THE HUMAN HYALURONAN SYNTHASE 2 GENE AND ITS NATURAL ANTISENSE RNA EXHIBIT COORDINATED EXPRESSION IN THE RENAL PROXIMAL TUBULAR EPITHELIAL CELL AND FIBROBLAST

Abdalsamed Altaher
MB ChB, MSc (Nephrology)

Thesis presented for the degree of MPhil
2012

Institute of Nephrology
School of Medicine
Cardiff University
Heath Park
Cardiff
CF14 4XN

DECLARATION

This work has not previously been accepted in substance for any degree and is not being concurrently submitted in candidature for any degree.

Signed…….. (Candidate) Date……..

STATEMENT 1

This thesis is being submitted in partial fulfilment of the requirements for the degree of MD.

Signed……. (Candidate) Date……

STATEMENT 2

This thesis is the result of my own independent investigation, except where otherwise stated. Other sources are acknowledged by explicit references.

Signed……. (Candidate) Date…….

STATEMENT 3

I hereby give consent for my thesis, if accepted, to be available for photocopying and for inter-library loan, and for the title and summary to be made available to outside organisation.

Signed…… (Candidate) Date……

STATEMENT 4: PREVIOUSLY APPROVED BAR ON ACCESS

I hereby give consent for my thesis, if accepted, to be available for photocopying and for inter-library loans **after expiry of a bar on access previously approved by the Graduate Development Committee.**

Signed…… (Candidate) Date……

Dedication

This thesis is dedicated to all of my family.

Acknowledgements

Firstly, I gratefully acknowledge the Department of Higher Studies, Ministry of Education Libya for funding the project.

I would like to thank my supervisors, Dr Timothy Bowen and Professor Aled Phillips, for their support, encouragement, and guidance throughout my MD.

I wish to sincere thank all my friends and colleagues in the Institute of Nephrology for their support, encouragement and advice, especially at the start of the project. Big thanks to Dr John Martin in particular for his technical help, support and friendship during the last four years.

Thanks to Dr Donald Fraser and Dr Bob Steadman for their useful discussion and good ideas in lab meeting.

Thank you to Dr Ruth Mackenzie, Kim Abberley and Cheryl Ward for their continuous assistance.

Finally, I would like to express my utmost gratitude to my close friends and family for their continuous support, during my study period.

Thesis Summary

Previous research at the Institute of Nephrology (IoN) has focused on the role of the vertebrate extracellular matrix (ECM) glycosaminoglycan, hyaluronan (HA), in renal fibrosis. The most effective predictors of disease outcome are interstitial accumulation of myofibroblasts and associated ECM expansion. The function of HA in the differentiation of resident and/or infiltrating fibroblasts to myofibroblasts, or by epithelial-to-mesenchymal transition of renal proximal tubular epithelial cells (PTCs) to a myofibroblastic phenotype, is therefore of great interest.

HA is synthesised by the HA synthase (HAS) enzymes, encoded by the corresponding *HAS* genes. Work at the IoN has shown HAS2 induction by fibrotic mediating cytokine transforming growth factor-β1 (TGF-β1) and pro-inflammatory cytokine interleukin-1 beta (IL-1β), and that HAS2 is the dominant HAS isoform in the regulation of fibroblast and PTC phenotype.

Recent data from the IoN showed coordinated expression of HAS2 and its natural antisense RNA, HAS2-AS1, in TGF-β1- and IL-1β-treated PTCs. The work described in this thesis began with confirmation of these findings, and this cytokine-driven coordinated expression pattern was then demonstrated in primary fibroblasts.

Forced expression of the HAS2 open reading frame in PTC induced up-regulated HAS2-AS1 transcription, while inhibition of HA synthesis down-regulated IL-1β-driven antisense up-regulation; HAS2 siRNA knockdown in PTC did not significantly change HAS2-AS1 expression. By contrast, and confirming previous IoN findings, siRNA knockdown of HAS2-AS1 expression also resulted in significant down-regulation of HAS2 mRNA synthesis, while novel data showed that forced HAS2-AS1 expression had no significant effect on HAS2 transcription.

In conclusion, TGF-β1 and IL-1β-driven coordinated expression of HAS2 and HAS2-AS1 was demonstrated for the first time in primary lung, oral mucosal, and dermal fibroblasts. Data from manipulation of HAS2 and HAS2-AS1 expression in PTC suggested that antisense transcription was regulated by HA-driven signalling, and that transcription of HAS2-AS1 antisense RNA stabilised and/or augmented HAS2 expression.

Presentation

Abdalsamed Altaher, Daryn R Michael, Aled O Phillips, Rachel D Neville, Min-young Kim, Timothy Bowen. The Human Hyaluronan Synthase 2 Gene and its Natural Antisense RNA Exhibit Coordinated Expression in the Renal Proximal Tubular Epithelial Cell. (Oral presentation). The Third Scientific Symposium for Libyan Students in UK Universities (Saturday 12 June 2010, Sheffied Hallam University).

Abdalsamed Altaher, Daryn R Michael, Aled O Phillips, Rachel D Neville, Min-young Kim, Timothy Bowen. The Human Hyaluronan Synthase 2 Gene and its Natural Antisense RNA Exhibit Coordinated Expression in the Renal Proximal Tubular Epithelial Cell. (Poster). The forth Scientific Symposium for Libyan Students in UK Universities (Saturday 15 January 2011, Cardiff University).

Contents

Chapter Six:

Glossary of Abbreviations

4MU	4-Methyl-Umbelliferone
α –SMA	Alpha-smooth muscle actin
β ACE-1	β-secretase-1
Anti-GBM	Anti-glomerular basement membrane
BMP-7	Bone Morphogenic Protein-7
BSA	Bovine Serum Albumin
cDNA	Complementary Deoxyribonucleic Acid
CD44	Cluster of differentiation-44
cREB	cyclic AMP Response element-binding protein
C_T	Threshold cycle
Da	Dalton (s)
dATP	deoxyadenosine triphosphate
dCTP	deoxycytidne triphosphate
dGTP	deoxyguanosine triphoshate
dTTP	deoxythymidine triphosphate
DMEM	Dulbecco's Modified Eagle's Medium
DNA	Deoxyribonucleic Acid
dNTP	Deoxynucleotide Triphosphate
ECM	Extracellular Matrix
EDTA	Ethylenediaminetetraacetic acid
EMT	Epithelial-Mesenchymal Transition
FAK	Focal Adhesion Kinase

FCS	Fetal Calf Serum
FGF	Fibroblast Growth Factor
GAG	Glycosaminoglycan
gDNA	Genomic dexoxyribonucleic acid
GPI	Glycosylphattidylinositol
h	Hour (s)
HA	Hyaluronan
HARE	HA Receptor for Endocytosis
HAS	Hyaluronan Synthase
HAS2AS	Hyaluronan Synthase 2 antisense
Has	Murine hyaluronan synthase
HEPES	N-2-Hydroxyethylpiperazine-N`-2-Ethanesulfonic Acid.
HK-2	Human Kidney-2
HYAL	Hyaluronidase
IαI	inter-α inhibitor
IαLI	Inter-α-like Inhibitor
IGF-1	Insulin-like Growth Factor-1
Il-1	Interleukin-1
iNOS	inducible nitric oxide synthase
IoN	Institute of Nephrology
Kb	kilobase pairs
L.B	Luria-Bertani broth (Lysogeny broth)
L-HAS2AS	Long HAS2AS isoform
µg	Microgram (s)

µl	Microliter (s)
µm	Micrometer (s)
ml	Milliliter (s)
mM	Millimolar
min	Minute (s)
mRNA	Messenger Ribonucleic Acid
MW	Molecular Weigh
NCBI	National centre for Biotechnology information
NF-kβ	Nuclear Factor Kappa-B
ng	Nanogram (s)
nm	Nanometer (s)
nM	Nanomolar
NS	Not Significant
ORF	Open Reading Frame
PBS	Phosphate Buffered Saline
PCR	Polymerase Chain Reaction
PDGF	Platelet-Derived Growth Factor
PMC	Peritoneal mesothelial cells
PαI	Pre-α-inhibitor
PTC	Proximal tubular epithelial cells
QPCR	Quantitative Real Time Polymerase Chain Reaction
qRT-PCR	quantitative Reverse Transcription Polymerase Chain Reaction
RARE	Retinoic acid response element
RHAMM	Receptor for HA-Mediated Motility

RNA	Ribonucleic Acid
rRNA	ribosomal RNA
rpm	Revolutions Per Minute
RT	Reverse Transcription
s	Second (s)
S-HAS2AS	short HAS2AS isoform
siRNA	Short Interfering Ribonucleic Acid
Smad	homologue of Drosophila protein mother Against decapentaplegic (MAD)
Sp-1	Stimulatory Protein-1
Sp-3	Stimulatory Protein-3
TIS	Transcription initiation site
TGF-β	Transforming Growth Factor-Beta
TFBS	Transcription factor binding site
TNF-α	Tumour Necrosis Factor-Alpha
TSG-6	Tumour Necrosis Factor-Alpha-Stimulated Gene 6
TSS	Transcription start site
UDP	Uridine Diphosphate
UTR	Untranslated region
UV	Ultraviolet
V	Volt (s)

Hyaluronan

1.1 History

Hyaluronan (HA), or hyaluronic acid, is a negatively charged and non-sulphated linear glycosaminoglycan (GAG) distributed broadly throughout vertebrate organs, fluids, connective tissue, epithelial and neural tissues. It was initially isolated from the vitreous of the eye [1], and its exact chemical structure was determined in 1954 as a large linear polymer composed of a repeated disaccharide sequence [2]. It is a ubiquitous component of the vertebrate exracellular matrix (ECM) and participates in a wide variety of cellular processes including differentiation, adhesion, migration and proliferation.

1.2 Chemical Structure and Morphology

The basic disaccharide motif that forms HA is comprised of N-acetylglucosamine and D-glucuronic acid, linked together via alternating β-1,4 and β-1,3 glycosidic bonds [2] and is shown in Figure 1.1. This disaccharide structure is then repeated to form a hyaluronan molecule or HA chain. The number of repeat disaccharides in a completed HA chain can approach 30,000 units in some tissues. It can therefore have a molecular mass of up to 10 $x10^6$ kilodalton (kDa), and an extended length of more than 25 μm, if straightened, much larger than any other member of the GAG family [3].

Molecules of HA are highly hydrophilic, with a stiffened helical configuration that gives the molecule an overall random coil structure [4][5]. This random-coil structure and the large size of HA enable it to interact with molecules of water, thereby forming solutions

with high elasticity and viscosity [5][6] that provide space-filling and lubricating functions in tissues such as cartilage. As a result of these properties, HA has been used as a therapeutic agent to treat the joints of race horses [7] and, in the 1980s, HA became an established aid in ophthalmic surgery [8][9].

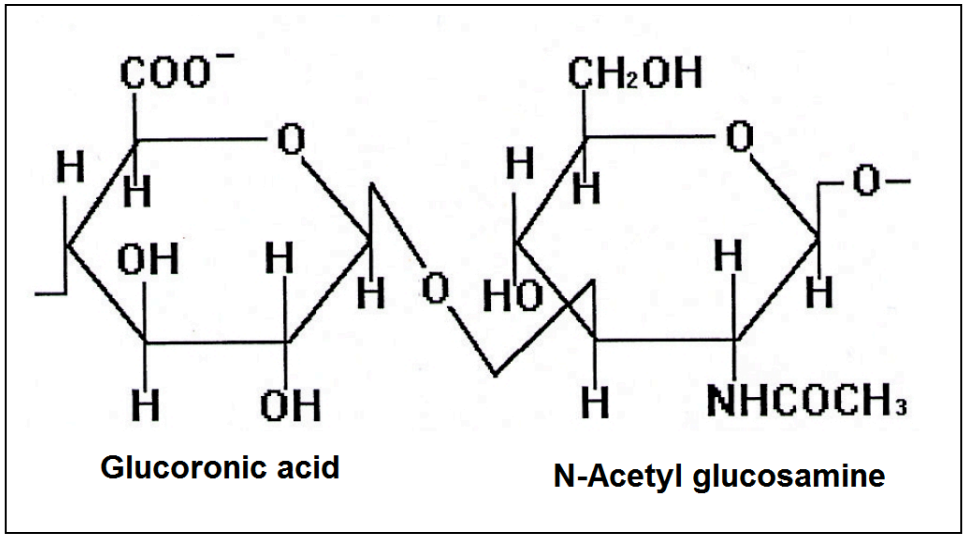

Figure 1.1 Chemical structure of HA .The repeating disaccharide unit is made of D-glucuronic acid and D-N-acetylglucosamine linked via alternating β-1, 4 and β-1, 3 glycosidic bands.

1.3 HA metabolism, assembly and signalling

1.3.1 HA synthesis

HA is synthesized by HA synthase (HAS) enzymes located within the plasma membrane. Three mammalian genes have been identified which encode HAS enzymes and these are known as HAS1, HAS2, and HAS3 [10,11] [12][13][14][15]. Each of the three mammalian HAS genes has been mapped to a different human autosome with HAS1 located at 19q13.3-13.4, HAS2 at 8q24.12 and HAS3 at 16q22.1 [14].

Each HAS enzyme catalyses the elongation of HA polymers via the addition of the uridine-diphospho (UDP) sugar nucleotide precursors UDP-glucuronic acid and UDP-N-acetyl glucosamine [16]. The HA chain is synthesized in the inner cytoplasmic surface of the cell membrane and then passes through the membrane to the extracellular space [17], as shown in figure 1.2.

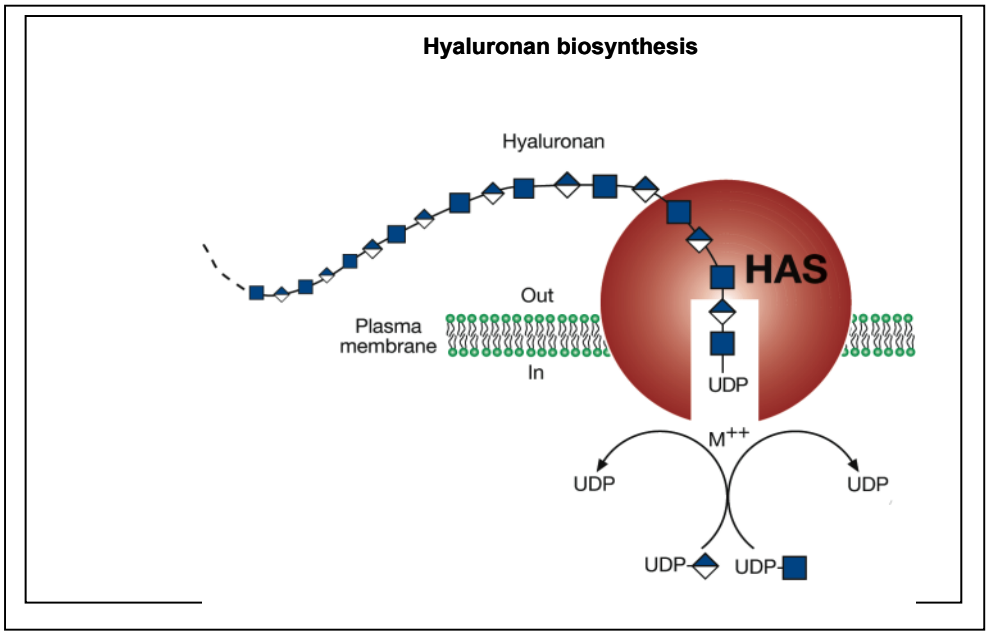

Figure1.2 Hyaluronan biosynthesis by hyaluronan synthase (HAS) occurs by addition of sugars (N-acetylglucosamine and glucuronic acid) to the reducing end of the polymer. M++ refers to a metal ion cofactor. Adapted from http://www.ncbi.nlm.nih.gov.

The properties, catalytic rate and mode of regulation for each isoenzyme are different and may underlie physiologically distinct functions [18][6]. Furthermore, many biological and physiological roles of HA have been related to its molecular weight. The molecular sizes of HA synthesised by the different HAS enzymes that are encoded by the respective HAS genes have therefore also been established. HAS1 has been shown to be the least active enzyme and drives the synthesis of high molecular weight HA (up to 2 x10^6 Da). HAS2 has a higher catalytic activity than HAS1 also, and generates high molecular weight HA polymers of greater than 2 x10^6 Da in size. In comparison, HAS3 produces lower molecular weight HA chains ranging from 2 x 10^5 to 3 x 10^5 Da *in vitro*. HAS3 is the most active of the three isoforms and drives the synthesis of large amounts of lower molecular weight HA chains [18][19][6].

1.3.2 HA Degradation

The degradation of HA is as essential as the synthesis of HA in maintaining tissue homeostasis, and it is estimated that about a third of the HA within the human body is removed and replaced during an average day [6]. The catabolic rate of HA differs extensively between tissues, and its half-life ranges from two to five minutes in circulating blood to roughly 70 days in the vitreous body [20].

The enzymes involved in HA degradation are the hyaluronidase enzymes (HYALs). Several hyaluronidase-like genes have been identified, however, only three (HYAL1, HYAL2 and HYAL3) encode proteins expressed in human tissues [21][22]. In humans, the three genes coding for these enzymes are tightly clustered at chromosome 3p21.3 [21]. HYAL1 cleaves high molecular weight HA into small oligosaccharides [23]. HYAL2 is glycosylphosphatidylinositol (GPI)-anchored to the plasma membrane and cleaves HA at a much slower rate to intermediate size fragments of approximately 50 disaccharides (roughly 20 KDa) [23]. HYAL3 does not appear to possess any hyaluronidase activity and very little is known about it [21][22]. HA degradation can occur also via two beta-exoglycosidases; beta-glucuronidase and β-N-acetyl-glucosaminidase (24][25], and has been demonstrated in the presence of reactive oxygen species [26].

Following HA degradation, pieces of HA are then taken up either into the surrounding tissues or into the lymph nodes and liver via endocytic uptake where it is then further degraded within lysosomes [20]. The endocytic uptake of HA is mediated through the

HA receptors Cluster of differentiation-44 (CD44), receptor for hyaluronan mediated motility (RHAMM) [27][28][6] and HARE (HA receptor for endocytosis) [29]. Alternatively, the high molecular weight HA may bind to the GPI-anchored HYAL2 on the plasma membrane, which degrades high molecular weight HA into 20 KDa fragments [30]. These fragments are then transported via endosomes to lysosomes where they are further degraded [31][32][28][33]. Once in lysosomes, further degradation of HA occurs through HYAL1, β-glucuronidase, and β-N-acetyl-glucosaminidase [24][25][33].

1.3.3 HA Assembly

1.3.3.1 HA binding proteins and organisation of the HA matrix

The HA binding proteins are known as hyaladherins. Most of the known hyaladherins and HA receptors couple to HA via an approximately 100 amino acid globular binding domain known as the link module, which is essential for ligand binding [34]. The consensus link module structure comprising an immunoglobulin domain and two adjacent link modules is common to many hyaladherins including versican and aggrecan. The immunoglobulin domains are most likely responsible for the link protein-proteoglycan interaction, whereas the link modules mediate binding to HA [34][35][36].

The hyaladherins can be further divided based upon their cellular or extracellullar location, and by the amino acid sequence of their HA binding site. The location of various hyaladherins is important for the formation of HA matrices and the balance

between these hyaladherins maintains an equilibrium that regulates the assembly of HA in the pericellular and extracellular matrix [37][38].

The extracellular hyaladherin group comprises many proteoglycans including aggrecan, versican, neurocan, and brevican. These proteoglycans can form large complexes with HA that are stabilised by the link module. These stable proteoglycan HA complexes can provide the load-bearing function in articular cartilage, contribute to maintaining the structural of numerous tissues, for example skin, and give elasticity in blood vessels [36][39][40].

A number of extracellular hyaladherins have been recognized that do not contain the link module domain. These include inter-α-trypsin inhibitor (IαI), pre-α-inhibitor (PαI) and inter-α- link inhibitor(IαLI), which cannot form link protein-stabilised complexes with HA, although heavy chains of IαI are known to covalently bind to HA and are also essential components of HA structures [41][42]. The heavy chains have been demonstrated to be an important component of pericellular HA structures and have been implicated in regulating cellular processes such as HA-mediated cell motility [37][43].

Tumour necrosis factor stimulated gene 6 (TSG-6) is secreted in response to inflammatory stimuli [44][45] and is known to contain a link module [46]. TSG-6 has been implicated in the stabilization of ECM structure, particularly by supporting the

formation of cross-linked HA networks [47]. TSG-6 catalyses the transfer of IαI heavy chains to HA forming a stable, covalently linked complex which has an important role in formation of the pericellular matrix [37][38][48]. Fülöp et al have also shown that TSG-6 -/- mice are infertile due to their inability to form a HA-rich extracellular matrix [48].

Recent studies from our laboratory have investigated the role of hyaladherin Inter-α-Inhibitor (IαI) family of proteins together with TSG-6 and the HA-binding proteoglycans bikunin and versican in the macro-molecular assembly of HA by renal proximal tubular epithelial cells (PTC) [37][49][38].The results demonstrated that the TSG-6-mediated formation of IαI heavy chain-HA complexes was critical for the formation of a peri-cellular HA matrix. As discussed above, it has been suggested that the TSG-6-mediated transfer of heavy chains from IαI to HA is necessary for the formation of the HA pericellular matrix [37].

Knudson et al, have demonstrated that HA binding sites or "receptors" participate in the assembly and retention of the HA-dependent aggrecan-rich portion of the chondrocyte pericellular matrix [50]. Matrix assembly was monitored on live, intact cells by the use of phase-contrast microscopy in combination with a particle exclusion assay. With this assay, the extent of the matrix was described as a "coat" surrounding the chondrocytes [50]. The HA rich pericellular matrix is anchored to the surface of cells through interactions with its principle receptor CD44 [50].CD44 has also been shown to be

important in the retention of pericellular matrix by chondrocytes and it is the main receptor associated with the formation of HA pericellular matrix [50]. Morphological and biochemical studies of matrix re-growth show that monoclonal antibodies directed against the HA receptor CD44 blocked chondrocyte pericellular matrix assembly [50].

1.3.3.2 Hyaladherins as HA receptors

The cellular hyaladherins comprise the receptors CD44 and RHAMM. The genes encoding CD44 and RHAMM can undergo alternate splicing of multiple variant exons, leading to the formation of numerous isoforms [51][34][52][53].

CD44 is a multifunctional trans-membrane glycoprotein [54]. CD44 is expressed on the plasma membrane where it can bind to and organise the actin cytoskeleton, and is also involved with the endocytotic uptake of HA at the cell surface [27][55] [56]. CD44 can also exist as a soluble form, shed from the plasma membrane, and can compete with membrane-associated CD44 for HA binding [57]. In addition, O-glycosylation of CD44 can occur resulting in an increased affinity for HA [58]. CD44 has been shown to be critical in the maintenance of local HA homeostasis. HA-CD44 interactions participate in a wide variety of cellular functions, including cell-cell aggregation, retention of pericellular matrix, matrix cell and cell-matrix signalling, receptor mediated internalization/ degradation of HA, cell migration and proliferation [59][60]. For this reason, HA-CD44- mediated interactions are critical in wound healing. For example,

CD44 plays an important part in regulating leukocyte extravasation into inflammatory sites [61] and mediated phagocytosis [62].

Isoforms of RHAMM can be located on cell surface, within the cytoplasm, or within the nucleus depending on the isoform expressed [63]. RHAMM does not contain the link module [34], instead it binds to HA through a 9-11 amino acid sequence containing multiple basic amino acids [64].

1.3.3.3 CD44 and HA signalling

It is clear that in some cell types, the multivalent interaction of polymeric HA with CD44 causes clustering of CD44 in the plasma membrane and that this event is associated with glycosylation and phosphorylation of CD44, interaction with the cytoskeleton and changes in cell behaviour [65][52][54]. It has been shown that CD44-HA interactions lead to activation of various components of the intracellular signaling pathways including NF-kB [66][67], phosphoinositide 3'-kinase [68], Src kinase [69] and Rac1[70][71]. Rearrangement of cytoskeletal elements such as ankyrin [72] and ezrin [73] result from the interaction of HA with CD44 in different cell types as show in figure 1.3. CD44 can also function as a co-receptor, physically co-localising with receptors such as TGF-β type I and type II receptors and resulting in modulation of intracellular transduction pathways involved in TGF-β signaling [74][75].

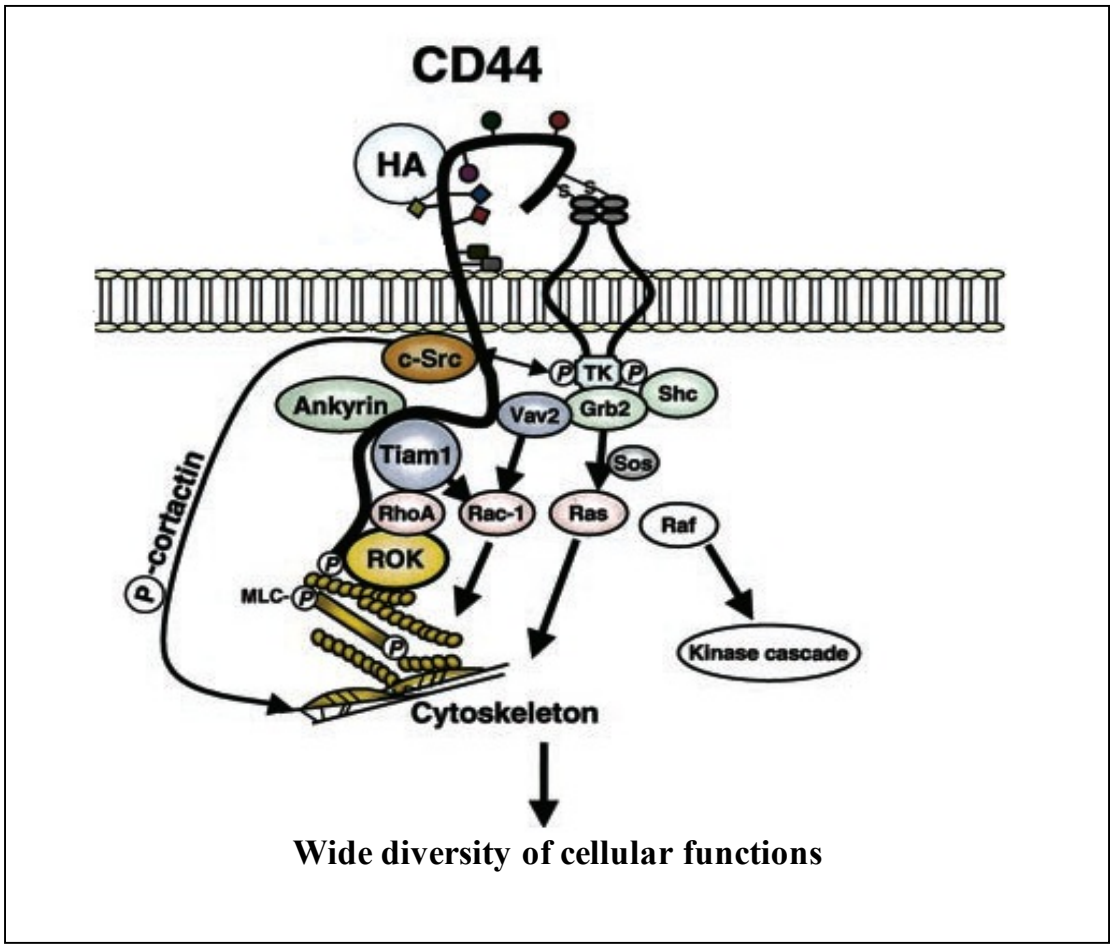

Figure 1.3 A current model for hyaluronan dependent, CD44-specific signaling pathways. CD44-hyaluronan interaction promote tyrosine kinase (TK) activity of the non-receptor kinase, Src. Src phosphorylates cortactin, which recruits it to the cell membrane. CD44-HA interactions also activate RHOA and Rac1, and CD44 binds to Tiam 1 and Vav2. HA also promotes the association of CD44 forms with cytoskeletal proteins such as ankyrin. Activation of these signaling pathways contributes to the role of CD44 in a wide diversity of cellular functions. Adapted from [63].

1.3.3.4 RHAMM and HA signalling

The HA receptor and hyaladherin RHAMM is unique in that it can be present at the cell surface, within the cytoplasm, and in the nucleus depending on alternative splicing of the transcript. It is expressed in many cell types and, depending on which isoform is present, contributes to HA–mediated migration, cytoskeletal reorganization and intracellular signal transduction [76]. Interaction of HA with RHAMM can trigger a number of cellular signaling pathways, including those that involve protein kinase C, focal adhesion kinase, MAP kinase, NF-κB, phosphatidylinositol kinase, tyrosine kinase, Src [36][77][78][79][63], Ras [80][81] and extracellular signal-regulated kinase (Erk) [82]. As shown in figure1.4, interacellular RHAMM is localized in the centrosome and modulates cell cycle control and mitotic spindle formation through cross-linking and association with actin and microtubule cytoskeletal elements [36]. RHAMM is also involved in regulating cell migration and has been shown to compensate for the loss of CD44 [83], whereby loss of CD44 resulted in increased HA accumulation allowing increased signalling of HA through RHAMM [83].

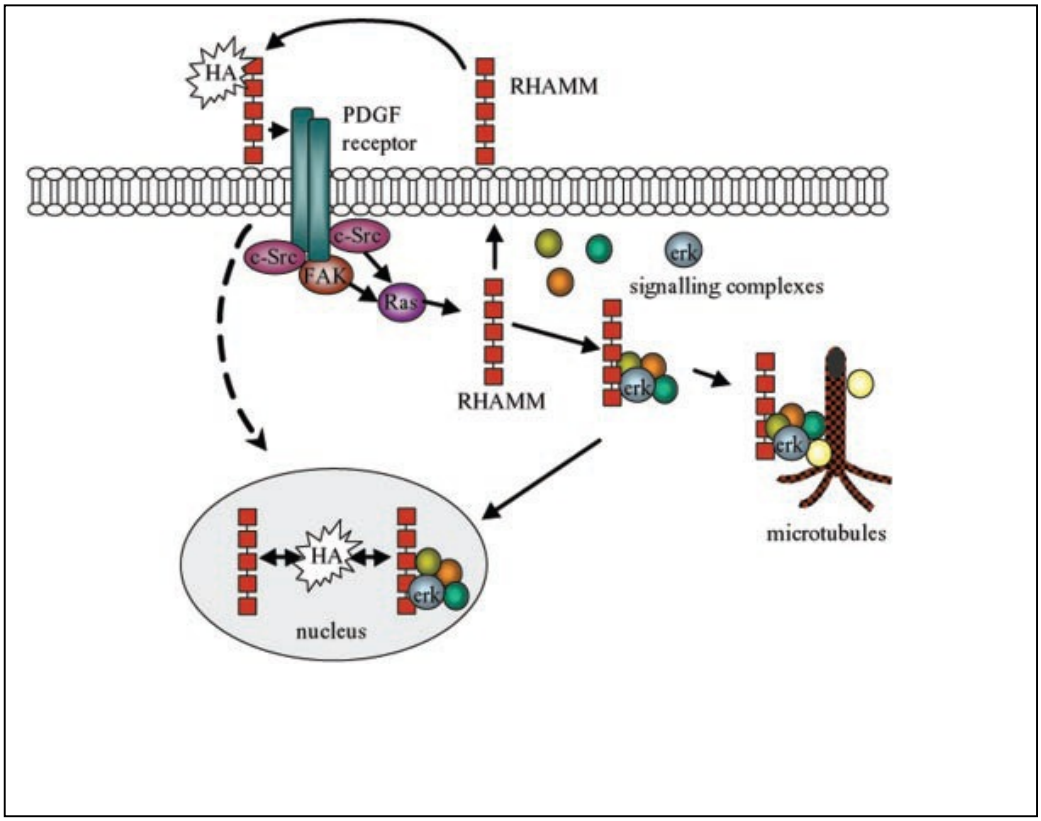

Figure 1.4 A current model for hyaluronan (HA)-dependent, RHAMM-mediated signaling pathways. Cell surface RHAMM-HA interactions regulate signaling through Ras and Src. Cell surface RHAMM modifies the ability of the PDGF receptor to activate Erk kinase, a key map kinase involved in cell motility. Intracellular RHAMM proteins possess multiple kinase recognition sites. Intracellular forms also associate with the cytoskeleton, notably interphase and mitotic spindle microtubules. Adapted from [63].

1.4 Biological function of HA

It was believed for many years that HA was an inert material which simply performed space-filling by organizing and modifying the extracellular matrix (ECM), however, numerous functions of HA have since been identified. Much of the work investigating the functionality of HA has come from studies on cancer, development and embryogenesis. As a result, HA has now been implicated in a wide range of extra-cellular matrix (ECM) - mediated processes including migration [84], differentiation [85], and proliferation [86].

1.4.1 HA in cell migration

Numerous studies suggest that HA may be involved in epithelial cancer cell migration and metastatic potential [87][88]. HA may actively promote tumour metastasis by promoting tumor cell adhesion and/or migration and may also protect against immune surveillance [36]. Furthermore, the level of HAS2 expression influences lamellipodial outgrowth, a key function in the migration process [6]. Nevertheless, over-expression of HAS2 and HAS3 genes in Chinese hamster ovary cells resulted in greater than 1000-fold enhancement of HA production and inhibited cell migration [6][89], suggesting that cell type is a crucial factor in determining the function of HA. In addition, HA synthesis has been shown to correlate with cell migration in a number of other cell types, and several reports have shown that cell movement can be inhibited by HA degradation or blocking HA receptor occupancy [90][91][92]. The extravasation of leukocytes from the blood into the vascular wall involves HA anchored to the surface of the endothelial cells by CD44 or RHAMM [93].

1.4.2 HA in cell differentiation

Previous work *in vivo* has demonstrated that differentiation of endothelial cells to mesenchymal cells is essential for the development of the atrioventricular canal (AVC) and subsequent septation and valve formation [85]. HA has multiple functions during AVC morphogenesis [45]. For example, HA promotes Ras-dependent differentiation into pre-valvular mesenchyme [85]. Camenisch et al, have shown that induction of cardiac endothelial-cell differentiation by a HA-modulated pathway involves ErbB2 and ErbB3 activation [85].

1.4.3 HA in cell proliferation

HA has long been implicated in malignant transformation and tumor progression [94][95], and an increase in HA accumulation has been observed around malignant cells found in breast, stomach and colon carcinoma [96][97][98]. Genetic manipulation of HAS genes in cancer cells has allowed investigation of the role of HA in tumour formation and progression. Over-expression of HAS2 and increased production of HA enhanced anchorage-independent growth and proliferation of human fibrosarcoma cells [99]. Similarly, over-expression of HAS3 promoted the growth of a prostate cancer cell line along with increased angiogenesis [100]. An altered balance in the ratio of synthesis to catabolism of HA is essential in both proliferation and migration, both of which have been shown to be enhanced in melanoma cells following the over-expression of either HAS1 or HAS2 genes [99][101].

Increased HA accumulation has been described in arterial disease where HA is thought to enhance the growth of vascular lesions through its effects on smooth muscle and endothelial cell proliferation and extracellular matrix synthesis [93][102]. Atherosclerosis and re-stenosis are characterized by marked changes in the content and distribution of HA [93]. The accumulation of HA in atherosclerotic lesions is frequently associated with increased expression of molecules that associate with HA, such as CD44 and TSG-6 [93].

1.5 HA in health

1.5.1 HA in development

HA is essential during embryonic development [103], where both the synthesis and turn-over of HA are required for heart formation [104][105]. Genetic deletion of the HAS isoforms *in vivo* has shown that mice deficient in HAS1 and HAS3 were embryonically viable [106], however deletion of HAS2 resulted in death at embryonic day ten due to failed development of the heart [45][106], indicating that HAS2 is vital to cardiac development.

1.5.2 HA in joint stability

The rheological properties that HA solutions exhibit (e.g. in synovial fluid) have also led to speculation about its role in the lubrication of joints and tissues. HA is commonly found in the body between surfaces that move along each other, for example, cartilage surfaces. HA solutions demonstrate similar visco-elastic properties shown by joint fluid [107][5].

1.5.3 HA in renal medulla

In the normal kidney, HA is expressed mainly in the interstitium of the renal papilla. Alterations in papillary interstitial HA has been implicated in regulating renal water handling by affecting the physiochemical characteristics of the papillary interstitial matrix and thus influencing the interstitial hydrostatic pressure [108]. HA plays a role in the urinary concentrating process [108][109].The lipid-laden interstitial cells are thought

to be the major source of HA synthesis in the inner medulla. These cells regulate hydration, as the amount of medullary hyaluronan has been shown to correlate with the hydration state [110].

1.6 HA in large organ fibrosis

Increased expression of HA has been detected in numerous fibrotic conditions associated with organ dysfunction such as lung [111], liver [112][113] and kidney [114][115][116].

1.6.1 HA in lung fibrosis

Pulmonary fibrosis is a component of interstitial lung disease, a diverse group of disorders that are characterized by chronic inflammation and progressive fibrosis of the pulmonary interstitium [117]. Elevated levels of HA have been established in numerous interstitial lung diseases, for instance idiopathic pulmonary fibrosis [118]. Furthermore, experimental models of pulmonary fibrosis have shown a substantial increase in HA accumulation in lung tissue and broncho-alveolar lavage fluid in rats with bleomycin-induced pulmonary fibrosis [119].

1.6.2 HA in liver fibrosis

In the liver, the concentration of HA in normal conditions is low. But, in the fibrotic liver it accumulates, and increased serum levels of HA are found in liver diseases of a variety of causes for instance alcoholic cirrhosis [120], chronic viral hepatitis [121] and primary biliary cirrhosis [122]. Serum HA levels have been found to correlate with the severity of

liver fibrosis [100][112], and HA has the potential to be a useful non-invasive biomarker for monitoring liver function, evaluating the extent of liver fibrosis and assessing response to therapy.

1.6.3 HA in renal fibrosis

Chronic kidney disease (CKD) is characterized by fibrosis, and in all renal diseases the progression of renal insufficiency leading to end-stage renal failure is closely correlated to the degree of fibrosis in the renal corticointerstitum. Increased expression of both HA and CD44 have been established in the cortical interstitium in a variety of interstitial and glomerular diseases such as ischemic renal injury [116], diabetic nephropathy [123], IgA nephropathy [124], anti-GBM nephritis [125], lupus nephritis [126], interstitial nephritis [127] and allograft rejection [128]. Stenvinkel and colleagues demonstrated that serum HA levels in a pre-dialysis population were strongly inversely correlated with survival on dialysis [129].

1.7 Tubulointerstitial fibrosis

Fibrosis is defined as expansion of stromal elements at the expense of highly differentiated parenchymal cells within the tissue. In renal disease, the expansion of stromal elements disrupts the kidney architecture and impairs fluid and solute exchange. The pathological changes associated with CKD and end-stage renal disease (ESRD) are progressive expansion of the tubulointerstitial space and subsequent fibrosis. The expansion of the interstitial volume is the result of proliferation of fibroblasts within the

interstitium, infiltration of monocytes and the excessive production of matrix within the interstitium by all these cells and by the tubular epithelial cells.

1.7.1 The histological changes of interstitium in tubulointerstitial fibrosis

Under physiological conditions, comparatively few renal fibroblasts reside in the interstitium. During renal fibrogenesis, fibroblast accumulation occurs in the tubulointerstitium. These pathologic, activated fibroblasts directly mediate fibrosis by leading to excessive deposition of ECM, and also by secretion of many pro-fibrotic factors such as transforming growth factor-Beta (TGF-β), platelet derived growth factor (PDGF) and fibroblast growth factor (FGF)[130].

There are several potential origins for the fibroblasts that drive tubulointerstitial fibrosis including local proliferation of resident fibroblasts, migration from the perivascular region, and recruitment of bone marrow derived precursors[131] [132].

In addition to being a source of profibrotic cytokines, PTCs may directly mediate fibrosis by acquiring a myofibroblast phenotype during renal injury via a process known as epithelial-mesenchymal transition (EMT) [133][134]. During EMT, tubular epithelial cells acquire mesenchymal gene expression and a migratory phenotype, accumulate excess ECM and secrete pro-fibrotic factors. A series of reports has shown that TGF-β1 is a vital pro-fibrotic factor in renal fibrosis, and is the principal stimulus of related processes, including EMT [135].

1.8 Previous work carried out at the IoN

Research in our laboratory has demonstrated that in normal conditions HA promotes renal proximal tubular epithelial cell (PTC) migration through interaction between CD44 and HA *in vitro* [84]. In addition, cell migration can be inhibited by an increase in HA degradation [90][21][136].

Work carried out at the Institute of Nephrology (IoN) has also demonstrated that the HA plays a pivotal role in regulating TGF-β1-driven cellular differentiation, facilitating fibroblast-myofibroblast transition [137][138]. Different TGF-β1-induced patterns of HA generation were associated with varying proliferative responses by dermal and oral mucosal fibroblasts, and inhibition of HA synthesis in dermal fibroblasts abrogated the TGF-β1-mediated induction of proliferation [137]. Lung fibroblasts also differentiate to a myofibroblastic phenotype [139], in response to TGF-β1 [140][141].

1.9 The Importance of the pericellular matrix HA in the regulation of cell phenotype

A number of cell types exhibit highly hydrated, HA pericellular matrices or "coats" that are usually 5-10 μm in thickness and can be removed by hyaluronidase treatment [142][143][144]. These pericellular matrices provide the essential environment for biological processes such as proliferation and migration [145]. Embryonic mesenchymal cells, including the precursors of muscle and cartilage, embryonic glial cells, neural crest cells and even some embryonic epithelial cells exhibit prominent pericellular matrices.

Recent IoN research has shown that the assembly of a HA pericellular matrix is necessary for myofibroblastic differentiation, and that sustained formation of a HA pericellular matrix may play an important role in maintaining the myofibroblast phenotype [138]. The role of HA can vary depending upon cell type and the HAS isoform expressed: in PTC, HAS2 has specifically been shown to be involved in the formation of a HA pericellular matrix [37], whereas HAS3 appears to be critical for HA cable formation [38]. In addition, De la Motte et al. showed that the increase of leukocyte binding was due to their interaction with HA cable-like structures, and that IαI has a crucial role in the formation of these cables [146].

Other work at the IoN has shown that HA can form pericellular cable-like structures in proximal tubular cell culture when stimulated with bone morphogenic protein-7 (BMP-7) [49]. Further research has shown that pericellular HA cables are anti-inflammatory and

inhibit the activation of monocytes [38], and that peripheral blood monocytes can bind to HA pericellular cable-like structures in a CD44 dependent manner [49]. These observations indicate that packaging of HA into pericellular cables plays an important role in HA function.

1.10 Organisation of the fibroblast pericellular HA matrix in myofibroblastic transdifferentiation

Fibroblasts are mesenchymal cells that *in vivo* have a bipolar spindle shape [147]. They have prominent nuclei, indicating a high level of protein synthesis. Fibroblasts play a central role in synthesis, degradation, and remodeling of the extracellular matrix in both health and disease [148][149][150][151][152][153]. In fibrosis, fibroblasts undergo activation to myofibroblasts [140][154][139][137][155] and this cell type perpetuates injury leading to organ fibrosis. The myofibroblast has a contractile phenotype characterized by the expression of a distinct actin isoform, α-smooth muscle actin (α-SMA) [153].

HA is essential for fibroblast to myofibroblast differentiation [138][137][156][157][158], and previous IoN work has demonstrated a functional role for HA in the differentiation of myofibroblasts from dermal fibroblasts, this regulatory role being deficient in aged fibroblasts that resist myofibroblastic differentiation [156]. In the renal cortico-interstitum, fibroblasts may be resident or derived from EMT of PTC [159].

The presence of myofibroblasts at biopsy is a marker of fibrotic progression, correlating to clinical outcome in CKD [160][161][162][163]. As the formation of the HA pericellular matrix accompanies myofibroblastic differentiation, it is likely that it may be involved in modulating this process [139]. Consequently, the formation of a HA pericellular matrix during myofibroblastic differentiation represents a potential target for the attenuation of progressive fibrosis.

Research at the IoN has shown an increased accumulation of high molecular weight HA during myofibroblast differentiation and demonstrated that it is organized into a pericellular matrix [139]. HA synthesis has been shown to be important for promoting this differentiation process, dermal fibroblast differentiation was associated with an induction of HAS1 and HAS2 transcription and assembly of pericellular HA coats, whereas resistance to differentiation in oral fibroblasts was associated with failure of pericellular coat assembly [138]. It therefore appears that inhibition of HA synthesis results in a corresponding reduction in this phenotypic change and maintenance of fibroblastic phenotype.

Webber et al. demonstrated that inhibition of autocrine TGF-β1 signalling and loss of the myofibroblast phenotype was associated with suppression of the expression of hyaladherin TSG-6, which has been demonstrated in numerous cell types to be a critical regulator of HA coat assembly [37][48]. This suppression of TSG-6 expression was associated with a loss of myofibroblast pericellular HA [141].

Simpson et al. confirmed a role for TSG-6 in facilitating fibroblast differentiation by demonstrating that siRNA knockdown of TSG-6 gene expression led to an inhibition of TGF-β1-dependent induction of α-SMA. This result suggests that TSG-6 facilitation of HA pericellular coat assembly is necessary to allow TGF-β1-dependent phenotypic activation of fibroblasts [156]. The importance of the pericellular HA coat in regulating the fibroblast-myofibroblast activation process is further highlighted by data demonstrating that inhibition of coat formation by hyaluronidase also prevented TGF-β1 mediated phenotypic conversion [156].

1.11 Organisation of pericellular renal proximal tubular epithelial cell (PTC) HA in Epithelial-to-Mesenchymal transition

PTC contribute to pathological changes in the renal interstitium by the generation of cytokines and alterations in the composition of the extracellular matrix [164][165][166][167]. PTC also play a key role in fibrosis as they undergo EMT to acquire a myofibroblastic phenotype [168]. The principal growth factor implicated in the phenotypic transition of EMT *in vitro* and in progressive disease *in vivo* is TGF-β1 [169] [170][171].

Work at the IoN has demonstrated that TSG-6 is also a major factor mediating the mechanism of EMT in PTC and thereby contributes to changes in cell phenotype in renal pathology [172].

It has been proposed that the HAS isoforms may have an essential role in differentiation from one cellular phenotype to another. Forced expression of HAS2 by adenoviral transfection promotes EMT in Madin-Darby canine kidney cells and MCF-10A human mammary epithelial cells [173].

HAS activity has also been shown to have an influential role in the organisation of HA pericellular structures. The forced expression of HAS3 in PTC leads to the formation of pericellular cables [38], while the forced expression of HAS2 in the same cells leads to the formation of HA pericellular matrix, and inhibits HA cable formation [37]. In PTCs *in vitro*, formation of HA cables/ coats and how they are put together can lead to different functional effects. Pericellular HA coat formation is associated with cell migration [38], while HA cables modify epithelial –mononuclear leukocytes interactions and decrease fibrotic effects by binding of monocytes to these structures, thereby attenuating monocyte-dependent PTC generation of TGF- β1 [38].

1.12 HAS2-driven HA synthesis

1.12.1 Role of HAS2 expression in the regulation of epithelial cell phenotype

HAS2 expression and HA metabolism are thought to have a role in EMT, which drives a wide range of physiological processes such as tissue remodelling, organ development and wound healing, and may also contribute to pathophysiological processes. HAS2-driven HA synthesis may be important in CKD, where EMT causes tubular epithelial cells to transform into myofibroblasts [174][168].

At the IoN and in other laboratories, it has been demonstrated that increased HA synthesis in PTC is accompanied by up-regulation of HAS2 expression in the presence of disease-related stimuli such as elevated concentrations of glucose and IL-1β [175]. Furthermore, data from the IoN have suggested that both HAS2 transcriptional induction and subsequent HAS2-driven HA synthesis may impact on renal fibrosis through their role in the phenotypic modulation and alteration of the PTC function. For example, forced-expression of HAS2 in PTC resulted in the formation of peri-cellular HA coats and an increase in cell motility - an essential early stage in EMT [37][133][38].

Other work has shown that HAS2 expression is important for EMT both *in vitro* [173] and *in vivo* [45]. HAS2 inactivation in the mouse embryo is lethal because of failure of

cardiac endothelial cells to undergo epithelial to mesenchymal transition [45]. Phenotypic alteration in human mammary epithelial cells may be driven by adenoviral expression of HAS2, the increase of synthesis of HA through this induction of HAS2 then initiating epithelial-mesenchymal transformation [173]. In addition, in renal epithelial cells there is an increase in HA following the up-regulation of HAS2 transcription in autoimmune renal injury [176].

1.12.2 Role of HAS2 expression in the regulation of fibroblast phenotype

Work carried out at the IoN has shown the importance of HAS2-isoform-dependent effects on fibroblast phenotype. In lung fibroblasts for example, HAS2 mRNA synthesis and HA peri-cellular coat formation are associated with the myofibroblastic phenotype, [139], and increased HA synthesis together with up-regulated HAS2 transcription have been reported in lung fibrosis [177]. Furthermore, work at the IoN has shown that TGF-β1 stimulation was associated with induction of HAS2 in dermal fibroblasts, while there was a lack of induction of HAS2 transcription in oral fibroblasts which are resistant to phenotype activation [138]. In addition, the impaired ability of ageing dermal fibroblasts to acquire a myofibroblastic phenotype was associated with failure of HAS2 induction following TGF-β1 stimulation, and this study shows that over-expression of HAS2 in older dermal fibroblasts, aged *in vitro*, restores their TGF-β1-responsiveness [156]. Moreover, in human lung fibroblasts, knockdown of HAS2 expression using a HAS2-specific siRNA resulted in attenuated differentiation to the myofibroblast phenotype and decreased expression of α-SMA [141]. In addition, scratch-wound studies using skin

keratinocyte monolayers show an increase in HA following an up-regulation of HAS2 transcription [178,179].

1.13 Regulation of HAS2 expression

HAS2 transcription can be induced by a variety of stimuli. Epidermal keratinocytes, for example, show an increase in HAS2 expression in response to epidermal growth factor [178][179], and also to keratinocyte growth factor [180]. Other cytokines and growth factors reported to induce HAS2 expression include PDGF in both corneal endothelial cells [181] and mesothelial cells [182], tumor necrosis factor-α (TNF-α) in periodontal ligament cells [183], as well as fibroblast growth factor (FGF) and insulin-like growth factor-1 (IGF-1) in human articular chondrocytes and osteosarcoma cells [184].

In addition, previous reports from the IoN and other laboratories have demonstrated that a number of cytokines, including IL-1β and TGF-β1, are implicated in transcriptional regulation of the HAS2 gene. For example, IL-1β has been reported to increase HAS2 expression in PTC via NF-κB signaling [175], and IL-1β was reported to induce HAS2 expression in periodontal ligament cells [183]. IL-1β stimulation of human peritoneal mesothelial cells (PMC) [185] and adult dermal fibroblasts [186] resulted in the up-regulation of HAS2 and an associated rise in HA synthesis.

TGF-β1, on other hand, can either stimulate or suppress HAS2 expression, depending on the cell type. For instance, it has been shown to increase the transcription of HAS2 in corneal endothelial cells via Smad signaling [181], whereas TGF-β1 downregulates HAS2 in rat epidermal keratinocyte cells [179] and also suppresses HAS2 gene expression in mesothelial cells [182]. Moreover, work at the IoN has shown that TGF-β1 was associated with induction of HAS2 in dermal fibroblasts, while there was a lack of induction of HAS2 transcription in oral fibroblasts [138]. In addition, the impaired ability of ageing dermal fibroblasts to acquire a myofibroblastic phenotype was associated with failure of HAS2 induction following TGF-β1 stimulation [156].

In high glucose concentrations *in vitro*, to model mimic diabetic nephropathy, PTC synthesise high levels of HA, which is coincident with specific up-regulation of transcription at the HAS2 locus [175].

1.14 Genomic structure of HAS2

The human HAS2 gene has been mapped to 8q24.12 [14]. Work at the IoN reconstructed the putative genomic structure for each human HAS isoform, including the HAS2 gene, identifying the putative upstream proximal promoter region in each case [187]. Figure 1.5 shows a schematic representation of the genomic structure of each human HAS gene, compared with their murine Has orthologues [19][187].

The genomic structure for the HAS2 isoform spanned four exons, exon one forming a discrete 5′-untranslated region (5′-UTR), with the translation start site at nucleotide one of exon two. The mouse Has2 and human HAS2 isoforms have similar genomic structures [19] and a comparison between human HAS2 intron/ exon boundaries and the corresponding regions in murine Has2 gene [19][188] established there is high level of both nucleotide and amino acid sequence identity among human and mouse orthologues.

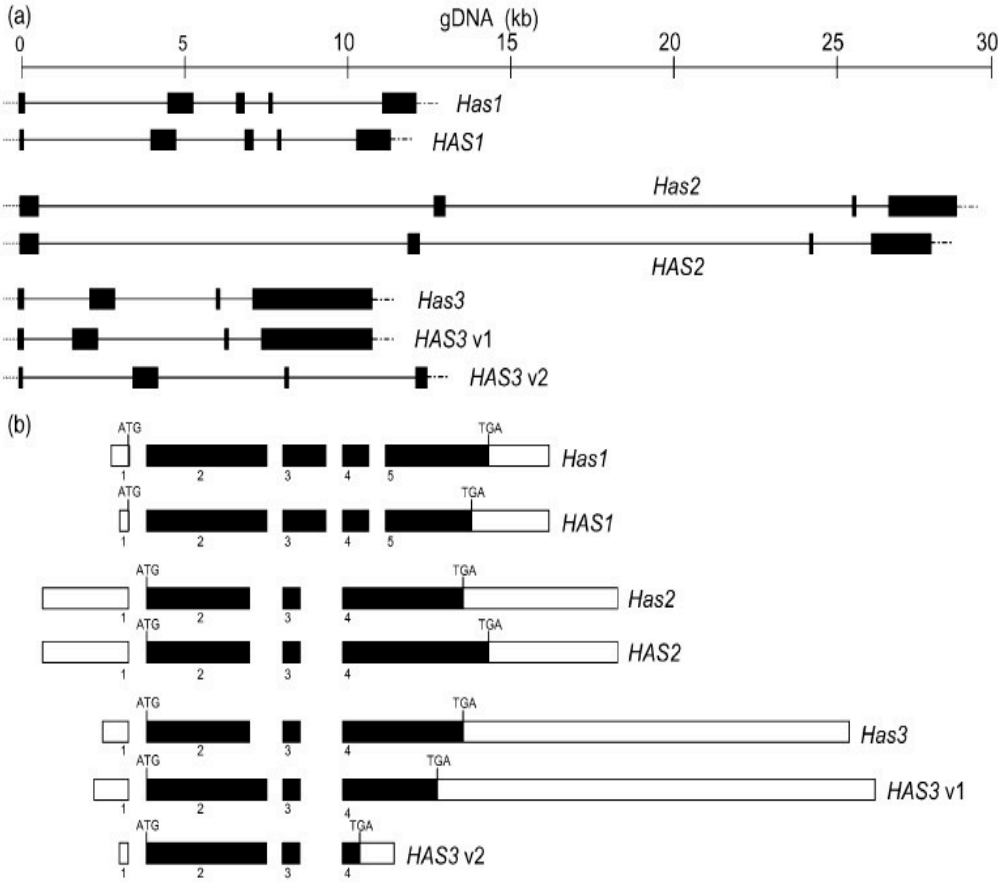

Figure 1.5 Genomic structures for human HAS1, HAS2, HAS3v1 and HAS3v2 are drawn to scale in 5'-3' orientation together with murine Has 2 orthologues [82].(a) Exons are represented by filled boxes and are separated by introns (solid lines), preceded by promoter regions (dotted lines) and followed by downstream 3' sequences (dotted and dashed lines). (b) The second part of the figure shows the alignment of the exons of the human HAS genes and murine Has orthologues [82] in 5'-3' orientation, showing the translation start (ATG) and termination codons (TGA). Exons are represented by numbered boxes, with the coding regions filled and the 5'-and 3'-UTRs empty. Adapted from Monslow et al. 2003 [187].

1.15 Transcriptional regulation of HAS2

1.15.1 *Role of the promoter in constitutive and stimulated HAS2 gene transcription*

Promoters are combinations of DNA sequence elements that are usually located in the immediate upstream region of the gene, often within 200 bp of the transcription start site, that serve to initiate transcription. The binding of RNA polymerase II at the core promoter is a key stage in gene transcription, and gene expression is initiated via the binding of transcription factors and other key elements such as tissue specific transcription factors to the promoter and the formation of a transcriptional complex with RNA polymerase II.

Recent work at the IoN has investigated the regulatory elements responsible for the transcription of the human HAS2 gene [187][189]. This work detected an extended sequence for HAS2 exon 1 and relocated the HAS2 transcription initiation site (TIS) 130 nucleotides upstream of the reference HAS2 mRNA sequence [189]. Data from *in silico* analysis in our laboratory of the newly-defined HAS2 promoter region highlighted a cluster of three Sp1/Sp3 recognition sites immediately adjacent to the relocated TSS [189]. Later work demonstrated that transcription factors Sp1 and Sp3 act as co-activators at these sites, mediating HAS2 constitutive transcription in PTC [190].

Previous work at the IoN has also shown that IL-1β stimulation of PTC *in vitro* leads to HAS2 up-regulation via an NF-κB dependent mechanism [175][190] and identified an NF-κB site 250 bp upstream of the HAS2 TSS in silico. The presence of p50 and p65, the NF-κB sub-units typical of the canonical pathway up-regulation, in PTC nuclei following IL-1β stimulation was also demonstrated, although NF-κB binding to HAS2 promoter was not seen [190]. More recently, quantitative qRT- PCR data demonstrated that siRNA knockdown of Sp1 and Sp3 inhibits HAS2 induction following incubation with IL-1β, and that the TGF-β1 induction of HAS2 in PTC is abrogated by siRNA knockdown of Smad2 and Smad3 [191].

Saavalainen et al. showed that, in keratinocytes, the human HAS2 promoter is under the control of the inducible transcription factors NF-kβ and retinoic acid receptor (RAR), as well as constitutively active Sp1 [192][193]. These regulatory proteins share common cofactors, providing numerous possibilities for functional interaction between associated signalling pathways. Moreover, Makkonen et al found that cyclic AMP Response element-binding protein (cREB) and retinoic acid regulate the human HAS2 gene [194].

1.16 Genomic organization of HAS2-AS1, a natural antisense RNA to HAS2

In addition to transcription, HAS2 expression may also be regulated at the post-transcriptional, translational and post-translational levels. Post-transcriptional regulation of HAS2 expression by natural antisense RNA, HAS2-AS1, has recently been described [195].

The human HAS2-AS1 gene is transcribed from the opposite genomic DNA strand to HAS2 at locus 8q24.12, and comprises four exons, as shown below in Figure 1.6.This antisense transcript was originally designated as human HASNT (for HAS2 antisense), and the symbol Hasnt was used for the corresponding mouse orthologue [195]. NCBI has since annotated the human transcript as HAS2-AS1.

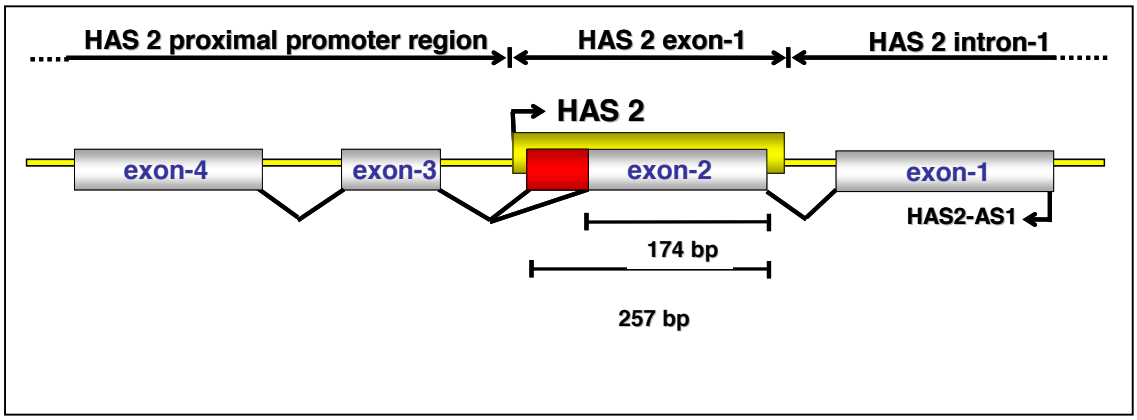

Figure 1.6 Genomic organization of the HAS2-AS1 gene with respect to HAS2. The red box indicates the difference in nucleotide composition of the long and short splice-variants of HAS2AS exon 2.

As shown in Figure 1.6, the HAS2-AS1 exon 1 sequence lies within intron 1 of the HAS2 gene, the second HAS2-AS1 exon is complementary to a portion of HAS2 exon 1, and the nucleotide sequences of HAS2AS exons 3 and 4 are located upstream of HAS2.

Expression of a "long" HAS2-AS1 splice-variant, L-HAS2-AS1, and a corresponding "short" alternatively-spliced product, S-HAS2-AS1, has been reported in osteosarcoma cells [195]. This length variation involves a difference of 83 nucleotides of the HAS2-AS1 exon 2 sequence and thus changes the length of complementary sequence with HAS2. L-HAS2-AS1 shares 257 nucleotides with HAS2 exon 1, while S-HAS2-AS1 has a corresponding 174 nucleotide region of complimentarity [191][195].

1.17 Post Transcriptional Regulation of HAS2 gene expression by HAS2-AS1

Natural antisense RNAs have been found in viruses, prokaryotes and eukaryotes, and are plentiful in mammals, including human and mouse [196]. They have a wide range of potential functional roles, including the regulation of gene expression [197][195][184][198]. Chao and Spicer demonstrated that overexpression of the HAS2-AS1 gene down-regulated both HAS2 mRNA transcription and HA synthesis in osteosarcoma cells [195]. These finding suggested that HAS2-AS1 may regulate HAS2

transcription *in vivo*, and the authors predicted that HAS2 and HAS2-AS1 transcriptional activity was independent and mutually exclusive [195].

At the beginning of the work described in this thesis, the data summarized above described the extent of knowledge on the expression of HAS2-AS1 and its interaction with HAS2. As described above, previous work at the IoN had implicated HA in renal fibrosis. From *in vivo* studies, HA was shown to be a correlate of fibrosis in analysis of renal biopsy samples from diabetic nephropathy patients [114]. In addition, HAS2-driven HA synthesis has been shown to play a role in the modulation of the phenotype of two cell types: transdifferentiation of fibroblasts to myofibroblasts and EMT of PTC to an activated, myofibroblastic phenotype [37][38][138][139][141][156].

To pursue further the connection between HAS2 expression and HAS2-driven HA synthesis and renal fibrosis, the work outlined in this thesis set out to establish the role of HAS2-AS1 in the regulation of HAS2 expression. Following experiments showing coordinated expression of sense and antisense RNAs in response to three disease-related stimuli in PTC, simultaneous transcriptional induction of HAS2-AS1 and HAS2 expression was also demonstrated in a variety of fibroblasts cell types in response to cytokine stimulation. Since these data suggested that sense: antisense relationship in these cells was different to that described previously in osteosarcoma cell [195], further experiments were designed to modulate the expression of HAS2-AS1 or HAS2 and to observe any changes in expression of the other RNA.

1.18 Project Aims

The aim of this project is to further ongoing work looking at regulation of HAS2. In particular, this thesis examines the relationship between HAS2 and HAS2-AS1 in order to give us some functional insight into what HAS2-AS1 does and how HAS2-AS1 RNA may regulate HAS2 mRNA expression. The specific aims were:

1) To compare and contrast the regulation of HAS2 and HAS2-AS1 expression in PTC in response to the pro-inflammatory cytokine IL-1β and the pro-fibrotic cytokine TGF-β1, that are known to be implicated in kidney fibrosis. In addition, elevated glucose concentration was also investigated as this mimics diabetic nephropathy and has been reported to drive HA synthesis. Having established these patterns of expression in PTCs, to extend these observations to the other cell types, lung, dermal and oral fibroblasts.

2) To use forced expression or siRNA knockdown of HAS2 mRNA to determine the effect of this manipulation of expression on the inducibility of HAS2-AS1 RNA in response to IL-1β or TGF-β1.

3) To use forced expression or siRNA knockdown of HAS2-AS1 RNA to determine the effect of this manipulation of expression on the inducibility of HAS2 mRNA in response to IL-1β or TGF-β1.

2.1 Tissue culture

Human proximal renal tubular epithelial cell (PTC) line HK-2 and human lung fibroblasts were cultured in 75 cm^2 tissue culture flasks at 37˚C in a humidified incubator (Cell House 170, Heto Holten, Derby, UK) with an atmosphere containing 5% CO_2 and 95% air. Spent medium was removed by aspiration and fresh growth medium was added every 3 to 4 days until the cells reached 100% confluence [199]. When sub-cultured, the content of each original 75 cm^2 (T-75) flask was divided into three new flasks.

HK-2 cells were purchased from the American Type Culture Collection (Manassas, VA, USA) and grown in 1:1 (v/v) mixture of glucose-free D-MEM : F-12 Ham (NMF-12) medium (10 mmol/l glucose; Gibco/BRL Life Technologies Ltd, Paisley, UK) supplemented with 10 ml of HEPES (Gibco) per 500 ml medium, 5µg/ml of insulin (Sigma, Poole, Dorset, UK), 5µg/ml of transferrin (Sigma), 5 ng/ml of sodium selenite (Sigma), 400 ng/ml of hydrocortisone (Sigma) and 10% foetal calf serum (FCS; Autogen Bioclear Ltd, Calne, Wiltshire, UK).

Primary human lung fibroblasts (AG02262) were purchased from Corriel cell repositories (Coriell Institute for Medical Research, NJ, USA). These cells were cultured in D-MEM supplemented with 2 mM of L-glutamine, 100 µg/ml of penicillin (Sigma), 100 µg/ml of streptomycin (Sigma) and supplemented with 10% foetal calf serum (FCS).

Dermal and oral mucosal fibroblasts were obtained by biopsy from consenting adults undergoing routine minor surgery, and ethical approval for the biopsies was obtained from the South East Wales Research Ethics Committee.

2.2 Sub-culture of cells

Confluent cell monolayers for passage were sub-cultured using the following method.

1. Spent medium was aspirated from the cell monolayer and the cells were washed once with 10 ml of PBS.
2. A sufficient volume of a 1:9 (v/v) solution of trypsin : PBS was added to cover the cell monolayer.
3. Cells were inspected by light microscopy and, after 4-5 min incubation at 37˚C, were detached from the flask by gentle agitation.
4. Trypsin protease activity was neutralised by the addition of 30 - 40 ml of fresh growth medium, containing 10% FCS, to prevent cell lysis of the cells.
5. The cell suspension was transferred to a sterile 50 ml universal tube.
6. Cells were pelleted by centrifugation at 1,500 rpm at 4˚C for 6 min.
7. The supernatant was aspirated and the cells were re-suspended in 45 ml of fresh supplemented medium containing 10% FCS and seeded into appropriate culture vessels: 2 ml / well in a 6-well plate, 5 ml / T-25 flask, 15 ml per T-75 flask.

2.3 Serum starvation / Growth arrest

All experiments were carried out following a period of growth arrest for the cells. Growth medium was removed from confluent cell monolayers, which were then washed

twice with PBS. Fresh, serum-free growth medium was then added and the cells were incubated for a further 48 h at 37˚C.

2.4 Cell stimulation

Serum-free growth arrest medium was aspirated and replaced with control serum-free medium or medium containing 1 ng/ml of recombinant interleukin-1-beta (IL-1β; R&D Systems Europe Ltd., Abingdon, Oxfordshire, UK) or 10 ng/ml of recombinant transforming growth factor-beta1 (TGF-β1; R&D). The duration of cell stimulation was determined in time course experiments.

2.5 RNA Extraction

1. Supernatants were removed and 1 ml of TRI-Reagent solution (Sigma) was added per well of a 6 well plate, incubated at room temperature for 1 min, then pipetted repeatedly to ensure complete cell lysis.
2. Each cell lysate was transferred to a sterile 1.5 ml tube and incubated at room temperature for 5 min to ensure complete dissociation of nucleoprotein complexes. Lysates were then stored at -80˚C, until ready for RNA extraction.

   The following steps were performed on ice.
3. Samples were defrosted and 200 µl of chloroform was added per 1 ml lyaste. The samples were agitated by inversion for 15 s, until completely emulsified.
4. Samples were incubated at room temperature for 5 min to allow clear phase separation.
5. Centrifugation was carried out at 12,000 rpm for 15 min at 4˚C.

6. The colourless upper aqueous phase (approximately 0.5 ml) was transferred carefully to a fresh tube for each sample, removing any of the interface. The lower organic phase was discarded.

7. To precipitate RNA, 0.5 ml of isopropanol was added to each sample per 0.5 ml of upper aqueous phase. The samples were then mixed by inversion and stored overnight at -20˚C.

8. Samples were defrosted, centrifuged at 12,000 rpm for 15 min at 4˚C, and supernatants were decanted to leave an RNA pellet. Each pellet was washed with 1.5 ml of ice-cold 75% ethanol, vortexed briefly and centrifuged at 12,000 rpm for 15 min at 4˚C.

9. Supernatants were decanted and RNA pellets were air-dried for 1 h to remove all traces of ethanol.

10. Pellets were re-suspended in 20 µl of water, and vortexed to ensure all the RNA had been solubilised.

11. The absorbance at 260 nm (A_{260}) of a 1:50 dilution of each sample was analysed spectrophotometrically and RNA concentrations were calculated using the following equation:

$$\frac{A_{260} \text{ x dilution factor x extinction coefficient}}{1000} = [\text{RNA}]\ (\mu l/\mu g)$$

12. The integrity of extracted RNA was determined by flat-bed electrophoresis 1µl of each RNA extract though a 2% agarose gel (see Appendix 1). The presence of discrete bands representing the 28S and 18S subunits of ribosomal RNA indicated intact RNA suitable for experimental analysis.

2.6 Reverse Transcription

1. Reverse transcription was carried out using the High Capacity cDNA Reverse Transcription Kit with RNase Inhibitor (Applied Biosystems, Warrington, Cheshire, UK). The final volume of the reverse transcriptase (RT) master mix (MM) was adjusted for the number of RNA samples, and included sufficient for one no template control reaction with no RNA.

2. These ingredients comprised the MM (totalling 10 µl per sample)

10 x RT Buffer	2.0 µl
25 x dNTP Mix (100 mM)	0.8 µl
10 x RT random primers	2.0 µl
Multi-Scribe reverse transcriptase	1.0 µl
RNase inhibitor	1.0 µl
nuclease-free H_2O	3.2 µl
	10.0 µl

3. A total of 1 µg of each RNA sample was diluted in 10 µl of water

4. An aliquot of 10 µl of MM was added to each RNA sample, making a total reaction volume of 20 µl. Reverse transcription was carried out in a thermocycler, using the following cycling protocol.

	Step 1	**Step2**	**Step 3**	**Step 4**
Temperature	25˚C	37˚C	85˚C	4˚C
Time	10 min	120 min	5 s	

2.7 Quantitative Reverse Transcription-Polymerase Chain Reaction (qRT-PCR)

Master mixes (MMs) for qRT-PCR of HAS2 and 18S ribosomal (r) RNA, and HAS2-AS1, were made up as shown below, in each case comprising a total reaction volume of 20 µl.

MM for HAS2

TaqMan fast universal PCR master mix	10 µl
HAS2 primer and probe	1 µl
cDNA from RT reaction	1 µl
H_2O	8 µl
	20 µl

MM for HAS2-AS1

TaqMan fast universal PCR master mix	10 µl
HAS2-AS1 primer and probe	1 µl
cDNA from RT reaction	2 µl
H_2O	7 µl
	20 µl

MM for 18S rRNA

TaqMan fast universal PCR master mix	10 µl
18S rRNA primer and probe	1 µl
cDNA from RT reaction	1 µl
H_2O	8 µl
	20 µl

Taqman assay reagents for qRT-PCR analysis of HAS2, HAS2-AS1 and 18S rRNA were obtained from Applied Biosystems. Samples were processed in an Applied Biosystems Fast Optical 96-well reaction plates in a Fast Real-Time PCR system with cycling parameters of 95˚C for 10 min followed by 40 cycles of 95˚C for 15 s and 60˚C for 1

min. Onboard SDS software was used for the analysis of output data from biological triplicates. The process of Q-PCR is summarised in figure 2.1.

The comparative C_T method was used for relative quantification of gene expression. The C_T (threshold cycle where amplification is in the linear range of the amplification curve) for the standard reference gene 18S ribosomal RNA (rRNA) was subtracted from the target gene C_T to obtain the ΔC_T for each sample. The mean ΔC_T values for similar samples were then calculated. The expression of the target gene in experimental samples relative to expression in control samples was calculated:

$$\textbf{Relative Expression} = 2^{-(\Delta CT\,(1) - \Delta CT\,(2))}$$

Where ΔC_T (1) is the mean ΔC_T value calculated for the experimental samples, and ΔC_T (2) is the mean ΔC_T value calculated for the control samples. Data were analysed using "RQ Manager" software from Applied Biosystems UK Ltd.

C_T , or the threshold cycle, is a number of PCR cycles needed to detect fluorescence associated with the amplification of a specific product. If efficiency of the reaction is 100%, with every PCR cycle the number of copies of the product is doubled. Therefore, 1 cycle different (i.e. ΔC_T =1) between two samples means that there was initially 2-fold difference in expression of a particular gene between those samples. The difference of 2 cycles (ΔC_T =2) means 4-fold (2^2) difference in expression, ΔC_T =3 means 8-fold (2^3) difference, and so on.

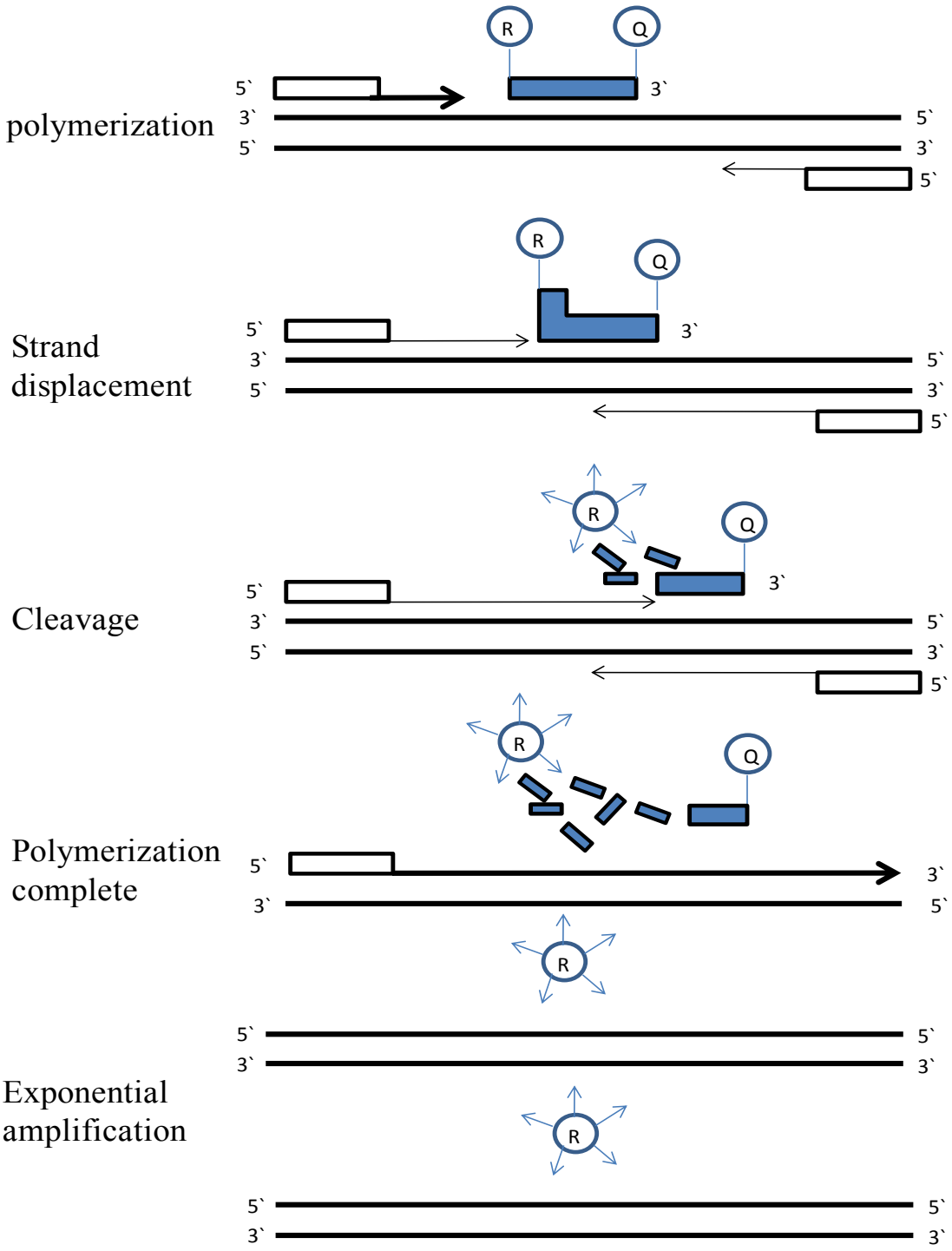

Figure 2.1: Mechanism of Q-PCR.
The forklike-structure-dependent, polymerisation- associated, 5`to 3` nuclease activity of AmpliTaq Gold Polymerase. The subsequent release of the fluorescent reporter is related directly to the exponential accumulation of PCR products.
Modified from the Taq Man Universal PCR Master Mix protocol (Applied Biosystems).

Detection of the PCR product relies on the cleavage of the TaqMan probe. The TaqMan probe contains a reporter dye at the 5' end a quencher dye at the 3' end. When the probe is intact, the proximity of the quencher dye to the reporter dye enables the quencher dye to suppress the fluorescence of the reporter dye. If the target gene is present, during the PCR reaction, the probe will specifically anneal between the forward and reverse primer sites. During the reaction, cleavage of the probe occurs due to the forklike-structure-dependent polymerisation-associated 5'to 3' nuclease activity of the AmpliTaq Gold DNA polymerase. This releases the fluorescent reporter from the probe, and close proximity of the quencher, therefore allowing the reporter to fluoresce. Fluorescence of the reporter allows detection of PCR products, and the increase in fluorescence is directly related to the amount of PCR product. This process occurs in every cycle and does not interfere with the exponential increase of PCR product. The 3' end of the probe is blocked to prevent extension of the probe during PCR. If the target sequence is not present the probe will not hybridise to the cDNA, therefore the probe will not be cleaved and the fluorescence of the reporter will remain suppressed.

2.8 qRT-PCR reagents

qRT-PCR down by Taqman gene expression assays were purchased from Applied Biosystems.The qRT-PCR reaction was carried out using standard protocols as recommended for the Taqman assay reagents.

Gene	Primer/ Probe Catalogue Number
HAS2	Hs_00193435_ml
HAS2-AS1	AI5H05G

Table: Taq Man Gene Expression Assays (Applied Biosystems).

2.9 Transforming competent cells for pCR-3.1 and pCR-3.1 HAS2 expression vector

Prior to the transformation procedure, a water bath was equilibrated at 42˚C, an appropriate volume of SOC medium was pre-warmed to room temperature and selective LB plates (see Appendix 2) were pre-warmed at 37˚C for 30 min.

1. One vial of One Shot TOP10 chemically competent *E. coli* cells (Invitrogen) were thawed on ice for each transformation.
2. Approximately 10 ng of each plasmid DNA (kind gifts from Dr Russell Simpson, Institute of Nephrology, Cardiff University School of Medicine) was added to the bacterial cells and mixed by gentle flicking.
3. Vial(s) were placed on ice for 30 min with mixing by gentle flicking of the tube every 10 min.
4. Cells were heat-shocked for 30 s at 42˚C without mixing.
5. Vial(s) were placed on ice for 2 min and then 250 µl of pre-warmed SOC medium was added aseptically to each vial.
6. Vial(s) were capped tightly and shaken at 37˚C for 1 h at 225 rpm in an orbital shaking incubator.
8. Aliquots of 5 µl and 50 µl from each transformation were spread on pre-warmed selective LB plates, which were then inverted and incubated overnight at 37˚C.
9. A suitable single colony was picked and processed by mini-preparation and restriction endonuclease digestion to confirm presence of the transformed HAS2 expression plasmid as overleaf.

2.10 Plasmid DNA Extraction by Alkaline Lysis

A single colony was picked from an agar plate showing growth of appropriate density and used to inoculate 5 ml of LB broth + 50 μg/ml ampicillin and incubated at 37˚C overnight in an orbital shaker. An aliquot of 4 ml was then screened, as outlined below, for the presence of plasmid vectors containing HAS2 promoter sequence (see Monslow et al., 2004).

1. The bacterial cells in each 4 ml aliquot of broth culture were pelleted by sequential addition to, and centrifugation in, a sterile 1.5 ml Eppendorf tube. After each spin, the supernatant was decanted and the final pellet was taken up in 100 μl of a resuspension solution comprising 50 mM glucose, 10 mM EDTA and 25 mM Tris-HCl, pH 8.0.
2. Samples were vortexed briefly and left to stand at room temperature for 5 min.
3. A total of 200 μl of a freshly-prepared lysis solution of 0.2 M NaOH in 1% SDS was added and placed on ice for 5 min.
4. A freshly-prepared aliquot of 150 μl of a neutralizing solution of 3 M potassium / 5 M acetate was added, the mixture was then vortexed for 10 s, placed on ice for a further 5 min and then centrifuged at 13, 000 rpm for 5 min.
5. Supernatants were decanted to sterile 1.5 ml Eppendorf tubes, and an equal volume of approximately 400 μl of phenol/chloroform was added (bottom layer) and vigorous brief vortexing was carried out, followed by centrifugation at 13, 000 rpm for 2 min.
6. Supernatants were decanted to sterile 1.5 ml Eppendorf tubes, and 2 volumes (approximately 800 μl) of ice-cold ethanol.

7. Brief, vigorous vortexing was followed by 5 min centrifugation at 13,000 rpm, after which supernatants were decanted.

8. Pellets were washed by the addition of 1 ml of ice-cold 70% ethanol followed by brief vigorous vortexing until the white pellet was detached from bottom of tube, after which centrifugation was carried out at 13,000 rpm for 5 min.

9. Supernatants were decanted and pellets were allowed to air dry.

10. A volume of 30 µl of H_2O + 0.5 U/ µl of RNase A (Qiagen, Crawley, West Sussex, UK) was added to each pellet, brief vigorous vortexing was carried out and extracts were left to stand at room temperature for 30 min prior to commencing restriction endonuclease digestion.

11. Digestion with restriction endonucleases (NEB UK Ltd, Hitchin, Hertfordshire, UK) of e.g. HAS2 (insert) was set up as shown below:

Not I	0.3 µl
*Kpn*I	0.3 µl
Multi-copre TM 10xbuffer	1.0 µl
BSA	1.0 µl
Water	7.4 µl
	10.0 µl

and incubated at 37˚C for 2 h.

12. Following incubation, 3 µl of loading buffer was added to each sample. Samples were then applied to a 2% agarose gel prepared in TAE buffer containing 0.5 µg/ml of ethidium bromide, separated by electrophoresis at 75 V for 90 min and visualised using ultra-violet light. The HiSpeed Plasmid Midi Kit (Qiagen) was used to prepare larger quantities of vectors from larger volumes of positive cultures according to the manufacturer's instructions. Prepared plasmids were sequenced to ensure fidelity of amplification and ligation, used in downstream analyses and glycerol stocks of cultures were stored in addition to purified

plasmid preparations. As described above. Following this, an aliquot of one positive culture was used to inoculate a starter culture for midi-preparation of a larger-scale column-based plasmid purification using kit reagents according to the manufacturer's instructions (Promega).

2.11 Forced HAS2 expression in lung fibroblasts

Lung fibroblasts were transfected with the pCR-3.1 expression vector containing the HAS2 open reading frame using Lipofectamine LTX Reagent (Invitrogen).

For each sample, the transfection complex for each well was prepared as follows:

1. A mixture of 1 μg of the HAS2 vector insert was diluted in 200 μl Opti-MEM I Reduced Serum Medium (Invitrogen) without serum and mixed thoroughly.
2. A mixture of 1 μg of the empty vector was diluted in 200 μl Opti-MEM I Reduced Serum Medium (Invitrogen) without serum and mixed thoroughly.
3. A volume of 1.0 μl of PLUS Reagent (Invitrogen) was added directly to the diluted DNA, mixed gently and incubated at room temperature for 5 min.
4. An aliquot of 2.5 μl of Lipofectamine LTX Reagent (Invitrogen) was then added to the diluted DNA, mixed thoroughly and incubated at room temperature for 30 min, after which time the transfection complexes were ready.
5. A total of 200 μl of the DNA-Lipofectamine complexes was added to each well containing cells, mixing was carried out by gentle rocking of the plate.
6. Cells were incubated at 37˚C in a CO_2 incubator for 24 h. A time course of transfection of 24 h, 48 h, 72 h and 96 h was carried out to optimize HAS2 expression, with RNA extraction carried out using TRI-Reagent as described above. Transfection with empty pCR-3.1 vector was carried out as a negative control.

2.12 Transfection of HK-2 Cells with HAS2 and HAS2-AS1 specific siRNAs

1. HK-2 cells were cultured to approximately 30-50% confluence.
2. Cells were washed with PBS and then growth arrested for 3-4 h prior to transfection.
3. Similarly to the experiments described above for the transfection of the HAS2 vector, transfection complexes for the transfection of siRNAs were prepared using a working concentration of 30 nM in Opti-MEM I Reduced Serum Medium, and Lipofectamine 2000 (Invitrogen) was used as the transfection reagent according to the manufacturer's instructions.

2.13 siRNA reagents

siRNA reagent for specific gene knockdown experiments were purchased from Applied Biosystems. The qRT-PCR reaction was carried out using standard protocols as recommended for the Taqman assay reagents.

Gene	siRNA Catalogue Number
HAS2	117326
HAS2-AS1	4426961

2.14 Effect of glucose concentration on HAS2 and HAS2-AS1 gene expression in HK-2 cells

PTCs were grown to confluence and stimulated under serum-free conditions with normoglycemic (5 mM), high (25 mM) D-glucose concentration and an osmotic control of 5 mM D-glucose + 20 mM D-Mannitol for 0, 24, 48, 72 and 96 h time course . At each time point, cells were harvested by homgenisation in TRI-reagent. At the end of the experiment, RNA extraction was carried out prior to quantitative reverse transcription PCR (qRT-PCR) for HAS2 mRNA and HAS2-AS1 RNA expression as described previously. (Section 2.7).

2.15 HAS2-AS1 Overexpression

HK2 cells were grown to sub confluency in 24 well plates, and were growth arrested in serum free medium for over 4h prior to transfection.

To study the biological activity of HAS2-AS1 three plasmid preparation were transfected into HK2-cells.

1. Full length HAS2-AS1 in pcDNA3.1 purchased from Epoch Biolabs, INC. Missouri City Texas, USA.
2. L HAS2-AS1 exon 2 in pc DNA3.1 as described by Chao and Spicer [195] (prepared earlier in our laboratory by Dr D. Michael).
3. Empty vector PCR 3.1.

Transfection was carried out in triplicate and the incubation continued for both 24 hours and 48 hours time points post transfection.

1. RNA was collected in Tri reagent (Sigma) as per manufacturer's instructions, RNA was purified and quantified, RT was carried out on 1μg of the total RNA extracted from each sample and qRT-PCR was the carried out on the resultant cDNA to determine HAS2 expression.

   The transfection mixtures were prepared in advance to reduce any bias in transfection condition.

2. Lipofectamine LTX (Invitrogen) was used to transfect the cells as per manufacturers instructions in 500 μl/well in medium containing 10% serum.
3. 100 μl Optimem was used per well (x3 so 300 μl) of Optimem was prepared for each transfection.
4. 500 ng DNA was added per well (x3 so 1.5 μg) DNA (4.8 μl empty vector), (9.15 μl HASAS) or 9.3 μl L-HAS2AS).
5. 0.5 μl PLUS /well was added (x3 so 1.5 μl) and the samples were then mixed and incubated for 10-15 min at RT.
6. 2.5 μl LTX was then added per well (x3 so 7.5 μl), and the samples incubated for a further 30 min at RT. 100 μl was then added to each well containing 500 μl of medium with 10% serum.

2.16 HA synthesis inhibition by 4-methyl-umbelliferone (4-MU) blocks the stimulated effect of HAS2

1. HK2 cells were seeded into a 24 well plate and grown until the cells were 80% confluent.
2. Six groups of quadruplicate wells were treated as follows: empty vector (pcdna4, 500 ng /well), over-expressing HAS2 vector, empty vector plus 4-MU treatment, over-expressing HAS2 vector plus 4-MU, empty vector plus IL-1β (1 ng/ml) and empty vector plus both IL-1β and 4-MU.
3. HA synthesis inhibitor 4-MU was prepared by preparing a stock of 1 M in DMSO, diluting this to 1 mM in medium immediately before use, and then adding this at 50:50 to the medium in the well to give a final concentration of 0.5 mM on the cells. IL-1β was used at a final concentration on 1 ng/ml.
4. Transfection was carried out using Lipofectamine LTX.
5. Briefly, for each well, 0.5 µg vector was added to 100 µl Optimem and 0.5 ml "Plus reagent" added and incubated for 10 min at room temperature in a 1.5 ml tube.
6. Then 2.5 µl LTX was added for each well, and the incubation continued for a further 20 mins. 100 µl of this DNA Lipofectamine complex was added to each well of cells, together with 150 µl medium (+ or – IL-1β) and a further 250 µl of medium (+ or – 4-MU) was added to each well, giving a final volume of 0.5 ml.
7. The incubation was continued for 3 days, after which the medium was removed, the cells washed with PBS, and the RNA extracted as previously described for analysis by qRT-PCR.

2.17 Statistical Analysis

All experiments were performed at least in triplicate. Arithmetic mean, standard deviation and standard error were calculated and the data are represented as ± Standard Error of Mean (SEM). Comparisons were performed using an unpaired Student's t-test. The value of $P < 0.05$ was considered as statistically significant. Using the "two sample assuming unequal variances" within Microsoft excel (2003 edition).

Expression of HAS2 and HAS2-AS1 in renal proximal tubular epithelial cell line HK-2 and lung, dermal and oral mucosal fibroblasts in response to IL-1β and TGF-β1

3.1 Introduction:

3.1.1 HA synthesis, HAS2 and HAS2-AS1 expression

One principal research theme at the Institute of Nephrology is the identification of mechanisms by which PTC and fibroblasts drive renal fibrosis. Fibrosis is the common end-point of CKD, and increased deposition of HA has been demonstrated to correlate with the degree of interstitial fibrosis in progressive renal dysfunction associated with diseases such as IgA nephropathy [200] and diabetic nephropathy [114]. Of the three HAS isoforms,work carried out at the IoN to date has focused specifically on expression of the HAS2 gene and HAS2-driven HA synthesis, as this isoform has been shown to be a key phenotypic modulator of both PTC [37] and fibroblast [138] in both cases driving a pro-fibrotic effect.

Post-transcriptional down- regulation of both HAS2 mRNA synthesis and subsequent HAS2-driven HA synthesis by the natural antisense RNA HAS2-AS1 has recently been reported in osteosarcoma cells [195]. HAS2-AS1 is transcribed from the opposite genomic DNA strand at the HAS2 locus, and exon two of HAS2-AS1 is complementary to the first HAS2 exon (see figure 3.1).

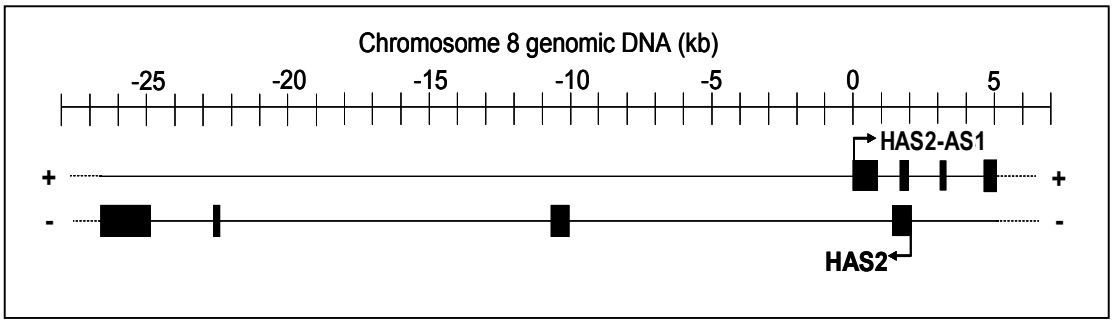

Figure 3.1 Genomic organisation of HAS2-AS1 and HAS2 at locus 8q24.12. The four exons of HAS2AS on the upper (+) strand of chromosome 8 at locus 8q24.12 are shown as filled boxes, with the transcription start site illustrated as an arrow. HAS2 on the lower (–) strand is depicted similarly, and the overlap of HAS2-AS1 exon 2 and HAS2 exon 1 is evident. Adapted from Michael et al. (2011) [191].

Previous work at the Institute on Nephrology has studied HAS2 regulation in depth. [37][138][188][189][192]. Most recently, coordinated expression of HAS2 and HAS2-AS1 expression in HK-2 cells, in response to IL-1β and TGF-β1, has been shown [191]. The relationship between HAS2 and HAS2-AS1 is, however, not fully defined, and it is possible that HAS2-AS1 may be a target through which HAS2 expression could be regulated. Further insight into factors regulating HAS2 expression and its relationship with its antisense RNA may therefore identify potential targets for future therapeutic intervention in the fibrotic process [201].

One of the diseases of interest at the IoN is diabetic nephropathy (DN). This chapter confirmed experiments showing coordinated HAS2 and HAS2-AS1 expression in response to addition of DN-associated stimuli cells from PTC line HK-2 [191], and then extended these observations to include other cell types.

3.1.2 Diabetic nephropathy

Diabetes mellitus is a condition characterised by the presence of elevated blood glucose levels. This may be caused by lack of insulin production (type I diabetes, ~5-10% patients with diabetes mellitus), or most often, inability to respond to insulin (type II diabetes). Over time, hyperglycaemia causes significant anomalies in the vasculature [202], which lead to micro- and macrovascular complications of diabetes: nephropathy, retinopathy, neuropathy, and atherosclerosis. Approximately one third of diabetic patients (both type I and II diabetes) suffer from kidney disease [203]. DN is therefore the most common single cause of ESRD, accounting for 20% of all patients requiring renal replacement therapy in the UK [204]. Furthermore, mortality is higher in diabetic patients in comparison with non-diabetic patients [204].

Clinically incipient nephropathy manifests initially as persistent microalbuminria (i.e. albumin excretion: 20-200 mg per day). Then, persistent proteinuria occurs (i.e. total protein excretion > 200 mg per day) and is an indication of overt DN. Following the onset of proteinuria, there is a progressive decline in kidney function, leading to ESRD. In approximately 50% of patients with overt nephropathy, progression is quick and kidney function is usually lost in less than five years [205].

3.1.3 Extracellular matrix expression in DN

The changes seen within the diabetic kidney are similar whether the underlying diagnosis is type I or II diabetes mellitus. The earliest histopathological change in DN is renal hypertrophy [206]. This may be explained by both mesangial and interstitial expansion. In the course of the disease, further damage in both the renal corpuscle and tubulointerstitium is observed. In addition to mesangial expansion, corpuscular changes include glomerular basement membrane thickening, glomerular sclerosis, and, at later stages of the disease, loss of podocytes [206]. In the tublointerstitium fibrosis develops. The tubular basement membrane thickens [207]. Tubules and peritubular capillaries are gradully replaced by extracellular matrix and interstitial cells. The latter include, apart from usual fibroblasts and resident macrophages, myofibroblasts and infiltrating immune cells [208]. As with all other couses of CKD the outcome correlates with interstitial fibrosis and the presence of myofibroblasts in renal biopses.

3.1.4 HA modulation of cell phenotype in DN

3.1.4.1 The renal proximal tubular epithelial cell (PTC), HA and diabetic nephropathy (DN)

In health, renal proximal tubular epithelial cells (PTCs) reabsorb the majority of filtered water and solutes, and contribute to tubular basement membrane formation via secretion of type IV collagen and laminin.

A number of *in vitro* studies carried out at the IoN have suggested that HA contributes to the pathogenesis of renal fibrosis via transition of PTC to a myofibroblastic phenotype, which is associated with increased HA synthesis [209].

3.1.4.2 Potential drivers of fibrosis in DN

Transforming growth factor-beta 1 (TGF-β1)

The cytokine and fibrotic mediator TGF-β1 has been implicated in progressive renal interstitial fibrosis [210][211][212]. Increased levels of TGF-β1 have been reported in a variety of diseases associated with renal fibrosis, including glomerulonephritis [213] and DN [214]. Moreover, the over expression of TGF-β1 has been shown to induce CKD [215], and inhibition of its action has been shown to prevent renal injury in animal models of glomerulonephritis [216] and also in a model of progression of interstitial fibrosis [217].

Interleukin-1 beta (IL-1β)

Inflammation may also play a part in the progression of fibrosis. Early stages of fibrosis are typically characterised by inflammation, and this leads to changes in renal interstitial matrix, tubular atrophy, cellular transformation and the accumulation of myofibroblasts [218,219, 220,221]. In many conditions the extent of renal fibrosis and the number of infiltrating inflammatory cells change in parallel, and these inflammatory cells are therefore thought to contribute to the loss of renal function and fibrosis. Support for this

comes from animal models of injury in which macrophages are depleted [222] and from animals lacking in genes encoding proteins involved in inflammatory cell recruitment [223][224]. Furthermore, even in conditions such as DN where the primary insult is considered to be metabolic, many studies have also implicated an inflammatory component in its pathogenesis [225][226][227].

Previous work at the IoN has shown that IL-1β increases HAS2 mRNA expression in HK-2 cells in an NF-κB-dependent manner [175]. IL-1β was also shown to increase the expression of CD44, the HA receptor and this was associated with internalization of HA, suggesting increase functional form of receptors facilitating this process [58]. IL-1β has numerous roles leading to the promotion of fibrosis, including promotion of leukocyte infiltration, inducing proinflammatory mediators and inducing production of TGF-β1, which is a key profibrotic growth factor [228][229].

Glucose and hyperglycaemia

In addition to pro-inflammatory and pro-fibrotic cytokines, disease-specific stimuli such as raised glucose concentration drive HA synthesis [230][231][232]. More specifically, increased HAS2 transcription, together with raised levels of HA synthesis, have been reported in PTC line HK-2 cells cultured *in vitro* in glucose concentration similar to those found in DN [175]. As previously demonstrated at the IoN, the combined effects of glucose and IL-1β may modulate the profibrotic potential of the PTCs in DN, by an increase in the TGF-β1 production [164]. It has been demonstrated that strict glycaemic

control is effective in prevention of development and progression of DN at early stages [233]. High glucose concentration may directly up-regulate the synthesis of TGF-β, a profibrotic cytokine, in mesangial cells and PTC, leading to increased production of extracellular matrix proteins [234]. There is evidence that in addition to increased synthesis of ECM components, glucose may also decrease degradation of matrix components which may also contribute to ECM accumulation in DN [235].

TGF-β1 may function in conjunction with hyperglycaemia, to mediate the changes seen within the tubulo-interstitium in DN. Phillips et al suggested that the role of hyperglycaemia may be to prime the kidney for an enhanced pro-fibrotic response to a second stimulus[164][199]. Addition of 25mM D-glucose to PTC in culture caused an increase in TGF-β1 mRNA. This increase was only seen following the application of a second stimulus (IL-1β) [164].

Macrophage influx previously has been implicated in the pathogenesis of DN, both in animal models and in human diease [236][237]. This suggests that the generation of macrophage-derived cytokines such as IL-1β, in combination with the effect of elevated glucose concentrations, may act synergistically to influence the pathogenesis of DN. In IoN has shown that increased HA synthesis in response to either IL-1β or elevated 25 mM D-glucose is associated with NF-κB activated transcription of HAS2 [175].

3.1.4.3 Oral mucosal and dermal fibroblasts

In the kidney, fibroblasts are mainly distributed in both cortical and medullary interstitium. In cortical interstitium and outer medullary interstitium, fibroblasts synthesise ECM and are the major source of HA in the inner medulla; medullary HA correlates with hydration state [110].

Fibroblasts located in the cortical and outer interstitium are responsible for most of the excessive ECM deposition seen in fibrosis [238]. Under physiological conditions, only a few renal fibroblasts can be found in the interstitium. However, during renal fibrogenesis, their number increases dramatically and they take on an activated, alpha smooth-muscle (α-SMA) expressing myofibroblast phenotype.

Phenotypic conversion from fibroblast to myofibroblast is associated with major changes in the synthesis and metabolism of HA, in which the activated myofibroblast phenotype is charactersed by the accumulation of intracellular and extracellular HA, and the assembly of enlarged HA pericellular matrices [139]. Furthermore, inhibition of HA synthesis (Meran et al., 2007), or removal of the pericellular HA coat (Simpson et al., 2009), inhibited phenotypic activation of dermal fibroblasts [138][156].

Progressive renal fibrosis can be thought as uncontrolled, aberrant scarring of renal tissue. Previous work from this laboratory using dermal fibroblasts as a model of a scarring fibroblast phenotype has shown that TGF-β1 drives phenotypic differentiation of

these cells from fibroblast to myofibroblast [138]. Meran et al. have confirmed that the resistance of non-scarring model cells oral mucosal fibroblasts to TGF-β1 mediated myofibroblastic change is associated with the failure of induction of HAS2 [138].

Meran et al. (2007) demonstrated that IL-1β stimulation induced HAS2 mRNA expression in both dermal and oral mucosal fibroblasts, but neither cell type differentiated to a myofibroblast phenotype [138]. IL-1β promotes fibroblast proliferation and, fibroblasts derived from diseased kidneys demonstrate greater IL-1β responsiveness than those from normal kidneys [239][240].

As outlined above, much is now known about the up-regulation of HAS2 mRNA synthesis by numerous disease-associated stimuli. However, significantly less is known about the mechanisms regulating HAS2 expression, including the relationship between the synthesis of HAS2 mRNA and the expression of natural antisense HAS2-AS1. The work in this chapter began with confirmation of coordinated regulation of HAS2 and HAS2-AS in HK-2 cells following TGF-β1 and IL-1β treatment [191]. Regulation of expression was then also analysed in response to elevated D-glucose levels in these cells. In addition, the effects of TGF-β1 and IL-1β stimulation on sense and antisense expression in primary human lung, dermal and oral mucosal fibroblasts were also investigated.

Aims:

1) To compare and contrast the regulation of HAS2 and HAS2-AS1 expression in response to the cytokines IL-1β and TGF-β1, and to elevated glucose concentration in PTC.
2) Having established patterns of expression in PTC, to see how these results apply more widely across different fibroblast cell types.

3.2 Results

3.2.1 RNA quality control

Following RNA extraction the integrity of RNA was determined by flat-bed electrophoresis of 1µl of RNA extract through a 1 % agarose gel. The presence of two bands representing18S and 28S subunits of ribosomal (r)RNA indicated intact, high-quality RNA suitable for use in further experiments (Figure 3.2).

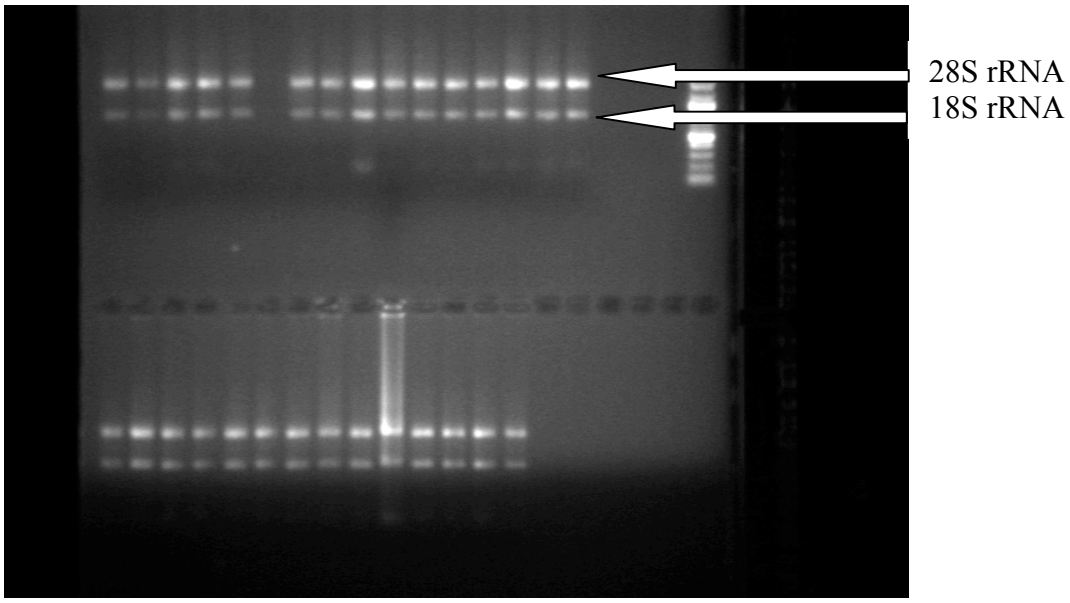

Figure 3.2: Flat-bed 1% Agarose gel electrophoresis of RNA extracts from HK-2 cells. The two discrete bands represent intact 28S and 18S rRNAs, showing that the samples contain undegraded total RNA suitable for use in further experiments.

3.2.2 qRT-PCR analysis of cDNA generated from RNA extracts

In figures 3.3 and 3.4, amplification of the endogenous control 18S rRNA was seen at comparatively low cycle number, due to its high abundance. HAS2 transcripts were not as abundant, and were therefore detected at higher cycle numbers.

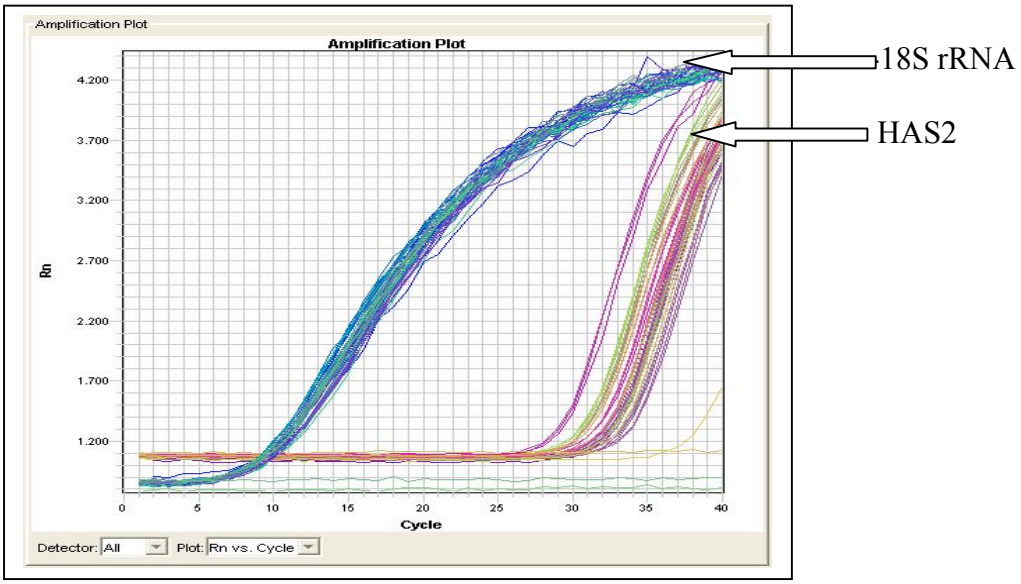

Figure 3.3 : Amplification plot of cycle number against normalised fluorescence, qRT-PCR reaction profiles from cDNA prepared from HK-2 cells, stimulated with IL-1β for 0 , 3, 12, and 24 h. Time course analyses were carried out in triplicate and each sample was assayed in triplicate. Amplification of endogenous control 18S rRNA reaction was evident between cycle numbers 10 and 15, with HAS2 amplification appearing after 27-33 cycles. A typical amplification curve starts with background fluorescence, followed by the exponential amplification phase, a linear phase, and final plateau. The threshold point at which a reaction reaches a predetermined fluorescent intensity above background is set early in the exponential phase of amplification. The PCR cycle at which the sample reaches the threshold is known as the threshold cycle (C_T).

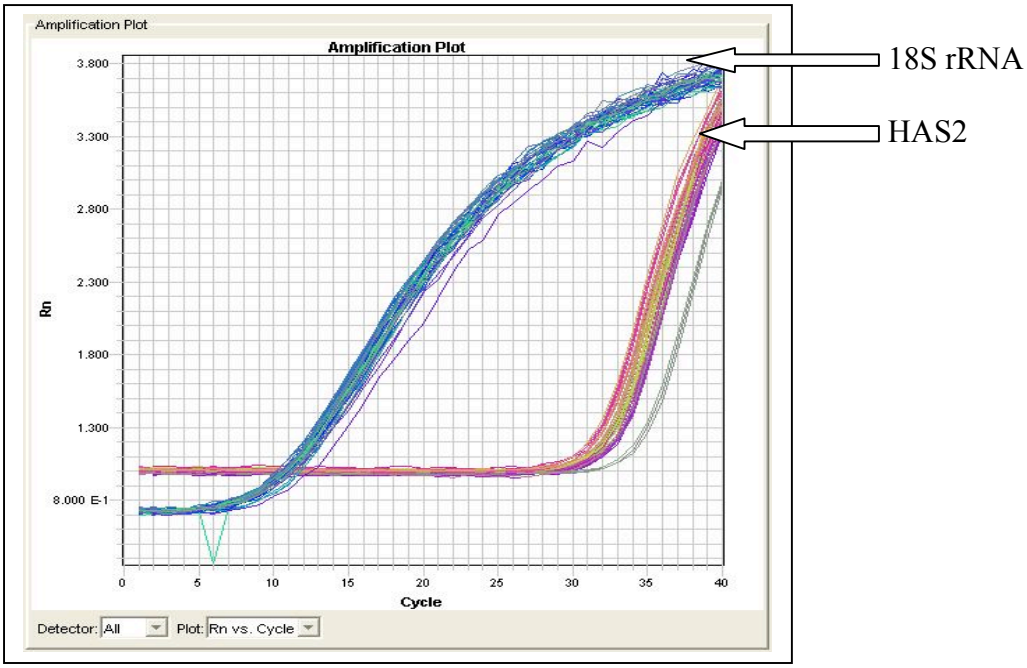

Figure 3.4: Amplification plot of cycle number against normalised fluorescence, the qRT-PCR reaction profiles from cDNA prepared from HK-2 cells, stimulated by TGF-β1 for 0, 3, 12, 24 h. Time course analyses were carried out in triplicate and each sample was run in triplicate.

3.3 Regulation of HAS2 and HAS2-AS1 in PTCs

3.3.1 Effect of IL-1β on HAS2 and HAS2-AS1 gene expression in HK-2 cells

To examine the effect of IL-1β on HAS2 and HAS2-AS1 transcription in growth arrested (serum deprived for 48 hours) HK-2 cells, 1 ng/ml of IL-1β was added to HK-2 cultures for 0, 3, 6, 9, 12, 24 and 48 h. At each time point, cells were harvested by homogenisation in TRI-reagent. At the end of the experiment, RNA extraction was carried out prior to qRT-PCR analysis for HAS2 mRNA and HAS2-AS1 RNA expression as described previously (section 2.7).

As shown in Figure 3.5.A, following stimulation by IL-1β there was a rapid induction in HAS2 mRNA expression which peaked at 3 h. Subsequent HAS2 expression levels declined, although these remained greater than those detected in the corresponding un-stimulated controls for the duration of the experiment. With the exception of the 12 h time-point, the difference between HAS2 transcription in IL-1β-treated and untreated cells was statistically significant.

A)

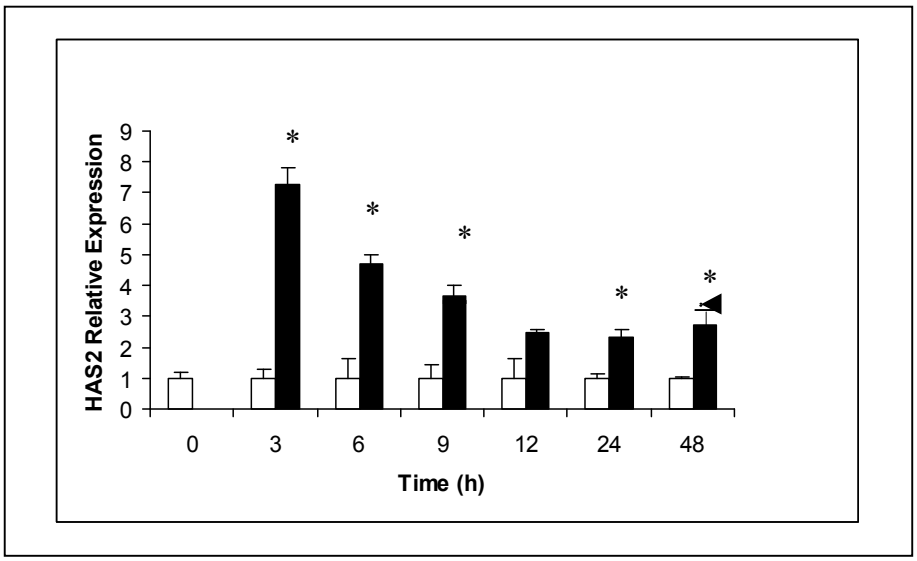

B)

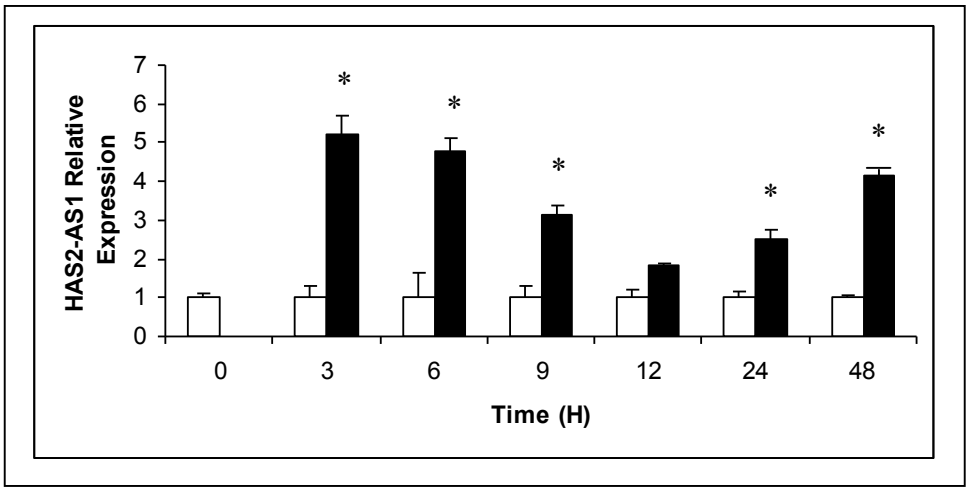

Figure 3.5. Transcriptional induction of A) HAS2 mRNA and B) HAS2-AS1 RNA in response to IL-1β-(1ng/ml) in HK-2 cells. Empty bars represent unstimulated PTC, filled bars represent IL-1β- treated cells. Collated data are shown from two reproducible experiments, each carried out in triplicate, and error bars show standard error of the mean (n = 6). Statistical analysis was performed by the Student's *t* test: *, $P < 0.05$.

Similarly, addition of 1 ng/ml of IL-1β stimulated a pattern of HAS2-AS1 transcriptional induction that exactly mirrored that of HAS2 expression (Figure 3.5.B). The maximal induction of HAS2-AS1 expression was also seen after 3h of IL-1β treatment, and stimulated cells showed a statistically significant increase in HAS2-AS1 transcription, with the exception of the 12 h time point.

The data from Figures 3.5.A and 3.5.B therefore demonstrated that IL-1β induction of HAS2 and HAS2-AS1 transcription in HK-2 cells was coordinated.

3.3.2 Effect of TGF-β1 stimulation on HAS2 and HAS2-AS1 gene expression in HK-2 cells

To examine the effect of TGF-β1 on HAS2 and HAS2-AS1 transcription in growth – arrested HK-2 cells, 10 ng/ml of TGF-β1 was added to HK-2 cultures for 3, 6, 9, 12, 24 and 48 h. At each time point, cells were harvested by homogenisation in TRI-reagent. At the end of the experiment, RNA extraction was carried out prior to quantitative reverse transcription PCR (qRT-PCR) for HAS2 mRNA and HAS2-AS1 RNA expression as described previously (Section 2.7).

As shown in figure 3.6.A, HAS2 expression increased over the time course of TGF-β1 stimulation, reaching a maximal level at 48 h. However, the difference in HAS2 expression between TGF-β1-treated and untreated cells was only statistically significant at the 24 h and 48 h time points. Similarly, Figure 3.6.B shows that a similar profile of HAS2-AS1 transcriptional up-regulation was seen, in response to TGF-β1 treatment, reaching statistical significance at the 24 h and 48 h time-points.

The data from Figure 3.6 demonstrated that both HAS2 mRNA and HAS2-AS1 RNA transcription were up-regulated in a coordinated fashion in response to TGF-β1.

These data show essentially the same results as those reported by Michael et al 2011 [191] with an increase in the expression of HAS2 and HAS2-AS1. Michael et al.

however, showed a significant increase at an earlier time point than reported here. This discrepancy may be due to the relatively large error bars for the 3, 6, 9 and 12 h time points, resulting from biological variation or experimental error. A larger number of experimental samples may have shown less variation and statistical significance at earlier time points.

The above data for coordinated expression of HAS2 and HAS2-AS1 in response to TGF-β1 and IL-1β confirmed the findings published previously from the IoN [191].

A)

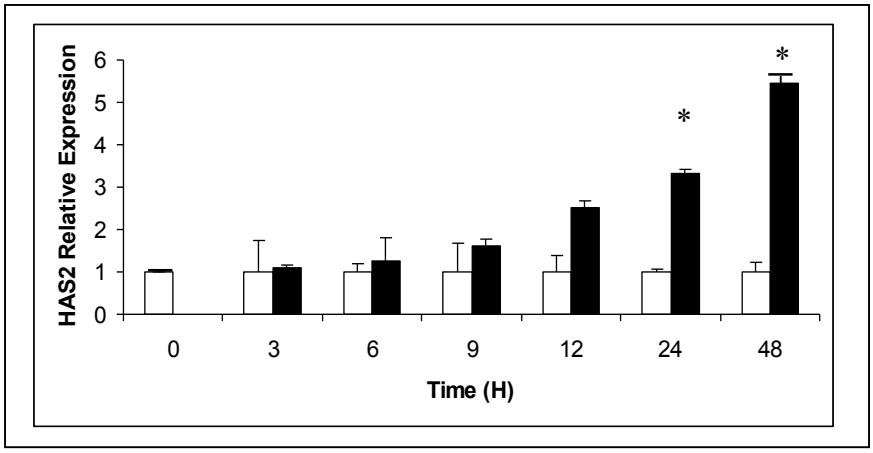

B)

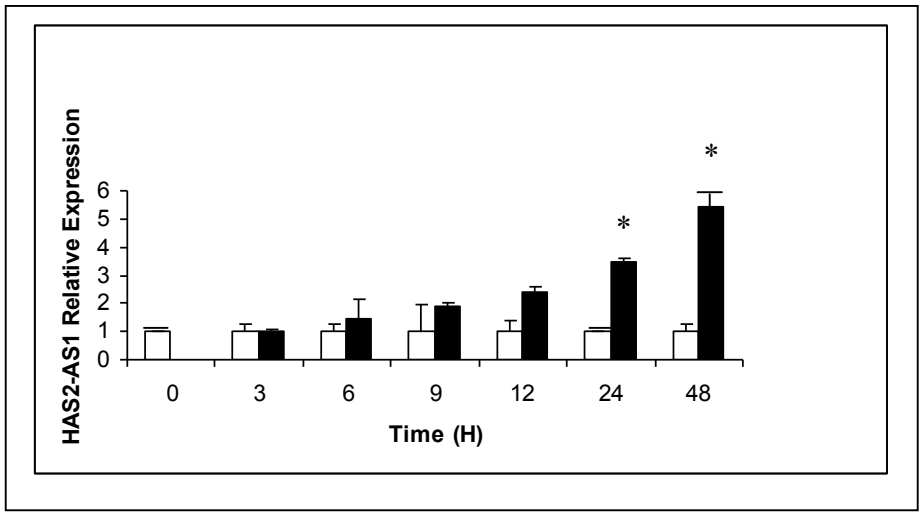

Figure 3.6 Transcriptional induction of A) HAS2 mRNA and B) HAS2-AS1 RNA in response to TGF-β1-(10ng/ml) in HK-2 cells. Empty bars represent unstimulated PTC, filled bars represent TGF-β1 treated cells. Collated data are shown from two reproducible experiments, each carried out in triplicate, and error bars show standard error of the mean (n = 6). Statistical analysis was performed by the Student's *t* test: *, $P < 0.05$.

3.3.3 Effect of glucose concentration on HAS2 and HAS2-AS1 gene expression in HK-2 cells

The effect of glucose concentration on HAS2 and HAS2-AS1 expression was investigated using normal (5 mM) and high (25mM) D-glucose concentration, and an osmotic control of 5 mM D-glucose + 20 mM D-Mannitol over a 96 h time course, as shown in Figure 3.7 below.

As seen in figure 3.7.A, HAS2 expression was up-regulated by 25 mM D-glucose after 48 h, 72 h and 96 h, and at the latter two time-points this up-regulation was statistically significant. Up-regulated HAS2 transcription was also seen in the osmotic control of 5 mM D-glucose + 20 mM D-mannitol at 96 h, but this was not statistically significant.

The effect of glucose concentration on HAS2-AS1 gene expression (Figure 3.7.B) followed a similar temporal profile to that for HAS2, and was statistically significant at the same time points.

A)

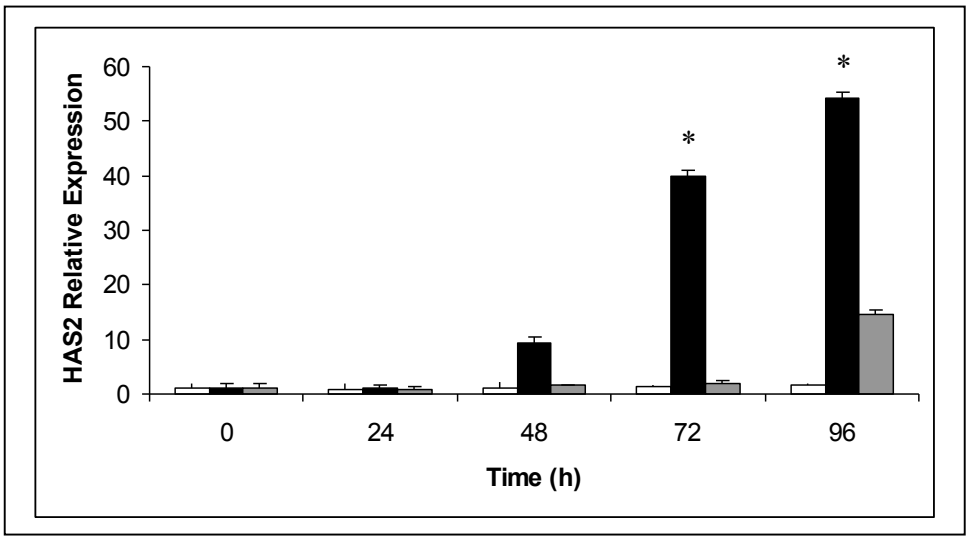

B)

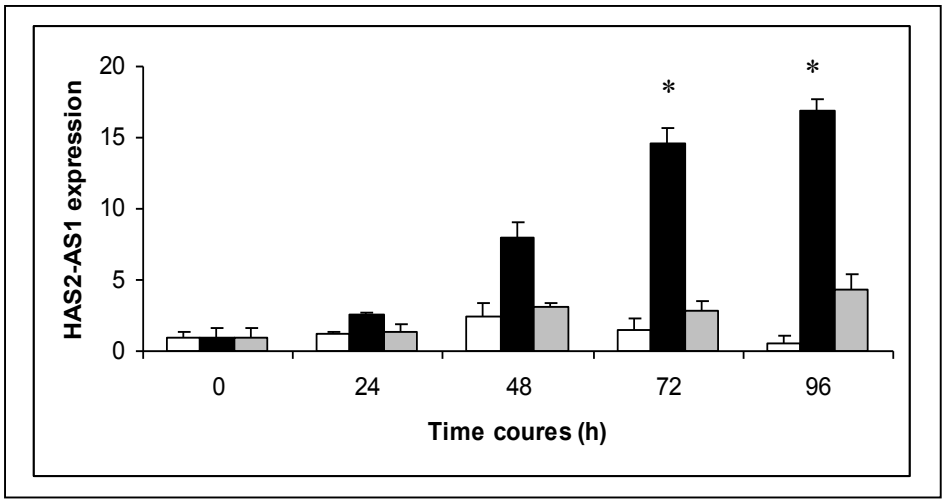

Figure 3.7 Transcriptional induction of A) HAS2 mRNA and B) HAS2-AS1 RNA in response to elevated glucose concentration in HK-2 cells. Empty bars represent the effect of 5 mM -D-glucose, black bars represent the effect of 25 mM D-glucose and grey bars represent the effect of 5 mM D-glucose + 20 mM D-mannitol. Data show one experiment, carried out in triplicate, and error bars show standard error of the mean (n = 3). Statistical analysis was performed by the Student's *t* test: *, $P < 0.05$.

3.4 Regulation of HAS2 and HAS2-AS1 in Fibroblasts

3.4.1 Effect of IL-1β stimulation on HAS2 and HAS2-AS1 gene expression in lung fibroblasts

Lung fibroblasts have been shown to differentiate into a myofibroblastic phenotype in a process involving peri-cellular HA coat formation [139]. Growth-arrested lung fibroblasts were treated with 1 ng/ml of IL-1β for 0, 3, 6, 9, 12, 24, 48 and 72 h. HAS2 and HAS2-AS1 transcription was then analysed by q-RT-PCR as described previously (section 2.7).

In response to IL-1β treatment (Figure 3.8.A) a statistically significant and discrete peak of HAS2 expression was seen after 12 h, but HAS2 expression in unstimulated cells was no different than the levels of stimulated HAS2 transcription at all other time points. Figure 3.8 B illustrates a similar temporal profile of HAS2-AS1 expression, with a distinct, statistically significant peak after 12 h.

A)

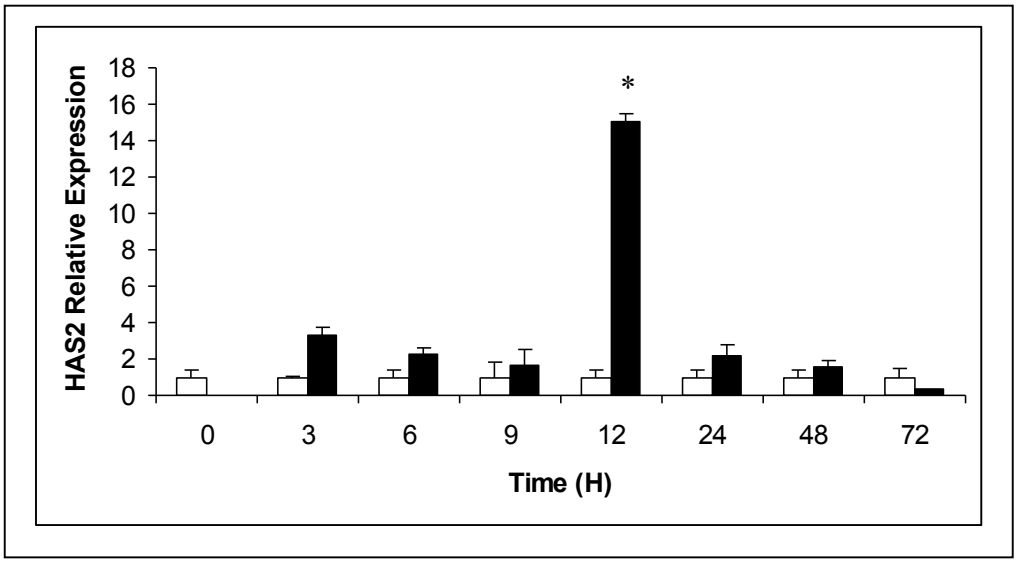

B)

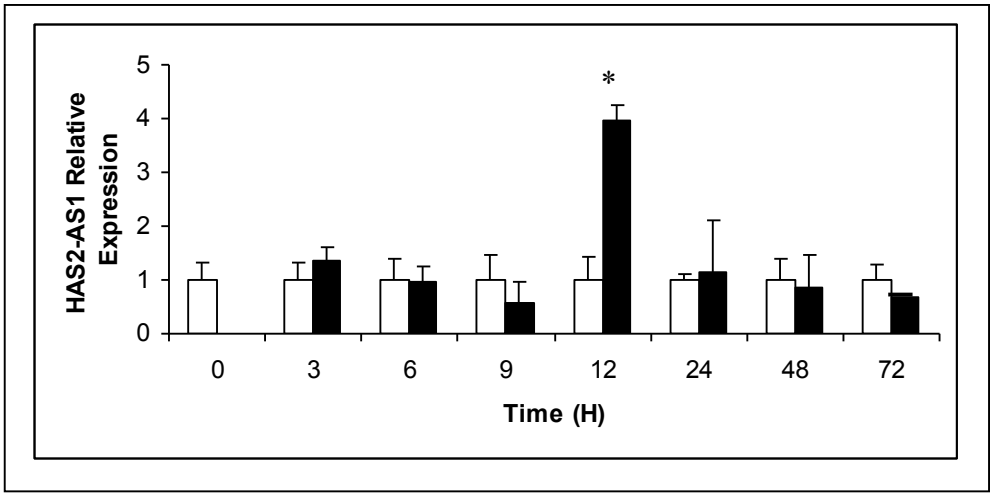

Figure 3.8 Transcriptional induction of A) HAS2 mRNA and B) HAS2-AS1 RNA by IL-1β (1ng/ml) treatment in lung fibroblasts. Empty bars represent unstimulated lung fibroblast cells, filled bars represent IL-1β treated cells. Collated data are shown from three reproducible experiments, each carried out in triplicate, and error bars show standard error of the mean (n = 9). Statistical analysis was performed by the Student's *t* test: *, $P < 0.05$.

3.4.2 Effect of TGF-β1 stimulation on HAS2 and HAS2-AS1 gene expression in lung fibroblasts

Growth-arrested lung fibroblasts cell were treated with 10 ng/ml of TGF-β1for 0, 24, 48 and 72 h. HAS2 and HAS2-AS1 transcription was then analysed by qRT-PCR (see section 2.7).

As seen in figure 3.9.A, in response to TGF-β1 treatment there was a statistically significant up-regulation in HAS2 gene expression only at the 48 h time point. Figure 3.9.B shows a similar temporal profile for HAS2-AS1 expression, with a discrete peak of expression after 48 h.

A)

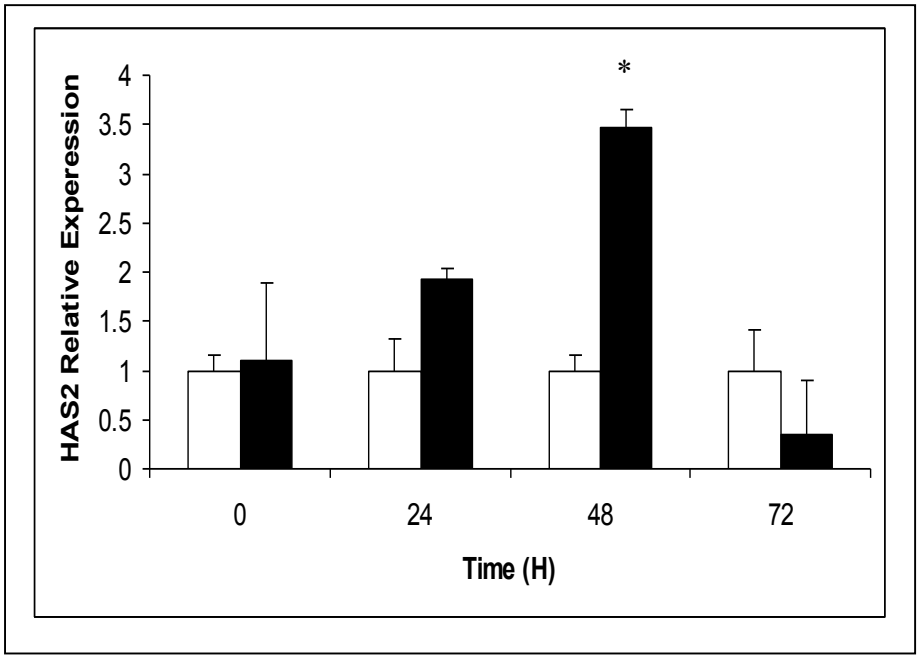

B)

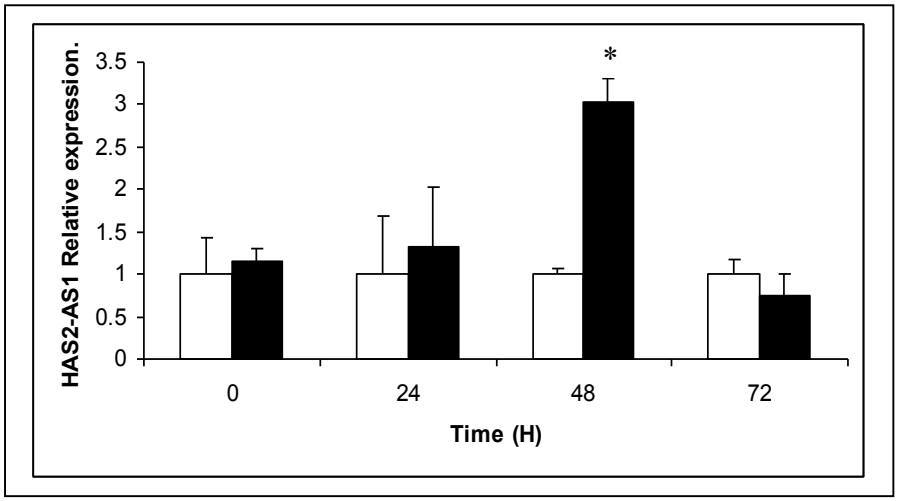

Figure 3.9 Transcriptional induction of A) HAS2 mRNA and B) HAS2-AS1 RNA by TGF-β1 (10 ng/ml) in lung fibroblasts. Empty bars represent unstimulated lung fibroblast cells, filled bars represent TGF-β1 treated cells. Collated data are shown from three reproducible experiments, each carried out in triplicate, and error bars show standard error of the mean (n = 9). Statistical analysis was performed by the Student's *t* test: *, $P < 0.05$.

3.4.3 Regulation of HAS2 / HAS2-AS1 gene expression in two models resistant to TGF-β1 stimulation of HAS2 expression

Simpson et al. (2009) demonstrated an age-dependent resistance to TGF-β1-mediated phenotypic activation of dermal fibroblasts, a functional change that may contribute to age related impaired wound healing. Age associated resistance to phenotypic activation is associated with decreased HAS2 expression and the failure of its induction by TGF-β1 [156]. In addition, Meran et al. (2007) have demonstrated that resistance of oral mucosal fibroblasts to TGF-β1 mediated myofibroblastic change is also associated with the failure of induction of HAS2 [138].

3.4.3.1 Aged model of TGF-β1 resistance

To investigate the effect of TGF-β1 on HAS2 and HAS2-AS1 transcription in dermal fibroblasts, cells were stimulated for 72 h. "Young" dermal fibroblasts were cells at passage 8; "Aged" dermal fibroblasts were cells at passage 15 as described previously [156].

A)

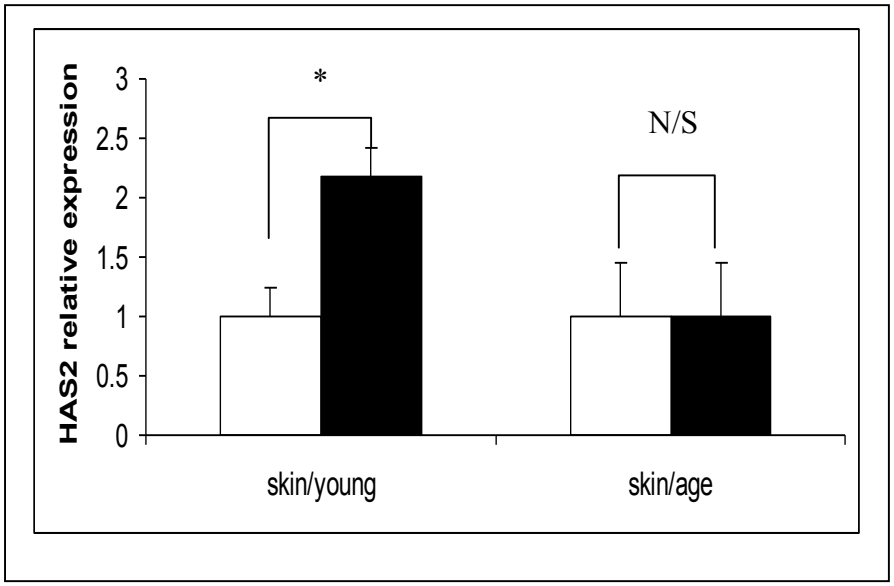

B)

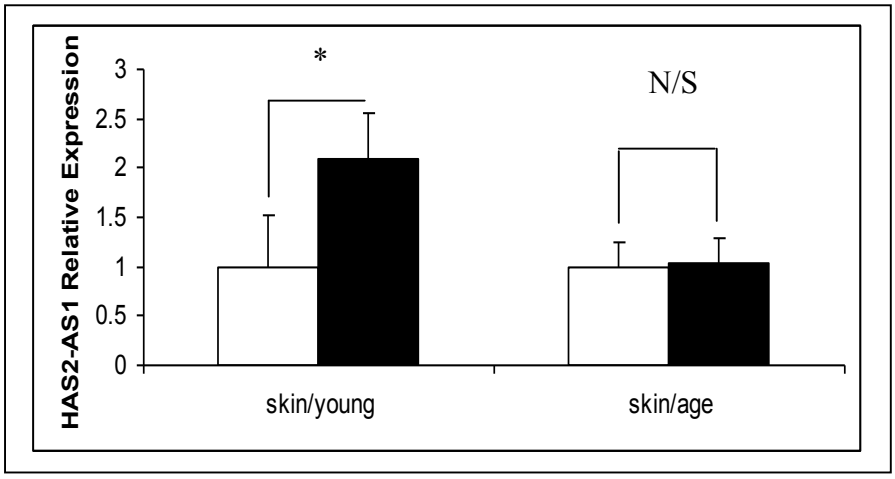

Figure 3.10 Transcriptional induction of A) HAS2 mRNA and B) HAS2-AS1 RNA by TGF-β1 (10 ng/ml) treatment in young and aged dermal fibroblasts. Empty bars represent unstimulated cells, filled bars represent TGF-β1treated cells. Data represent one experiment, carried out in triplicate, and error bars show standard error of the mean (n = 3). Statistical analysis was performed by the Student's *t* test:*, $P < 0.05$. N/S, not significant.

The data shown in figure 3.10 demonstrated that the addition of TGF-β1 to dermal fibroblasts leads to the coordinated transcription of HAS2 and HAS2-AS1 in young dermal fibroblast, a statistically significant change that was not seen in aged cell. In the aged cells, failure of induction of HAS2 following addition of TGF-β1 was also associated with a failure of induction of HAS2-AS1.

3.4.3.2 **Oral fibroblast model of TGF-β1 resistance**

Oral mucosal fibroblasts were growth arrested and then treated with 10 ng/ml of TGF-β1 for 72 h. Cells where used at passage 8.

The data displayed in Figure 3.11 showed that, following stimulation of oral mucosal fibroblasts with TGF-β1, both HAS2 and HAS2-AS1 expression was down-regulated, but that this reduction was not found to be statistically significant.

A)

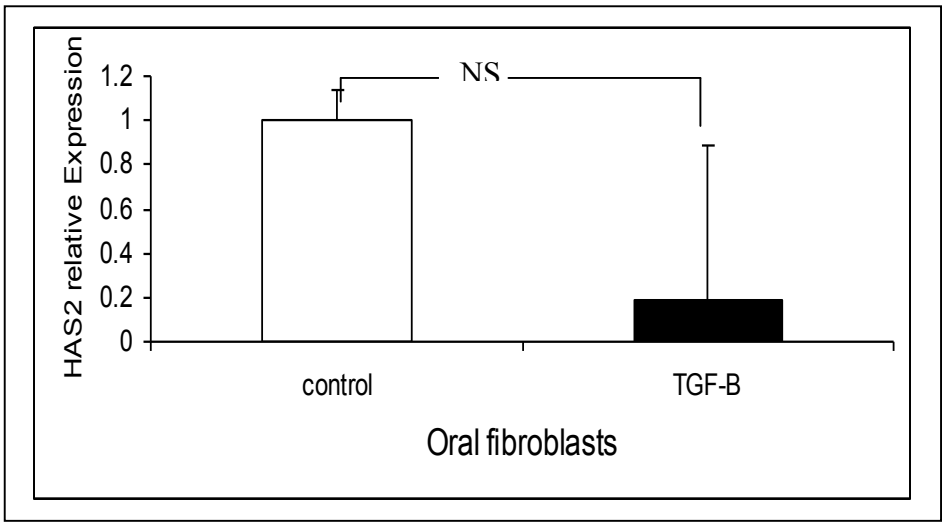

B)

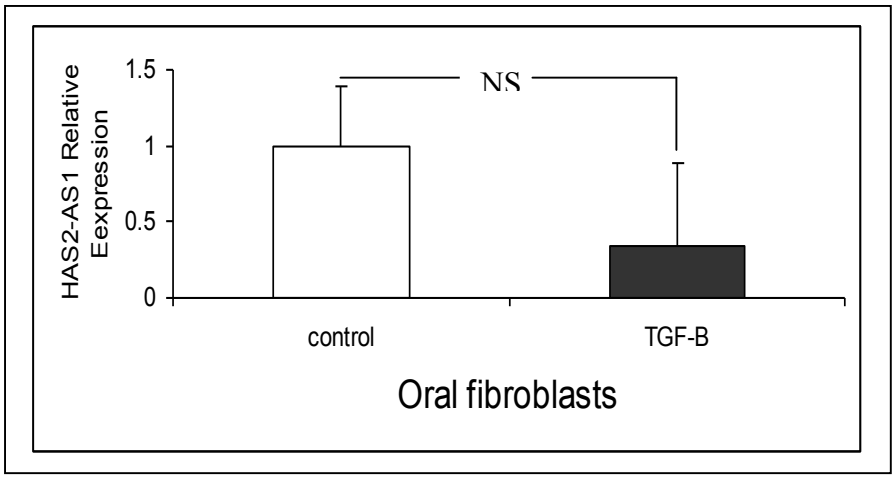

Figure 3.11 Transcriptional induction of A) HAS2 mRNA and B) HAS2-AS1 RNA by TGF-β1(10 ng/ml) in oral mucosal fibroblast cells. Empty bars represent unstimulated cells, filled bars represent TGF-β1 treated cells. Data represent one experiment, carried out in triplicate, and error bars show standard error of the mean (n = 3). Statistical analysis was performed by the Student's *t* test: N/S, not significant.

3.5 Discussion

The work described in this chapter is based on previous work carried out at the IoN showing that HAS2-driven changes in cell phenotype are important in the progression of fibrosis, and that there may be a relationship between disease-associated HAS2 transcriptional regulation and post-transcriptional HAS2 regulation by HAS2-AS1.

In PTCs, work from the IoN has shown that forced expression of HAS2 increased assembly of HA into pericellular coats, a phenotypic change that is associated with a migratory phenotype [37]. Migration of PTCs has been identified as one of the important steps of epithelial cell transdifferentiation [241], and is a key early stage in EMT. Furthermore, phenotypic alteration in renal epithelial cells may be driven by adenoviral expression of HAS2 [173]. This is consistent with previous data which examined the regulation of HA synthesis by renal PTCs *in vitro* [175] and demonstrated that increased HA synthesis was associated with the transcriptional activation of HAS2 by stimuli that are implicated in the pathogenesis of renal damage such as TGF-β1, elevated glucose concentration and the proinflammatory cytokine IL-1β. In the context of progressive renal disease, an increase in pericellular HA may therefore facilitate the fibrotic response and inducible HAS2 may contribute to renal injury.

Formation of pericellular HA coats are also associated with fibroblast to myofibroblast transformation [139]. Myofibroblasts mediate fibrosis and their numbers best predict the outcome in diverse models of renal injury [160][161][162][163][168]. Although the

primary interest of work at the IoN is in kidney fibrosis, due to the practical difficulties of culturing primary renal fibroblasts, *in vitro* models of TGF-β1 dependent lung and dermal fibroblast to myofibroblast activation are used. Using these models, previous data have shown the importance of HAS2-isoform-dependent effects on fibroblast phenotype.

In lung fibrosis, the accumulation of HA has been observed [242][243], and in other cases the up-regulation of HAS2 transcription has also been reported [183]. Furthermore, in lung fibroblasts, HAS2 mRNA synthesis and the HA peri-cellular coat formation are associated with the myofibroblastic phenotype [139]. The TGF-β1-driven activation of young dermal fibroblasts is associated with the induction of HAS2 transcription [156]. In contrast, *in vitro* studies show resistance to TGF-β1 mediated phenotypic differentiation and the induction of HAS2 mRNA in aged dermal [156] and oral mucosal fibroblasts [138].

Post- transcriptional regulation of HAS2 mRNA synthesis by the natural antisense RNA HAS2-AS1 has been reported [195]. Therefore, increasing our knowledge of the relationship between HAS2 and HAS2-AS1 will further our understanding of the function and mechanism of HAS2-AS1: HAS2 interaction.

In this chapter the coordinated transcriptional induction of both HAS2 and HAS2-AS1 transcripts in PTCs in response to the proinflammatory cytokine interleukin-1β, the fibrotic mediator transforming growth factor-β1, and elevated glucose concentration was

demonstrated. Furthermore, the data showed that coordinated expression of HAS2 and HAS2-AS1 was also seen in lung, dermal and oral fibroblasts.

In contrast, in aged dermal fibroblasts, no stimulation was seen following stimulation with TGF-β1 of either HAS2 or HAS2-AS1 transcription. In oral mucosal fibroblasts, following stimulation with TGF-β1, both HAS2 and HAS2-AS1 expression were down-regulated, but this effect was not statistically significant.

These results were not predicted on the basis of data described by Chao and Spicer in osteosarcoma cells in which forced expression of the complementary HAS2-AS1 exon 2 sequence down-regulated HAS2 transcription and HA synthesis [195]. In the range of cells used in the present study, induction of HAS2 sense and HAS2-AS1 antisense transcription occurred simultaneously in response to several stimuli. This so called "correlated" sense and antisense expression has been reported as one of a series of mechanisms by which natural antisense transcripts regulate their sense-strand counterparts via double-stranded RNA-dependent mechanisms [244][245]. Indeed, recent genomic data provide compelling evidence that gene expression at many loci is modulated by interaction between transcripts from the sense strand and complimentary transcripts from the opposite, anti-sense strand [244][246].

However, the phrase " natural anti-sense" RNA can be misleading since complementary, non-coding RNAs do not always accelerate degradation of their corresponding sense

strand messages, but may stabilize the coding strand transcript. The data presented here shows that HAS2-AS1 is widely co-expressed with HAS2 in a range of cells types.

The experimental data closely paralleled the recent observations of Faghihi and colleagues who have shown that β-secretase-1 (BACE1) mRNA expression is controlled by a regulatory non-coding RNA, BACE1-AS, that is partially complementary to BACE1 mRNA [247]. BACE-1AS increases BACE-1 stability leading to an increase in the BACE1 product and, by this mechanism, may drive Alzheimer`s disease-associated pathophysiology [247]. Similarly the data in this chapter suggest HAS2-AS1 RNA stabilizes HAS2 mRNA and leads to an increase in HAS2-driven HA synthesis, raising the possibilty that HAS2-AS1 expression may contribute to the phenotypic transition of cells thought to be important in the pathology of renal fibrosis.

An *in silico* study of the HAS2 proximal promoter region [248] and analyses of the sequences immediately upstream of HAS2-AS1 [191][248][249][250] have identified a similar range of putative upstream transcription factor-binding sits in both of these genes (see figure 3.12). This suggests that HAS2 and HAS2-AS1 may be controlled at least in part, by the same transcriptional "switches" to initiate the induction of transcription of both genes, and that the cytokine-stimulated up regulation of HAS2 and HAS2-AS1 transcription involves the simultaneous binding of transcription factors to both proximal promoters at the HAS2/ HAS2-AS1 locus.

The data in figure 3.9 show that no significant induction of HAS2 or HAS2-AS1 was observed in human lung fibroblasts following treatment with TGF-β1 for 72 h. By contrast, figure 3.10 shows significat TGF-β1-driven up-regulation of both transcripts after 72 h. These data highlight a potential tissue- specific fibroblast response to TGF-β1 that would be an interesting subject for further investigation, but that fell outside the scope of this project.

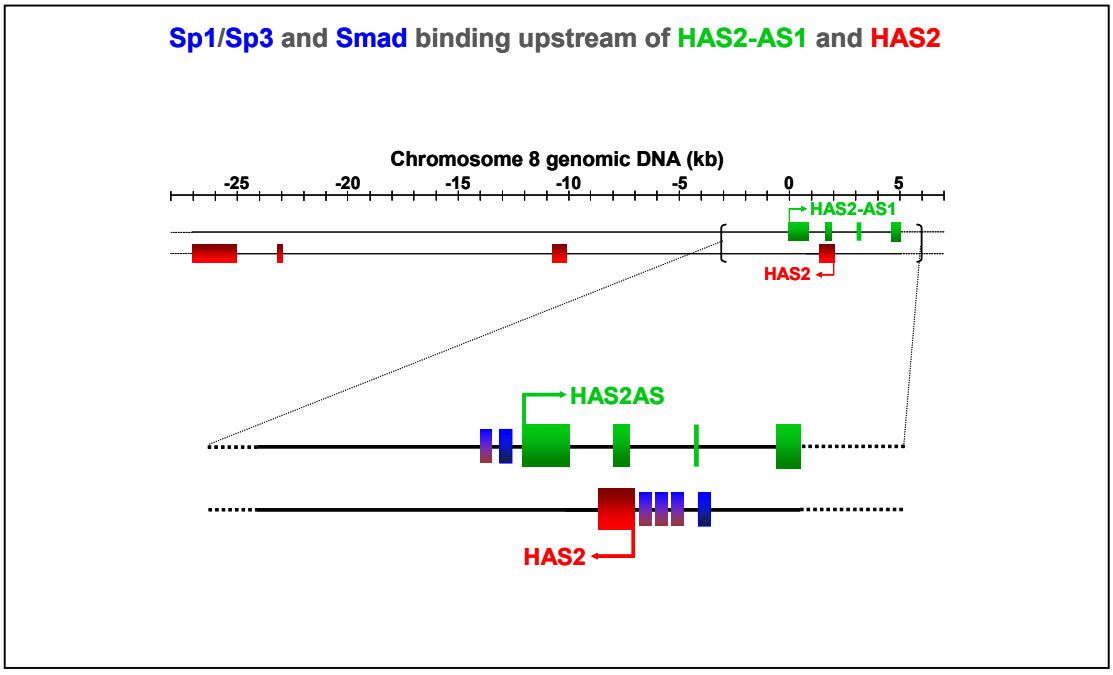

Figure 3.12 Sp1/Sp3 and Smad binding upstream of HAS2-AS1 and HAS2.
Genomic organization of HAS2-AS1 and HAS2 at locus 8q24.12 and locations of consensus transcription factor binding site motifs. Adapted from [189][190][191].

In this work, qRT-PCR was used because it is one of the most accurate methods for analyzing gene expression at the level of transcription. Prior to qRT-PCR, the most common method for determining expression levels were Northern blotting, RNase protection assays, or traditional (end-point) reverse transcription (RT) PCR. qRT-PCR was an improvement over the older methods such as Northern blotting, due to its ease of use and the much smaller amounts of RNA needed for the reaction and is run in real time. Whereas with other methods, the expression levels can only be observed after the completion of the entire reaction by running the end point of the reaction on an agarose gel.

While end-point RT-PCR can be useful to detect the presence or absence of a particular gene product at a predetermined cycle number, qRT-PCR has the advantage of measuring the starting copy number and detecting small difference in expression levels between samples during the amplification process. Therefore, using qRT-PCR, the entire amplification curve may be observed, and amplification and quantification occur simultaneously.

A typical PCR amplification plot has an exponential, linear, and plateau phase, where the amplification reaches a plateau as the reaction components are exhausted. Therefore, q RT-PCR quantifies the amplification products while the amplification reaction is in progress using a fluorescence detector in conjunction with the thermal cycler. In end-point RT-PCR, results are based on size discrimination, which may not be precise. Also,

since the precise reaction end point may vary between samples, gels may not be able to resolve variability in yield.

The need for accurate detection by qRT-PCR is particularly important for the work described in this thesis due to a lack of commercially-available HAS antibodies.

3.6 Conclusion:

In both HK-2 cells and fibroblasts, transcriptional induction of both HAS2 and HAS2-AS1 genes was coordinated in response to TGF-β1, IL-1β and elevated glucose concentration. Therefore, it is unlikely that the antisense transcript inhibits HAS2 induction, but that it has alternative functional significance for HAS2 expression.

Manipulation of HAS2 Expression in HK-2 cells and its effect on HAS2-AS1 expression

4.1 Introduction

In the previous chapter it was shown that the presence of a range of disease-associated stimuli led to coordinated expression profiles of HAS2 and HAS2-AS1 genes in a range of cell types. The aim of the work outlined in this chapter was to manipulate the expression of one gene to see the effect of this manipulation on the expression of the other gene, both under basal and stimulated conditions.

For the work described in this chapter, initial experiments were carried out in both lung fibroblasts and PTCs. Subsequently, it was decided to focus on the PTC. Through their role in matrix and cytokine generation, and acquisition of activated myofibroblastic phenotype via EMT, PTCs are thought to contribute to the initiation of renal fibrosis, and therefore represented a logical cell type in which to develop the experimental observations from chapter 3. Data are also presented on forced HAS2 expression in lung fibroblasts, in order to confirm the findings of the previous chapter regarding the general applicability of co-regulation of HAS2 and HAS2-AS1 expression.

4.1.1 Forced gene expression

Forced gene expression studies can be carried out using plasmid expression vectors containing the respective open-reading frame (ORF) insert to determine the effects of the expression of above average amounts of a target protein. This technique can be particularly useful when the target protein is present in small amounts under normal conditions, but may potentially be expressed in higher amounts in pathological situations.

4.1.2 Small interfering RNAs (siRNAs) knockdown of gene expression

Small interfering RNAs (siRNAs), sometimes known as short interfering RNAs or silencing RNAs, are recently-identified, naturally occurring 20-25 nucleotide long RNA molecules that modulate gene expression. The use of synthetic siRNAs for gene knockdown in mammalian cells has provided a wide range of experimental applications in biomedical research. In characterising the functional and phenotypic effects of HA in determining cell phenotype, previous work carried out in fibroblasts using siRNA has supported a role for HAS2 driving a pro-fibrotic phenotype [141][156].

The work outlined in this chapter was therefore designed to complement functional studies to further understand the relationship between HAS2 and its natural antisense HAS2-AS1.

Having previously demonstrated coordinated transcriptional regulation of HAS2 and HAS2-AS1, the series of experiments outlined in this chapter were designed to:

1- To use forced expression or siRNA knockdown of HAS2 mRNA to determine the effect of this manipulation of expression on the inducibility of HAS2-AS1 RNA in response to IL-1β or TGF-β1.
2- To use forced expression or siRNA knockdown of HAS2-AS1 RNA to determine the effect of this manipulation of expression on the inducibility of HAS2 mRNA in response to IL-1β or TGF-β1.

.

4.2. Results:

4.3 plasmid extraction

Figures 4.1 and figure 4.2 show plasmid extraction by mini-prep and Hi-speed plasmid midi kit methods.

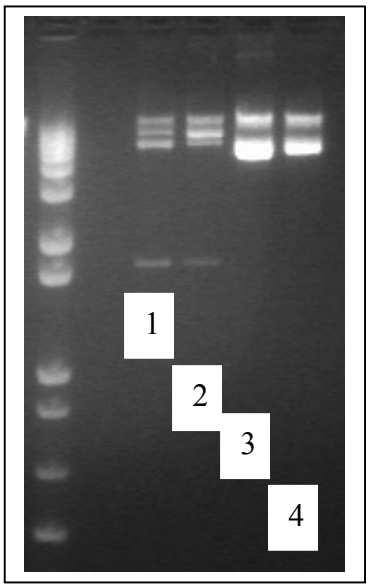

Figure 4.1 Mini-prep of pCR3.1 with the ORF insert HAS2, the purified plasmid was digested using Not I and Kpn I restriction endonucleases for 3 h, and digestion were loaded on to 1.5 % agarose gel. Lanes 1, 2 show PCR 3.1 and HAS2 (insert) at 1,650 base pairs, lanes 3-4 show empty vector pCR 3.1.

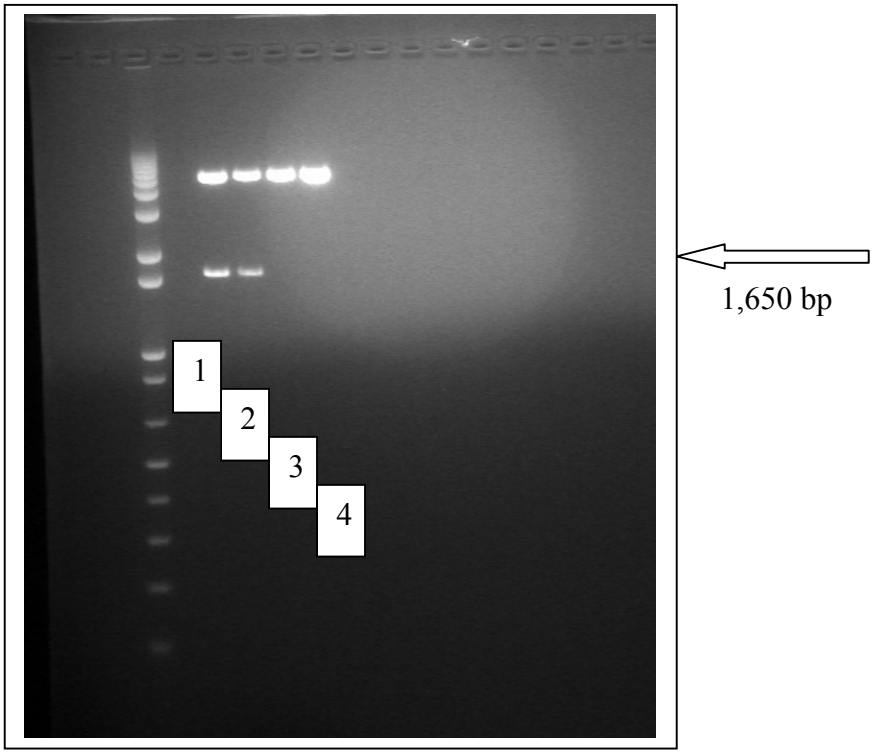

Figure 4.2 Agarose gel electrophoresis of pCR3.1 containing HAS2 using the Hi-speed plasmid Midi kit (QIAGEN). The purified plasmid was digested using Not I and Kpn I restriction endonucleases for 3 h and loaded on to 1.5 % agarose gel. Lanes 1 and 2 show pCR 3.1 and the HAS2 insert at 1,650 base pairs, lanes 3-4 show empty vector pCR 3.1.

4.4 Forced expression of HAS2 vector in lung fibroblasts

4.4.1 Confirmation of forced expression of HAS2 vector in lung fibroblasts

Lung fibroblasts were grown to approximately 70% confluence, growth arrested for 4 h and then transfected for 24 h with either the HAS2 expression vector or the empty vector as control (see 2.11). Transfection was carried out using Lipofectamine ^{TM} LTX Reagent (Invitrogen), the cells were incubated with vector and LTX for 24 h and the culture medium was renewed after 24 h. The following time points were examined in order to determine the optimum duration of HAS2 forced expression in subsequent experiments : 24, 48 , 72 , and 96 h. Cells were homogenized in TRI-Reagent, RNA was extracted and qRT-PCR was carried out for HAS2.

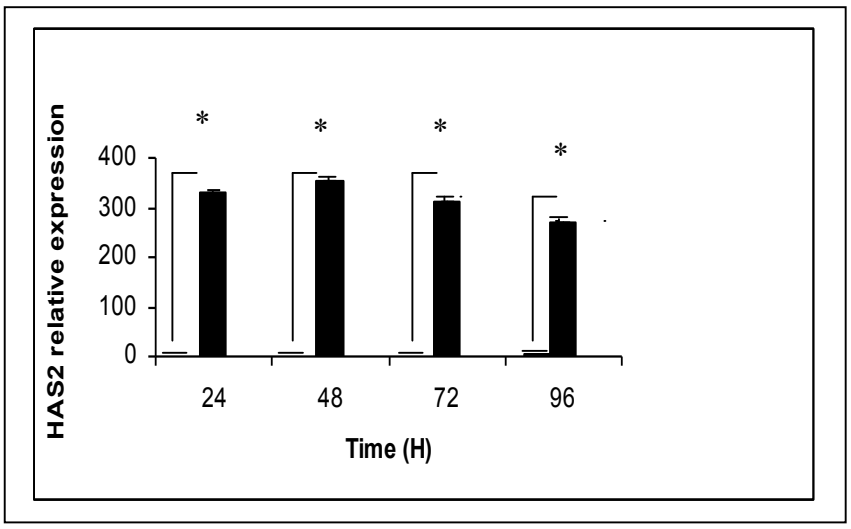

Figure 4.3 Time-course of forced expression of HAS2 in lung fibroblasts. Empty bars represent untransfected cells; filled bars represent cells transfected with HAS2 vector. Data are shown from one experiment, carried out in triplicate, and error bars show standard error of the mean (n = 3). Statistical analysis was performed by the Student's *t* test: *, $P < 0.05$.

The results demonstrated the optimal time-points for HAS2 forced expression were 24 h and 48 h. HAS2 expression was comparatively low in both untransfected cells and in cells transfected with empty vector.

4.4.2 Effect of HAS2 forced expression on HAS2-AS1 expression in lung fibroblasts

Lung fibroblasts were transfected for 24 h with either the HAS2 expression vector or the empty vector (see 2.11). Transfection was carried out using Lipofectamine ^{TM} LTX Reagent (Invitrogen). Following transfection, cells were incubated at 37ºC in a CO_2 incubator for 24 h and the culture medium was renewed after 24 h. In the following experiment, HAS2 and HAS2-AS1 expression were examined at 24 h and 48 h, cells were homogenized in TRI-Reagent, RNA was extracted and qRT-PCR was carried out for HAS2 and HAS2-AS1.

A)

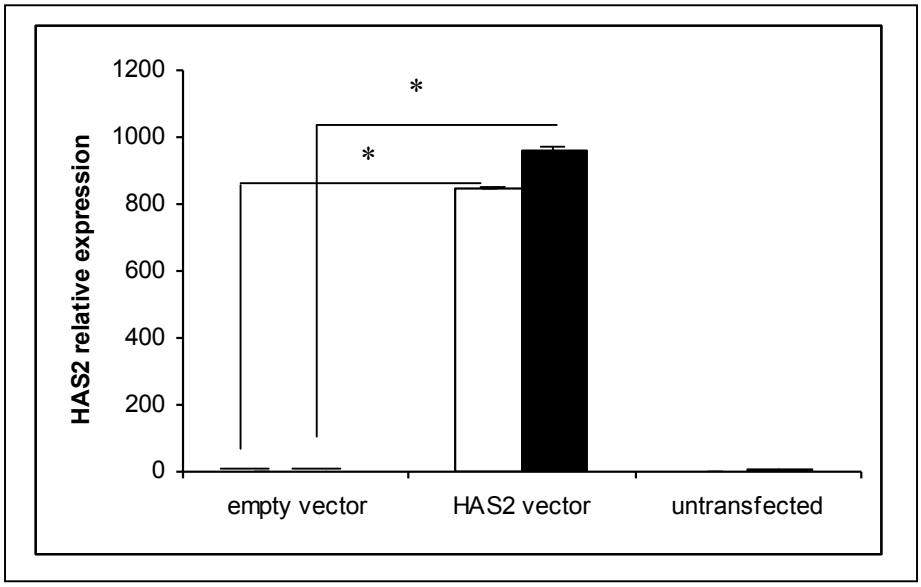

B)

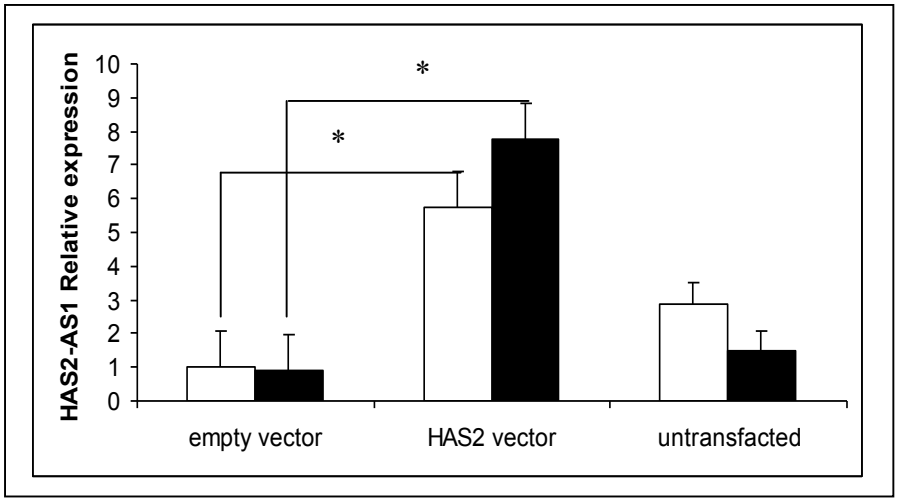

Figure 4.4 Forced expression of HAS2 in lung fibroblast cells at 24 and 48 h.
A) Relative expression of HAS2 mRNA. **B**) Relative expression of HAS2-AS1 mRNA. Empty bars represent the 24 h time-point and filled bars the 48 h time-point. Data show one experiment, carried out in triplicate, and error bars show standard error of the mean (n = 3). Statistical analysis was performed by the Student's *t* test: *, $P < 0.05$.

Statistically significant up-regulation of HAS2 was seen at both 24 h and 48 h following HAS2 vector transfection, with peak HAS2 expression at 48 h (Fig.4.4.A), while expression in untransfected cells and cells transfected with empty vector was comparatively low. At both time points, HAS2 forced expression resulted in statistically significant induction of HAS2-AS1 transcription. Peak HAS2-AS1 expression was seen at 48 h and once more expression in untransfected cells and cells transfected with empty vector was very low (figure 4.4.B). These data demonstrated that forced HAS2 expression in lung fibroblasts also lead to increased HAS2-AS1 expression.

4.5 HA synthesis inhibition by 4-MU stimulated effect of HAS2

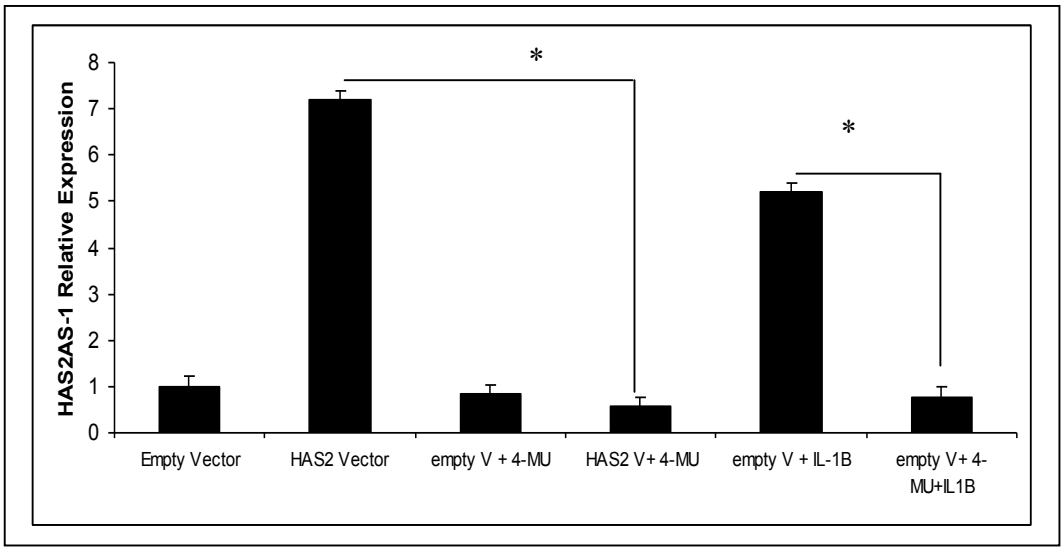

Figure 4.5 Transcriptional induction of HAS2-AS1 RNA in HK-2 cells. The data show two experiments, carried out in quadruplicate, and error bars show standard error of the mean (n=8). Statistical analysis was performed by the Student's t test:*, $P < 0.05$.

Data from figure 4.5 showed a significant decrease in HAS2-AS1 expression in HK-2 cell following forced HAS2 expression and treatment with 4-MU compared to cell transfected with HAS2 overexpression vector only. Similarly, cells transfected with empty vector, treated with 4-MU and stimulated with IL-1β showed a significant abrogation of IL-1β stimulated HAS2-AS1 induction compared to cells stimulated with IL-1β following transfection with empty vector.

4.6 siRNA knockdown of HAS2 expression in HK-2 cells

HK-2 cells were growth arrested at approximately 30-50% confluence and, where appropriate, stimulated with cytokine and/ or transfected with HAS2-specific siRNA (see section 2.12). At predetermined time points, cells were homogenised in TRI-Reagent followed, at the end of the experiment, by total RNA extraction and qRT-PCR to analyse the expression of HAS2 and HAS2-AS1.

4.6.1 Effect of siRNA knockdown of HAS2 on HAS2-AS1 expression following IL-1β stimulation of HK-2 cells

A)

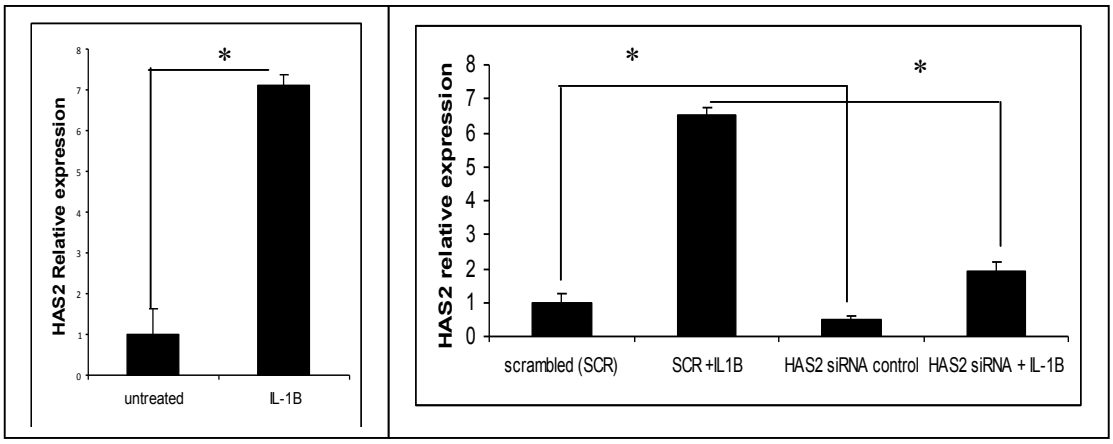

B)

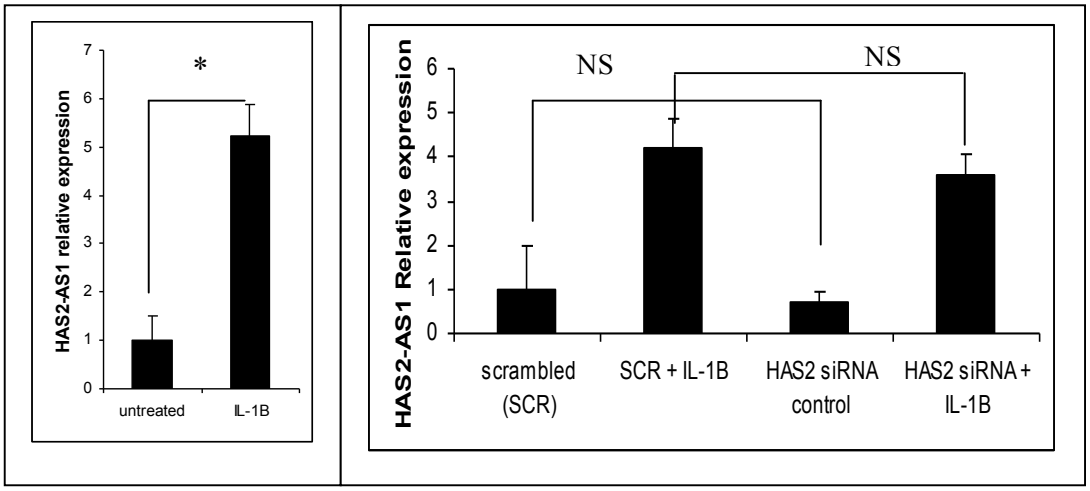

Figure 4.6: Relative expression of A) HAS2 mRNA and B) HAS2-AS1 RNA following HAS2 siRNA knockdown and / or IL-1β (1ng/ml) stimulation of HK-2 cells. Data are shown from one experiment, carried out in triplicate, and error bars show standard error of the mean (n = 3). Cells were transfected with either HAS2 siRNA or a scrambled oligonucleotide in the presence or absence of 1 ng/ml IL-1β for 3 h. Statistical analysis was performed by the Student's *t* test: *, $P < 0.05$.N/S, not significant. Control graphs (left) show the normal expression of untreated and IL-1β stimulated of HAS2 or HAS2-AS1 relative expression in absence of knockdown of the gene.

The data shown in Figure 4.6.A demonstrated that HK-2 cells transfected with HAS2 siRNA exhibited a significant attenuation in HAS2 expression when compared to cells transfected with scrambled control alone. Furthermore, cells transfected with HAS2 siRNA and stimulated with IL-1β for 3 h showed a significant abrogation of IL-1β stimulated HAS2 induction compared to cells stimulated with IL-1β following transfection with a scrambled control, demonstrating the efficacy of the HAS2-specific siRNA.

Data from figure 4.6.B showed that HK-2 cells transfected with HAS2 siRNA did not have significant lower HAS2-AS1 expression when compared to cells transfected with scrambled control alone. Similarly, cells transfected with HAS2 siRNA and stimulated with IL-1β showed no significant reduction in IL-1β stimulated HAS2-AS1 induction in comparison with cells stimulated with IL-1β following transfection with a scrambled control.

As described previously in chapter 3, the experimental data demonstrated coordinated up-regulation of both HAS2 and HAS2-AS1 in response to IL-1β. However, in this experiment, the failure of IL-1β to induce HAS2 transcription due to HAS2 siRNA did not significally abrogate HAS2-AS1 induction.

4.6.2 Effect of siRNA knockdown of HAS2 on HAS2-AS1 expression following TGF-β1 stimulation of HK-2 cells

A)

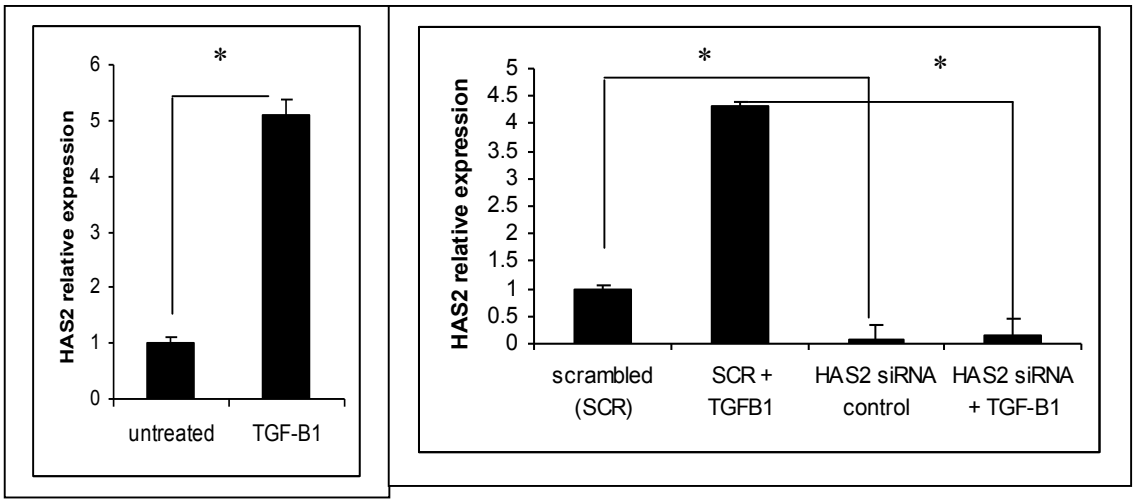

B)

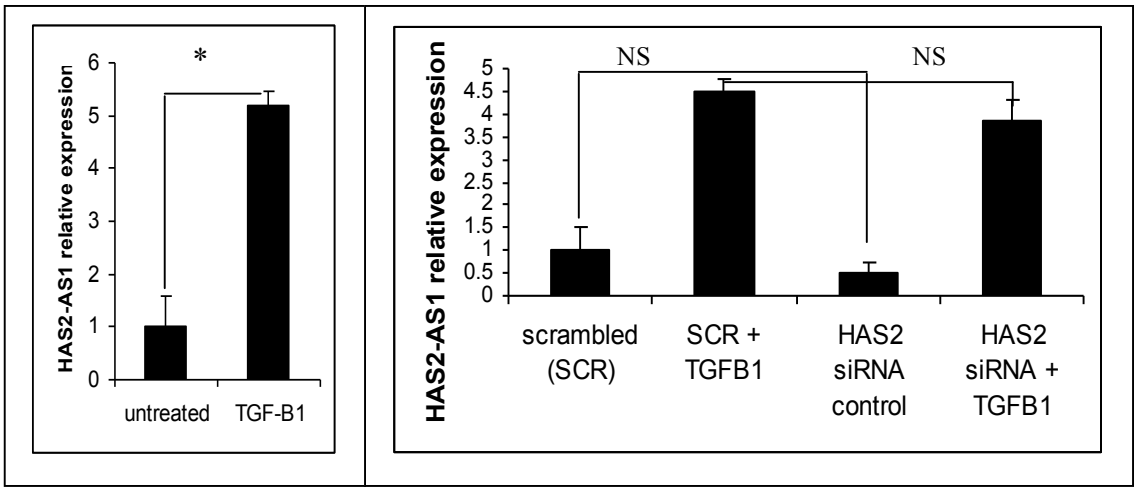

Figure 4.7. Relative expression of A) HAS2 mRNA and B) HAS2-AS1 RNA following HAS2 siRNA knockdown and / or TGF-β1 (10 ng/ml) stimulation of HK-2 cells. Data are shown from one experiment, carried out in triplicate, and error bars show standard error of the mean (n = 3). HK-2 cells were transfected with either HAS2 siRNA or a scrambled oligonucleotide in the presence or absence of 10 ng/ml TGFβ-1 for 48 h. Statistical analysis was performed by the Student's *t* test: *, $P < 0.05$. N/S, not significant. Control graphs (left) show the normal expression of untreated and TGFβ-1 stimulated of HAS2 or HAS2-AS1 relative expression in absence of knockdown of the gene.

The data shown in figure 4.7.A demonstrated that HK-2 cells transfected with HAS2 siRNA exhibited a significant attenuation in HAS2 expression when compared to cells transfected with scrambled control alone. In addition, cells transfected with HAS2 siRNA and stimulated with 10 ng/ml of TGF-β1 for 48 h showed a significant abrogation of TGF-β1-stimulated HAS2 induction compared to cells stimulated with TGF-β1 following transfection with a scrambled control.

Data from figure 4.7.B showed that HK-2 cells transfected with HAS2 siRNA did not show significantly decreased HAS2-AS1 expression when compared to cells transfected with scrambled control alone.Similarly, cells transfected with HAS2 siRNA and stimulated with TGF-β1 treatment at 10 ng/ml for 48 h showed no significant abrogation of TGF-β1-stimulated HAS2-AS1 induction in comparison with cells treated with TGF-β1 following transfection with a scrambled control.

As described previously in chapter 3, the experimental data demonstrated coordinated up-regulation of both HAS2 and HAS2-AS1 in response to TGF-β1. However, in this experiment, the failure of TGF-β1 to induce HAS2 transcription due to HAS2 siRNA did not significantly abrogate HAS2-AS1 induction.

4.7 siRNA knockdown of HAS2-AS1 expression in HK-2 cells

This work was carried out to investigate the relationship between HAS2 and HAS2-AS1, in order to determine whether regulation of HAS2-AS1 expression affects that of HAS2, and whether regulation of HAS2 expression affects HAS2-AS1 expression.

HK-2 cells were transfected with HAS2-AS1-specific siRNAs (see 2.12) using Lipofectamine ^{TM} 2000 (Invitrogen) transfection reagent. Following transfection, cells were incubated at 37ºC in a CO_2 incubator overnight. The following morning, the medium was replaced with serum-free medium and the cells were then left for a further 24 h prior to stimulation with IL-1β for 3 h, or TGF-β1 for 48 h.

At predetermined time points, the cells were lysed and total RNA was extracted. qRT-PCR was then carried out, as previously described, in order to analyse HAS2 and HAS-AS1 expression following siRNA treatment.

4.7.1 Effect of siRNA knockdown of HAS2-AS1 on HAS2 expression following IL-1β stimulation of HK-2 cells

A)

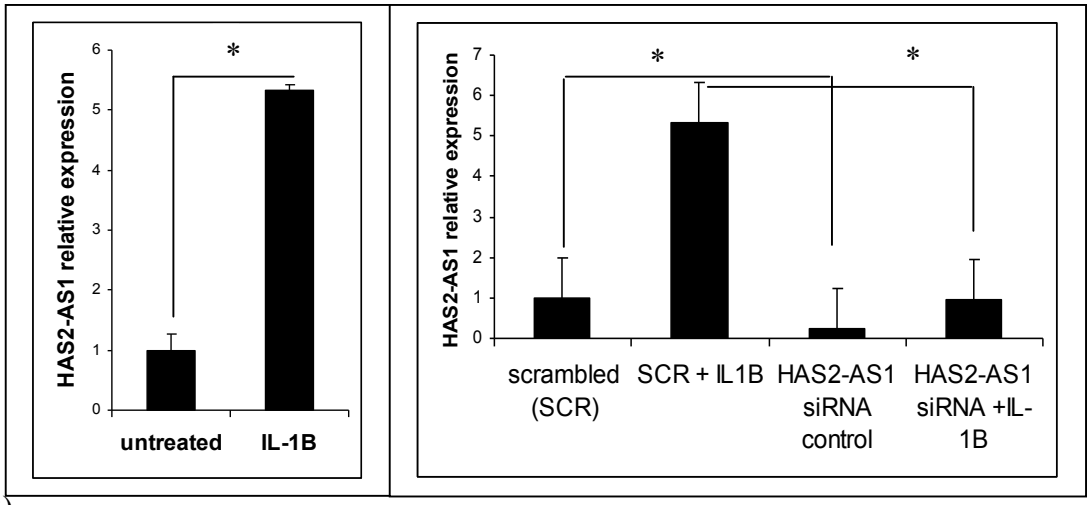

B)

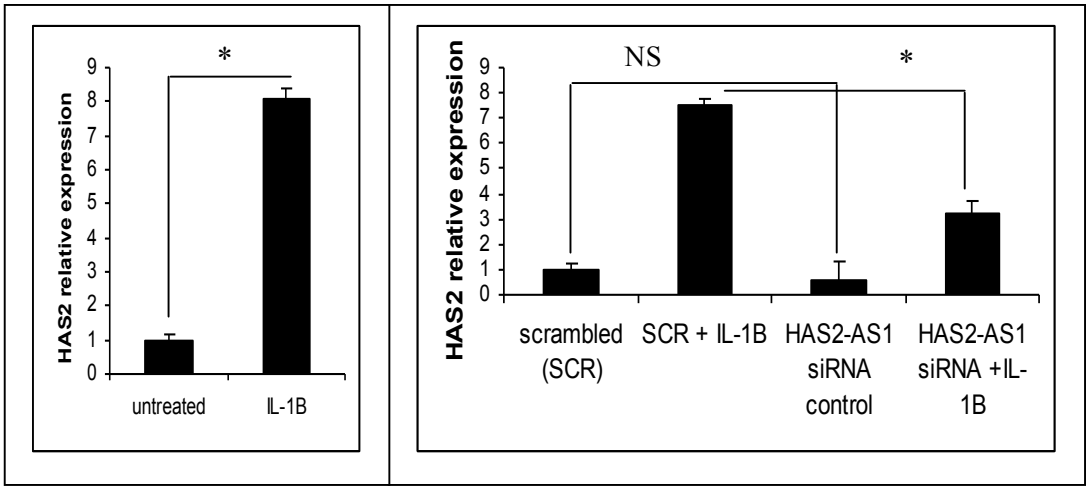

Figure 4.8 Relative expression of A) HAS2-AS1 RNA and B) HAS2 mRNA following HAS2-AS1 siRNA knockdown and /or IL-1β (1ng/ml) stimulation of HK-2 cells.
Data are shown from one experiment, carried out in triplicate, and error bars show standard error of the mean (n = 3). HK-2 cells were transfected with either HAS2-AS1 siRNA or a scrambled oligonucleotide in the presence or absence of 1 ng/ml IL-1β for 3 h. Statistical analysis was performed by the Student's *t* test: *, $P < 0.05$, N/S, not significant. Control graphs (left) show the normal expression of untreated and IL-1β stimulated of HAS2-AS1 or HAS2 relative expression in absence of knockdown of the gene.

The data shown in figure 4.8.A demonstrated that HK-2 cells transfected with HAS2-AS1 siRNA exhibited a significant attenuation in HAS2-AS1 expression when compared to cells transfected with scrambled control alone. Furthermore, cells transfected with HAS2-AS1 siRNA and stimulated with IL-1β for 3 h showed a significant abrogation of IL-1β stimulated HAS2-AS1 induction compared to cells stimulated with IL-1β following transfection with a scrambled control, demonstrating the efficacy of HAS2-AS1-specific siRNA.

Data from figure 4.8.B showed that HK-2 cells transfected with HAS2-AS1 siRNA did not have significantly decreased HAS2 expression when compared to cells transfected with scrambled control alone. However, cells transfected with HAS2-AS 1 siRNA and stimulated with IL-1β showed a significant abrogation of IL-1β stimulated HAS2 induction compared to cells stimulated with IL-1β following transfection with a scrambled control.

As described previously in chapter 3, the experimental data demonstrated coordinated up-regulation of HAS2-AS1 and HAS2 in response to IL-1β. In this experiment, the failure of IL-1β to induce HAS2-AS1 transcription due to HAS2-AS1 siRNA also prevented HAS2 induction.

4.7.2 Effect of siRNA knockdown of HAS2-AS1 on HAS2 expression following TGF-β1 stimulation of HK-2 cells

A)

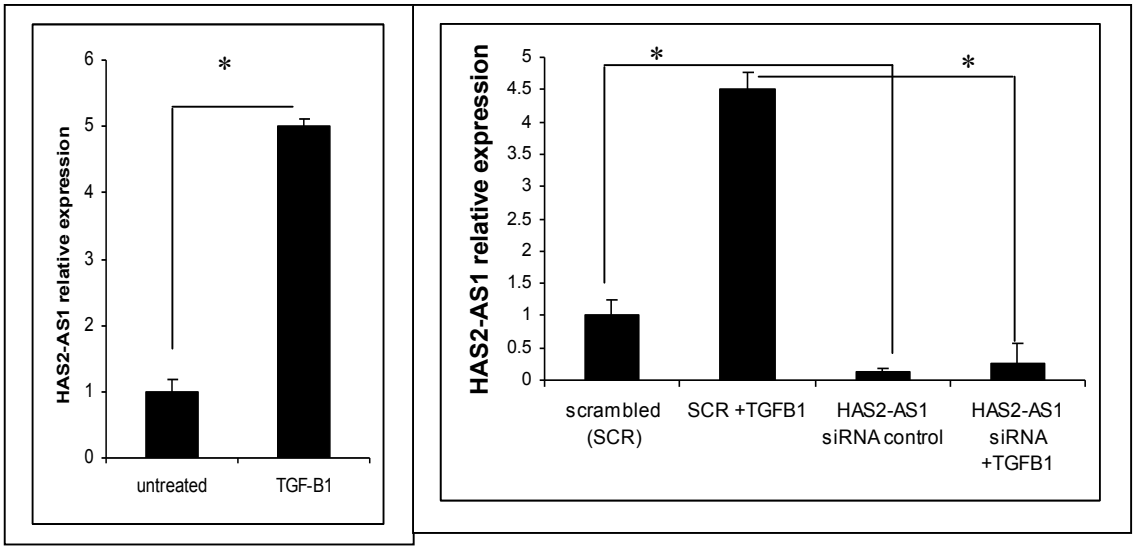

B)

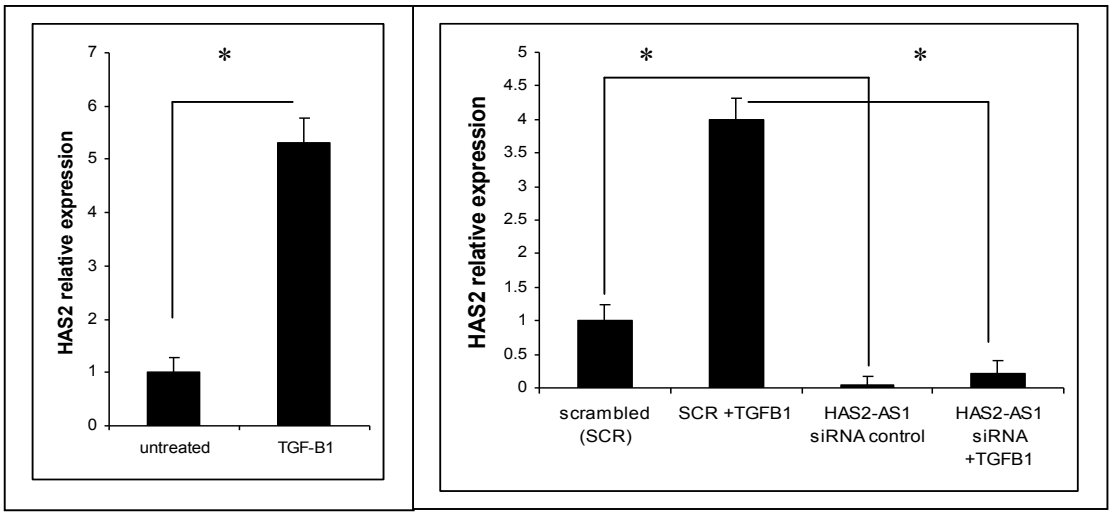

Figure 4.9 Relative expression of A) HAS2-AS1 RNA and B) HAS2 mRNA following HAS2AS siRNA knockdown and / or TGF-β1 (10 ng/ml) stimulation of HK-2 cells. Data shown from one experiment, carried out in triplicate, and error bars show standard error of the mean (n = 3). HK-2 cells were transfected with either HAS2-AS1 siRNA or a scrambled oligonucleotide in the presence or absence of 10 ng/ml TGF-β1 for 48 h. Statistical analysis was performed by the Student's *t* test: *, $P < 0.05$. Control graphs (left) show the normal expression of untreated and TGFβ-1 stimulated of HAS2-AS1 or HAS2 relative expression in absence of knockdown of the gene.

The data shown in figure 4.9.A demonstrated that HK-2 cells transfected with HAS2-AS 1 siRNA exhibited a significant attenuation in HAS2-AS1 expression when compared to cells transfected with scrambled control alone. Furthermore, cells transfected with HAS2-AS1 siRNA and stimulated with 10 ng/ml of TGF-β1 for 48 h, showed a significant abrogation of TGF-β1 stimulated HAS2-AS1 induction compared to cells stimulated with TGF-β1 following transfection with a scrambled control.

Data from figure 4.9.B showed that HK-2 cells transfected with HAS2-AS1 siRNA exhibited significantly decreased HAS2 expression when compared to cells transfected with scrambled control alone. In addition, cells transfected with HAS2-AS1 siRNA and stimulated with TGF-β1 showed a significant abrogation of TGF-β1 stimulated HAS2 induction compared to cells stimulated with TGF-β1 following transfection with a scrambled control.

As described previously in chapter 3, the experimental data demonstrated coordinated up-regulation of both HAS2-AS1 and HAS2 in response to TGF-β1. In this experiment, the failure of TGF-β1 to induce HAS2-AS1 transcription due to HAS2-AS1 siRNA also prevented HAS2 induction.

4.8 HAS2-AS1 forced expression

This work investigated whether forced HAS2-AS1 expression increased or decreased expression of HAS2.

To study the biological activity of HAS2-AS1, three plasmid preparations were transfected into HK2-cells:

1) Full length HAS2-AS1 in pcDNA3.1.

2) L-HAS2-AS1 exon 2 in pc DNA3.1 as described by Chao + spicer [195].

3) Empty vector PCR 3.1.

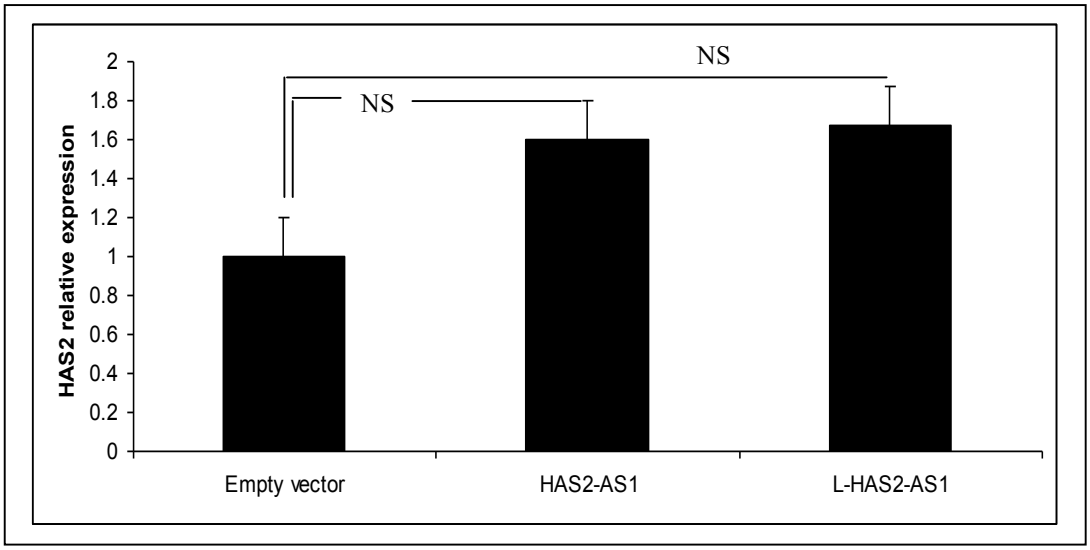

Figure 4.10 HAS2-AS1 forced expression in HK-2 cells. Transfection for 24 h. data are shown from one experiment, carried out in triplicate, and error bars show standard error of the mean (n=3). Statistical analysis was performed by the Student's t test: N/S, not significant.

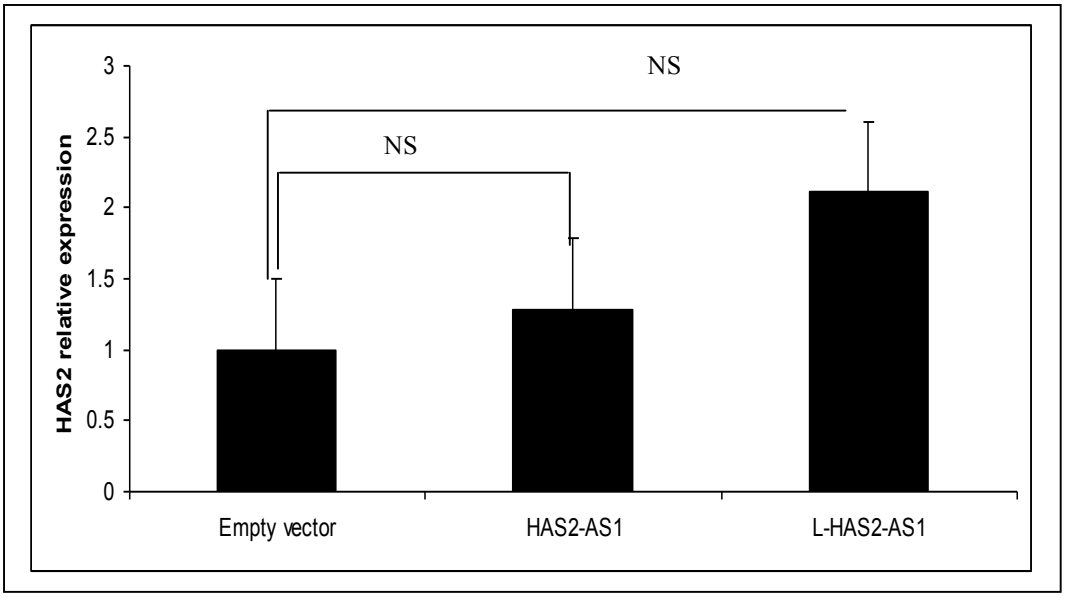

Figure 4.11 HAS2-AS1 forced expression in HK-2 cells. Transfection for 48 h. data are shown from one experiment, carried out in triplicate, and error bars show standard error of the mean (n=3). Statistical analysis was performed by the Student's t test: N/S, not significant.

Figures 4.10 and 4.11 show that forced expression of full-length HAS2-AS1 and L-HAS2-AS1 led to up-regulated HAS2 expression at 24 h and 48 h following transfection, respectively, but that this was not statistically significant in comparison to transfection with the empty vector.

4.9 Discussion

In the previous chapter the expression of human HAS2 and HAS2-AS1 genes was investigated, and showed coordinated transcriptional induction in response to several disease-related stimuli in four cell types. This coordinated temporal regulation suggested that HAS2-AS1 is unlikely to act as an antisense which inhibits HAS2 expression in these cells. These data, together with examples in the literature of interactions between complementary non-coding RNAs which stabilize and/ or facilitate expression of the respective mRNA suggest such a facilitatory role for HAS2-AS1 in the regulation of HAS2.

In this chapter, the aim was to manipulate the expression of either HAS2 or HAS2-AS1 to examine the resultant effect on the expression of the other gene to obtain more information on the potential functional relationship between HAS2 and HAS2-AS1.

Forced expression of HAS2 in both lung fibroblasts and PTCs, in the absence of cytokine stimulation, led to a significant up-regulation of HAS2-AS1 expression when compared to cells transfected with empty vector. In the previous chapter, it was postulated that coordinated regulation may be related to common transcription factor responsive elements in the promoter of HAS2 and HAS2-AS1. This, however, is unlikely to explain up-regulation of HAS2-AS1 following forced HAS2 expression. Another

possible explanation for this increase is that HA being produced by the forced HAS2 expression may drive expression of HAS2-AS1 via a signalling mechanism. It is well established that HA may activate numerous intracellular events, and that many of these effects are mediated via activation of intracellular signalling following engagement of HA with CD44, the principal extracellular HA receptor.

The work described here also investigated the possibility that the mechanism for up-regulation of HAS2-AS1 following forced HAS2 expression in HK2 cells was due to a subsequent increase in HA synthsis. HA synthesis was inhibited using 4-MU. This inhibition resulted in a significant decrease in the expression of HAS2-AS1 in these cells in comparison to forced HAS2 expression in the absence of 4-MU. These results imply that the increase in HAS2-AS1 seen in these experiments is due to the function of increased HA levels, rather than increased HAS2 mRNA synthesis. Depletion of the UDP-glucuronic acid pool by 4-MU has been shown previously to inhibit HA synthesis and peri-cellular HA coat formation in a number of cell types [137].

HAS2 siRNA knockdown did not result in statistically significant abrogation of HAS2-AS1 transcription under basal or cytokine-stimulated conditions. The basal result was not unexpected, since HAS2-AS1 is expressed at low abundance in unstimulated cells. One possible interpretation of the cytokine-stimulated data is that the down-regulation in HAS2-AS1 transcription due to decreased facilitatory interaction between HAS2 mRNA

and HAS2-AS1 RNA lacked statistical difference due to partial compensation by residual HAS2-driven HA synthesis resulting from incomplete HAS2 mRNA knockdown.

siRNA knockdown of HAS2-AS1 induction following cytokine stimulation (both IL-1β and TGF-β1) resulted in a statistically significant reduction in HAS2 transcriptional induction. This corroborates the findings at the IoN described by Michael et al 2011[191], and supports the case for a direct interaction between HAS2-AS1 and HAS2 that facilitates HAS2 transcription [191]. HAS2-AS1 siRNA knockdown showed no effect on the basal expression of HAS2, probably due to the low copy number of HAS2-AS1 in unstimulated cells as mentioned above. This is consistent with recent genomic data providing compelling evidence that gene expression at many genomic loci is modulated by interactions between transcripts from the sense strand and complimentary transcripts from the opposite, antisense strand [244][246] as discussed previously for BACE-1 [247].

Forced expression of either HAS2-AS1 or L-HAS2-AS1 exon 2 in HK-2 cells had no significant effect on HAS2 expression. Forced HAS2-AS1 exon 2 overexpression was show by Chao and Spicer to down-regulate HAS2 expression and subsequent HA synthesis in osteosarcoma cell [195]. However, on the basis of data show in chapter 3, we did not expect this to be the case in PTC. Indeed, we obtained no effect on HAS2 expression with the forced expression of this transcript. As this represents only part of L-

HAS2-AS1 RNA, we also carried out forced expression of the full-length antisense RNA. It may be important that, even in the presence of cytokine stimulation, the abundance of HAS2-AS1 is relatively low. Forced expression analyses therefore create an imbalance in the HAS2-AS1 RNA: HAS2 mRNA ratio that is never seen in PTC, either in health or disease. The fact that neither transcript affected HAS2 expression may therefore reflect a subtle mechanism of interaction between the two RNAs in the PTC cytoplasm, and their export to the cytoplasm following transcription will need to be analysed further.

4.10 In summary

Forced expression of HAS2 in lung fibroblasts, in the absence of any additional stimulus, lead to a significant an increase in HAS2-AS1 expression dependent on increase in HA synthsis. The experimental data described in this chapter also showed that siRNA knockdown of HAS2-AS1 RNA in HK-2 cells attenuated cytokine stimulated transcriptional induction of HAS2 mRNA. However, HAS2 siRNA and cytokine stimulation did not result in statistically significant abrogation of HAS2-AS1 induction. These findings suggest that the regulation of HAS2-AS1 may be related to HAS2-dependent generation of HA, whilst HAS2 regulation by HAS2-AS1 may be dependent on direct interaction between the complementary parts of the two RNA sequences.

General Discussion

1. Coordinated expression of HAS2 mRNA and HAS2-AS1 RNA in response to cytokine stimulation

The online Oxford English Dictionary (http://www.oed.com/) defines antisense as "Designating or pertaining to the strand of duplex DNA that acts as a template for the synthesis of mRNA in a cell; *also, designating or pertaining to RNA produced by the transcription of sense DNA, having a complementary base sequence to mRNA and able to bind with it, thereby preventing translation of the latter into protein."* The italicized part of this definition highlights the widely held belief that antisense sequences are negative regulators of "sense"-strand gene function at the translational level, as above, or at transcriptional or post-transcriptional levels.

On the basis of the experimental data contained in this thesis, the relationship between HAS2-AS1 RNA and HAS2 mRNA is not a traditional "antisense" interaction in which the expression of the antisense RNA leads to a down-regulation of HAS2 mRNA and a decrease in HA synthesis as described in osteosarcoma cells by Chao and Spicer (2005) [195].

Indeed, the simultaneous transcriptional up-regulation of HAS2-AS1 RNA and HAS2 mRNA in response to IL-1β and TGF-β1 demonstrated correlated expression of these genes. This demonstration of correlated expression suggested that HAS2 and HAS2-AS1

are co-ordinately regulated and that they may be controlled by the same transcriptional regulators. Thus, the cytokine-stimulated up-regulation of HAS2 and HAS2-AS1 transcription may involve simultaneous binding of transcription factors to both proximal promoters at the HAS2/HAS2-AS1 locus. This hypothesis is supported by an *silico* study of the HAS2 proximal promoter region [248] and analysis of the sequences immediately upstream of HAS2-AS1 [191][248][249][250] that have identified a similar range of shared putative upstream transcription factor-binding sites (TFBSs) in both of these genes.

At the IoN, previous *in silico* analysis of the HAS2 promoter region highlighted a cluster of three Sp1/Sp3 recognition sites immediately adjacent to the HAS2 TSS [189], and demonstrated that Sp1 and Sp3 acted as co-activators at these sites to mediate constitutive transcription [190]. These data were augmented by recent findings describing functional upstream elements in the HAS2 promoter, which may interact with Sp1 and Sp3 [193]. Further recent data from the IoN demonstrated that siRNA knockdown of Sp1 and Sp3 inhibits both HAS2 and HAS2-AS1 induction following incubation with IL-1β; and following knockdown of Smad2 and Smad3, the induction of HAS2 and HAS2-AS1 by TGF-β1 was blunted [191].

2. Regulation of HAS2-AS1 by HAS2 expression

Forced HAS2 expression in the absence of any further stimulus lead to a significant up-regulation of HAS2-AS1 expression. This is unlikely to be due to direct transcriptional up-regulation. One possible alternative mechanism is the interaction of HA with cell-surface receptors and subsequent signal transduction cascade leading to an up-regulation of HAS2-AS1. Inhibition of HA synthesis using 4-MU down-regulated HAS2-AS1 expression in HK-2 cells, suggesting that antisense expression was in this case modulated by up-regulated HA production and not increased transcription of HAS2.

HAS2-specific siRNA knockdown decreased HAS2 mRNA levels, but had no significant effect on HAS2-AS1 RNA. However, the presence of residual HA, possibly as a result of incomplete HAS2 siRNA knockdown, cannot be ruled out. It is well established that HA may activate numerous intracellular events, and that many of these effects are mediated via activation of intracellular signalling following engagement of HA with CD44, the principal extracellular HA receptor. It is therefore possible that the lack of statistical significance of the HAS2-AS1 attenuated response to both IL-1β and TGF-β1 following HAS2 siRNA knockdown supports a role for HAS2-driven HA in the regulation of HAS2-AS1 transcriptional regulation.

3. Regulation of HAS2 by HAS2-AS1 expression

HAS2-AS1-specific siRNA knockdown inhibited cytokine induced up-regulation of HAS2 mRNA and HAS2-AS1 RNA expression in HK-2 cells. These data suggest that HAS2-AS1 has a facilitatory role which stabilises and / or augments the expression of HAS2 mRNA in these cells. This so-called "correlated" transcription of RNA and mRNA from either genomic DNA strand at the same locus is one documented mechanism by which natural anti-sense transcripts regulate their sense-strand counterparts [244][245]. Clearly, it is possible that the influence of HAS2-AS1 on HAS2 expression may occur as a result of RNA: mRNA interaction. Indeed, research carried out at the IoN has provided evidence from both *in silico* and *in vitro* analyses that cytoplasmic interaction between sense and antisense transcripts was detected in the form of a double-stranded (ds) RNA duplex [191].

Another example of natural antisense regulation of sense expression is the recent study demonstrating that the Wilms'Tumor gene (WT1) locus encodes conserved antisense RNAs that may regulate WT1 expression via RNA: mRNA interactions, and this can become deregulated by a variety of mechanisms in Wilms' Tumour [251]. A similar interdependence has been reported between the β-secretase-1(BACE-1) gene and natural antisense BACE-1-AS. BACE-1 is a candidate gene for Alzheimer's disease that may drive disease associated pathology [247]. BACE-1 mRNA expression is up-regulated by increased transcription of the natural antisense RNA BACE-1-AS, leading to increased

BACE-1 protein levels *in vitro* and *in vivo* [247]. These data also parallel the recent observations of Matsui et al., where correlated expression of overlapping sense:antisense transcripts has been reported in the expression of rat inducible nitric oxide synthase (iNOS), where iNOS mRNA is stabilised by interaction with a natural antisense iNOS RNA [252].

As expected, forced HAS2-AS1 expression resulted in up-regulated HAS2-AS1 levels. However, no significant up-regulation of HAS2 mRNA was observed. These forced expression results are in contrast to the observation by Chao and Spicer; that over-expression of HAS2-AS1 in osteosarcoma cells down-regulated HAS2 mRNA synthesis and that subsequent HA synthesis was inhibited [195]. There are a number of possible reasons for the differences between these data and the findings in this work. These include the fact that the two studies were carried out in cells from different lineages, one malignant and one non-malignant, and differentiation in malignant cells is known to be different to non-malignant cells [253][254]. In addition, in the Chao and Spicer study, only RNA from the second exon of HAS2-AS1 was expressed, since this represented the extent of antisense sequence complementary to HAS2 mRNA [195]. This truncated antisense transcript might conceivably behave differently from the entire HAS2-AS1 RNA. Indeed, in their analyses on BACE-1 expression, Faghihi and colleagues expressed the full-length BACE-AS transcript in their corresponding control studies [247].

In addition, sense:antisense interaction may be cell-specific, and this may explain differences that occur as a result of the S- and L- HAS2-AS1 splice variants that differ only in their length of sequence complementarity with HAS2. As stated above, previous IoN data suggest these splice variants infer a role for HAS2-AS1 in the facilitation or augmentation of HAS2 expression in different cells and in HAS2-AS1:HAS2 interaction [191]. It is also possible that the presence of the HAS2-AS1 splice variants provides evidence of a potential additional level of regulation of HAS2 expression in these cells.

Reports from the IoN and other laboratories have demonstrated the importance of HAS2 expression in HA metabolism in kidney disease. An increase in HA expression in the renal corticointerstitium is commonly associated with the progression of interstitial fibrosis leading to ESRD. For example, in high glucose concentrations which mimic diabetic nephropathy, renal PTCs synthesise high level of HA, which is coincident with specific up-regulation of transcription at the HAS2 locus. Since HAS2-AS1 has a facilitatory role which stabilises and /or augments the expression of HAS2 gene, it is a potential target to modulate HAS2 expression, and therefore also represents a possible therapeutic target for intervention in renal fibrosis.

Future Work

Further investigation into the functional impact of the coordinated expression of HAS2-AS1 and HAS2 on cell phenotype would generate valuable data. For example, does this coordinated regulation have a synergistic effect on cell function? More specifically, it would be interesting to examine the effects of this expression on epithelial-to-mesenchymal transition, fibroblast-to-myofibroblast transdifferentiation, cell proliferation and cell migration.

Preliminary work by Simpson et al. has demonstrated that *in vitro* aged cells resist fibroblast to myofibroblast differentiation, and this resistance is associated with reduced HAS2 induction by TGF-β1 [156]. It is interesting to speculate, therefore, that a modification in HAS2-AS1 expression in aged dermal fibroblasts could contribute to this diminished HAS2 induction by TGF-β1. Previous data suggest that increased HAS2 mRNA levels promote transformation to a pro-fibrotic and migratory phenotype [37][38][139][141][156][174][255][256], so does the coordinated expression of HAS2-AS1 and HAS2 have a synergistic effect on cell function in this context?

In addition, if HAS2 over-expression is pathogenic [6][37][99][257], modulation of HAS2-AS1 expression could provide a novel method for the manipulation of HAS2 expression and could therefore have therapeutic potential effects.

References

1. Meyer, K. and Palmer, J.W., 1934. The polysaccharide of the vitreous humor. *J Biol Chem,* **107**, 629-634.
2. Weissmann, B., Meyer, K., Sampson, P. and Linker, A., 1954. Isolation of oligosaccharides enzymatically produced from hyaluronic acid. *J Biol Chem,* **208,** 417-29.
3. Toole, B.P., 2000. Hyaluronan is not just a goo. *J Clin Invest,* **106,** 335-6.
4. Laurent, T.C. and Fraser, J.R., 1992. Hyaluronan. *Faseb J, **6,*** 2397-404.
5. Laurent, T.C., Laurent, U.B. and Fraser, J.R., 1996. The structure and function of Hyaluronan: An overview. *Immunol Cell Biol,* **74,** A1-7.
6. Tammi, M. I., Day, A. J, and Turley, E.A., 2002. Hyaluronan and homeostasis: a balancing act. *J Biol Chem* **277**(7), 4581-4584.
7. Butler, J., N.W. Rydell, and E.A. Balazs. Hyaluronic acid in synovial fluid.VI. Effect of intra-articular injection of hyaluronic acid on the clinical symptoms of arthritis in track horses. *Acta Vet Scand*, 1970. **11**(2): 139-55.
8. Miller, D. and R. Stegmann. Use of sodium hyaluronate in human IOL Implantation. *Ann Ophthalmol*, 1981. **13**(7): 811-5.
9. Miller, D. and R. Stegmann. Secondary intraocular lens implantation using sodium hyaluronate. *Ann Ophthalmol*, 1982. **14**(7): 621-3.
10. Itano, N. and Kimata, K. 1996. Expression cloning and molecular characterization of HAS protein, a eukaryotic hyaluronan synthase. *J Biol Chem* **271**(17), 9875-9878.
11. Itano, N. and Kimata, K. 1996. Molecular cloning of human hyaluronan synthase. *Biochem Biophys Res Commun* **222**(3), 816-820.

12. Shyjan, A.M., Heldin, P., Butcher, E.E., Yoshino, T., Briskin, M.J. 1996. Functional cloning of the cDNA for a human hyaluronan synthase. *J Biol Chem* **271**(38), 23395-23399.
13. Spicer, A. P., Augustine, M.L. and McDonald, J.A., 1996. Molecular cloning and characterization of a putative mouse hyaluronan synthase. *J Biol Chem* **271** (38), 23400-23406.
14. Spicer, A. P., Olson, J.S. and McDonald, J.A., 1997. Molecular cloning and characterization of a cDNA encoding the third putative mammalian hyaluronan synthase. *J Biol Chem* **272**(14), 8957-8961.
15. Watanabe, K. and Yamaguchi, Y. 1996. Molecular identification of a putative human hyaluronan synthase. *J Biol Chem* **271** (38), 22945-22948.
16. DeAngelis, P. L. 1999. Hyaluronan synthases: fascinating glycosyltransferases from vertebrates, bacterial pathogens, and algal viruses. *Cell Mol Life Sci* **56** (7-8), 670-682.
17. Weigel, P. H., Hascall, V.C., Tammi, M. 1997. Hyaluronan synthases. *J Biol Chem* **272** (22), 13997-14000.
18. Itano, N., Sawai, T., Yoshida, M., Lenas, P., Yamada, Y., Imagawa, M., Shinomura, T., Hamaguchi, M., Yoshida, Y., Ohnuki, Y., Miyauchi, S., Spicer, A.P., McDonald, J.A., Kimata, K. 1999. Three isoforms of mammalian hyaluronan synthases have distinct enzymatic properties. *J Biol Chem* **274**(35), 25085-25092.
19. Spicer, A. P. and McDonald, J. A. 1998. Characterization and molecular evolution of a vertebrate hyaluronan synthase gene family. *J Biol Chem* **273** (4), 1923-1932.
20. Fraser, J. R., Laurent, T.C., Laurent, U.B. 1997. Hyaluronan: its nature, distribution, functions and turnover. *J Intern Med* **242**(1), 27-33.

21. Csoka, A. B., Scherer, S.W., Stern, R. 1999. Expression analysis of six paralogous human hyaluronidase genes clustered on chromosomes 3p21 and 7q31. *Genomics* **60**(3), 356-361.

22. Patel, S., Turner, P.R., Stubberfield, C., Barry, E., Rohlff, C.R., Stamps, A., Mckenzie, E., Young, K., Tyson, K., Terrett, J., Box, G., Eccles, S., Page, M.J. 2002. Hyaluronidase gene profiling and role of hyal-1 overexpression in an orthotopic model of prostate cancer. *Int J Cancer* **97**(4), 416-424.

23. Rai, S. K., Duh, F.M., Vigdorovich, V., Danilkovitch- Miagkova, A., Lerman, M.I., Miller, A.D. 2001. Candidate tumor suppressor HYAL2 is a glycosylphosphatidylinositol (GOI) - anchored cell-surface receptor for jaagsiekte sheep retrovirus, the envelope protein of which mediates oncogenic transformation. *Proc Natl Acad Sci USA* **98**(8), 4443-4448.

24. Csoka, A. B., Frost, G.I., Stern, R. 2001. The six hyaluronidase-like genes in the human and mouse genomes. *Matrix Biol* **20** (8), 499-508.

25. Stern, R. 2003. Devising a pathway for hyaluronan catabolism: are we they yet? *Glycobiology* **13**(12), 105R-115R.

26. Agren, U. M., Tammi, R.H., Tammi, M.I. 1997. Reactive oxygen species contribute to epidermal hyaluronan catabolism in human skin organ culture. *Free Radic Biol* Med **23** (7); 996-1001.

27. Knudson, C. B. 2003. Hyaluronan and CD44: strategic players for cell-matrix interactions during chondrogenesis and matrix assembly. *Birth Defects Res C Embryo Today* **69** (2), 174-196.

28. Knudson, W., Chow. G., Knudson, C.B. 2002. CD44-mediated uptake and degradation of hyaluronan. *Matrix Biol* **21** (1), 15-23.

29. Zhou, B., Weigel, J.A., Fauss, L., Weigel. P.H. 2000. Identification of the hyaluronan receptor for endocytosis (HARE). *J Biol Chem* **275** (48), 37733-37741.

30. Lepperdinger, G., Strobl, B., Kreil, G. 1998. HYAL2, a human gene expressed in many cells, encodes a lysosomal hyaluronidase with a novel type of specificity. *J Biol Chem* **273**(35), 22466-22470.

31. Culty, M., Nguyen, H.A., Underhill, C.B. 1992. The hyaluronan receptor (CD44) participates in the uptake and degradation of hyaluronan. *J Cell Biol* **116** (4), 1055-1062.

32. Hua, Q., Knudson, C.B., Knudson, W. 1993. Internalization of hyaluronan by chondrocytes occurs via receptor-mediated endocytosis. *J Cell Sci* **106** (Pt 1), 365-375.

33. Tammi, R., Rilla, K., Pienimaki, J.P., Maccallum, D.K., Hogg, M., Luukkonen, M., Hascall, V.C., Tammi, M. 2001. Hyaluronan enters keratinocytes by a novel endocytic route for catabolism. *J Biol Chem* **276** (37), 35111-35122.

34. Day, A. J. and Prestwich, G. D. 2002. Hyaluronan-binding proteins: tying up the giant. *J Biol Chem* **277**(7), 4585-4588.

35. Spicer, A. P., Joo, A., and Bowling, R. A., Jr. A hyaluronan binding link protein gene family whose members and physically linked adjacent to chondroitin sulfate proteoglycan core protein genes: the missing links. (2003) *The Journal of biological chemistry* **278** (23), 21083-21091.

36. Girish, K.S and Kemparaju, K. 2007. The magic glue hyaluronan and its eraser Hyaluronidase : a biological overview. *Life Sci* **80**(21), 1921-1943.

37. Selbi, W., Day, A.J., Rugg, M.S., Fulop, C., de la Motte, C.A., Bowen, T., Hascall, V.C., Phillips, A.O. 2006. Overexpression of hyaluronan synthase 2 alters

hyaluronan distribution and function in proximal tubular epithelial cells. *J Am Soc Nephrol* **17**(6), 1553-1567.

38. Selbi, W., de la Motte, C., Hascall, V.C., Day, A.J., Bowen, T., Phillips, A.O. 2006. Characterization of hyaluronan cable structure and function in renal proximal tubular epithelial cells. *Kidney Int* **70**(7), 1287-1295.
39. Yamaguchi, Y. Lecticans : organizers of the brain extracellular matrix. (2000) *Cell Mol Life Sci* **57**(2), 276-289.
40. Watanabe, H., Chenug, S. C., Itano, N., Kimata, K., and Yamada, Y. Identification of hyaluronan binding domains of aggrecan. (1997) *The Journal of biological chemistry* **272**(44), 28057-28065.
41. Blom, A., Pertoft, H., and Fries, E. (1995). Inter-alpha-inhibitor is required for the formation of the hyaluronan containing coat on fibroblasts and mesothelial cells. *The Journal of biological chemistry* **270**(17), 9698-9701.
42. Hess, K. A., Chen, L., Larsen, W.J. 1999. Inter-alpha-inhibitor binding to hyaluronan in the cumulus extracellular matrix is required for optimal ovulation and development of mouse oocytes. *Biol Reprod* **61** (20), 436-443.
43. Blom, A., Pertoft, H., and Fries, E. (1995). Inter-alpha- inhibitor is required for the formation of the hyaluronan containing coat on fibroblasts and mesothelial cells. *The Journal of biological chemistry* **270** (17), 9698-9701.
44. Horton, M. R., Mckee, C.M., Bao, C., Liao, F., Faber, J.M., Oliver, B.L.1998. Hyaluronan fragments synergize with interferon-gamma to induce the C-X-C chemokines mig and interferon-inducible protein-10 in mouse macrophages. *J Biol Chem 273* (52), 35088-35094.
45. Camenisch, T.D., Spicer, A. P., Brehm-Gibson, T., Biesterfeldt, J., Augustine, M. L., Calabro, A., Jr., Kubalak, S., Klewer, S. E., and McDonald, J.A. 2000.

Disruption of hyaluronan synthase-2 abrogates normal cardiac morphogenesis and hyaluronan-mediated transformation of epithelium to mesenchyme. *J.Clin. Invest*. **106**, 349-360.

46. Parkar, A.A. and A.J. Day, Overlapping sites on the link module of human TSG-6 mediate binding to hyaluronan and chrondritin-4-sulphate. *FEBS Lett*, 1997. **410** (2-3), 413-7.
47. Blundell, C.D., Mahoney, D.J., Cordell, M.R., Almond, A., Kahmann, J.D., Perczel, A., Taylor, J.D., Campbell, I.D., Day, A.J. Determining the Molecular Basis for the Ph-dependent interaction between the link module of Human TSG-6 and Hyaluronan. *Journal of Biological Chemistry*, 2007.**282** (17), 12979-12988.
48. Fulop, C., Szanto, S., Mukhopadhyay, D., Bardos, T., Kamath, R.V., Rugg, M.S., Day, A. J., Salustri, A., Hascall, V.C., Glant, T. T., and Mikecz, K., 2003. Impaired cumulus mucification and female sterility in tumor necrosis factor-induced protein-6-deficent mice. *Development* (Camb) **130**,2253-2261.
49. Selbi, W., de la Motte, C., Hascall, V.C., Phillips, A. 2004. BMP-7 modulates hyaluronan-mediated proximal tubular cell- monocyte interaction. *J Am Soc Nephrol* **15**(5), 1199-1211.
50. Knudson, W., Aguiar, D.J., Hua, Q., Knudson, C.B. 1996. CD44-anchored hyaluronan-rich pericellular matrices: an ultrastructural and biochemical analysis.*Exp Cell Res* **228** (2), 216-228.
51. Bourguignon, L. Y., Lokeshwar, V. B., He, J., Chen, X., and Bourguignon, G. J. (1992). A CD44- like endothelial cell transmembrane glycoprotein (GP116) interacts with extracellular matrix and ankyrin. *Molecular and cellular biology* **12**(10), 4464-4471.

52. Sleeman, J., Rudy, W., Hofmann, M., Moll, J., Herrlich, P., and Ponta, H. (1996). Regulated clustering of variant CD44 proteins increases their hyaluronate binding capacity. *The Journal of cell biology* **135**(4), 1139-1150.

53. Lesley, J., Hyman, R., English, N., Catterall, J.B., Turner, G.A. 1997. CD44 in inflammation and metastasis. *Glycoconj J* **14**(5), 611-622.

54. Knudson, W. and Knudson, C.B., 2000. The hyaluronan receptor, CD44. *In. Glycoforum.*

55. Knudson, C. B. and Knudson, W. 2004. Hyaluronan and CD44: modulators of chondrocyte metabolism. *Clin Orthop Relat Res* (427 Suppl), S152-162.

56. Tsukita, S., Oishi, K., Sato, N., Sagara, J., Kawai, A., and Tsukita, S. (1994). ERM Family members as molecular linkers between the cell surface glycoprotein CD44 and actin-based cytoskeletons. *The Journal of cell biology* **126**(2), 391-401.

57. Cichy, J. and Pure, E. 2003. The liberation of CD44. *J Cell Biol* **161** (5), 839-843.

58. Jones, S. G., Tto, T., phillips, A.O. 2003. Regulation of proximal tubular epithelial cell CD44- mediated binding and internalisation of hyaluronan. *Int J Biochem Cell* **35** (9), 1361-1377

59. Stern, R. and H.I. Maibach, Hyaluronan in skin: aspects of aging and its pharmacologic modulation. *Clinics in Dermatology*, 2008. **26** (2), 106-122.

60. Huebener, P., Abou-khamis, T., Zymek, P., Bujak, M., Ying, X., chatila, K., Haudek, S., Thakker, G., Frangogiannis, N.S. CD44 Is Critically involved in infarct Healing by Regulating the inflammatory and fibrotic Response. *J Immunol*, 2008. **180** (4), 2625-2633.

61. DeGrendele, H.C., P. Estess, and M. H. Siegelman, Requirement for CD44 in activated T cell extravasation into an inflammatory site. *Science*, 1997. **278** (5338), 672-5.

62. Vachon, E., Martin, R., Plumb, J., Kwork, V., Vandivier, R.W., Glogauer, M., Kapus, A., Wangx., Chow, C.W., Grinstein, S., Downey, G.P. CD44 is a phagocytic receptor. *Blood*, 2006. **107**(10), 4149-58.

63. Turley, E. A., Noble, P.W., Bourguignon, L.Y. 2002. Signaling properties of hyaluronan receptors. *J Biol Chem* **277**(7), 4589-4592.

64. Entwistle, J., Hall, C. L., and Turley, E.A. (1996). HA receptors regulators of signalling to the cytoskeleton. *Journal of cellular biochemistry* **61**(4), 569-577.

65. Lokeshwar, V.B., Fregien, N. and Bourguignon, L.Y., 1994. Ankyrin-binding domain of CD44 (GP85) is required for the expression of hyaluronic acid-mediated adhesion function. *J Cell Biol*, **126**, 1099-109.

66. Mc Kee, C.M., Lowenstein, C.J., Horton, M.R., Wu, J., Bao, C., Chin, B.Y., Choi, A.M. and Noble, P.W., 1997. Hyaluronan fragments induce nitric-oxide synthase in murine macrophages through a nuclear factor kappa B-dependent mechanism. *J Biol Chem*, **272**, 8013-8.

67. Fitzgerald, K.A., Bowie, A.G., Skeffington, B.S.and O`Nell, L.A., 2000. Ras, Protein kinase c zeta, and I kappa B kinases 1 and 2 are downstream effectors of CD44 during the activation of NF-kappa B by hyaluronic acid fragments in T-24 carcinoma cells. J *Immunol*, **164**, 2053-63.

68. Kamikura, D.M., Khoury, H., Maroun, C., Naujokas, M.A. and Park, M., 2000. Enhanced transformation by a plasma membrance-associated met oncoprotin: activation of a phosphoinositide 3-kinase dependent autocrine loop involving hyaluronic acid CD44. *Mol Cell Biol*, **20**, 3482-96.

69. Bourguignon, L. Y., Zhu, H., Shao, L., Chen, Y.W. 2001. CD44 interaction with c-Src kinase promotes cortactin-mediated cytoskeleton function and hyaluronic acid-dependent ovarian tumor cell migration. *J Biol Chem* **276**(10), 7327-7336.

70. Bourguignon, L.Y., Zhu, H, Shao, L. and Chen, Y.W., 2000. CD44 interaction with tiam1 promotes Rac1 signaling and hyaluronic acid mediated breast tumor cell migration. *J Biol Chem*, **275**, 1829-38.

71. Oliferenko, S., Kaverina, I., Small, J.V. and Huber, L.A., 2000. Hyaluronic acid (HA) binding to CD44 activates Rac1 and induces lamellipodia outgrowth. *J Cell Biol*, **148**, 1159-64.

72. Zhu, D. and Bourguignon, L.Y., 2000. Interaction between CD44 and the repeat domain of ankyrin promotes hyaluronic acid-mediated ovarian tumor cell migration. *J Cell Physiol*, **183**, 182-95.

73. Yonemura, S., Hirao, M., Doi, Y., Takahashi, N., Kondo, T. and Tsukita, S., 1998. Ezrin/radixin/moesin (ERM) proteins bind to a positively charged amino acid cluster in the juxta-membrane cytoplasmic domain of CD44, CD34, and ICAM-2. *J Cell Biol*, **140,** 885-95.

74. Bourguignon, L. Y., Singleton, P. A., Zhu, H., and Zhou, B. (2002). Hyaluronan promotes signalling interaction between CD44 and the transforming growth factor beta receptor I in metastatic breast tumor cells. *The Journal of biological chemistry* **277**(42), 39703-39712.

75. Ito, T., Williams, J.D., Fraser, D. J., and Phillips, A. O. (2004). Hyaluronan regulates transforming growth factor-beta-1-receptor compartmentalization. *The Journal of biological chemistry* **279**(24), 25326-25332.

76. Turley, E. A., and Harrison, M. (1999) RHAMM, a member of the hyaladherins. *In Glycoforum*.

77. Hall, C. L., Lange, L.A., Prober, D.A., Zhang, S., Turley, E.A. 1996. pp60(c-src) is required for cell locomotion regulated by the hyaluronanreceptor RHAMM. *Oncogene* **13**(10), 2213-2224.

78. Fieber, C., Plug, R., Sleeman, J., Dall, P., Ponta, H., Hofmann, H. 1999. Characterisation of the murine gene encoding the intracellular hyaluronan receptor IHABP (RHAMM). *Gene* **226**(1), 41-50.

79. Toole, B. P. 2004. Hyaluronan: from extracellular glue to pericellular cue. *Nat Rev Cancer* **4**(7), 528-539.

80. Wang, C., Thor, A.D., Moore, D.H 2nd ., Zhao, Y., Kerschmann, R., Stern, Watson, P.H., Turley, E.A. The overexpression of RHAMM, a hyaluronan-binding protein that regulates ras signalling, correlates with overexpression of mitogen-activated protein kinase and is a significant parameter in breast cancer progression. *Clin Cancer Res*, 1998. **4** (3), 567-76.

81. Mohapatra, S., Yang, X., Wright, J.A., Turley, E.A., Greenberg, A.H. Soluble hyaluronan receptor RHAMM induces mitotic arrest by suppressing Cdc2 and cyclin B1 expression. *J Exp Med*, 1996. **183** (4), 1663-8.

82. Lokeshwar, V.B and Selzer, M.G., 2000. Differences in hyaluronic acid mediated functions and signalling in arterial, microvessel, and vein-derived human endothelial cells. *J Biol Chem*, **275**, 27641-9.

83. Nedvetzki, S., Gonen, E., Assayag, N., Reich, R., Williams, R.O., Thurmond, R.L., Huang, J.F., Neudecker, B.A., Wang, F.S., Turley, E.A., Naor, D. 2004. RHAMM, a receptor for hyalyuronan-mediated motility, compensates for CD44 in inflamed CD44-knockout mice: a different interpretation of redundancy. *Proc Natl Acad Sci U S A* **101(**52), 18081-18086.

84. Ito, T., Williams, J.D., Al-Assaf, S., Phillips, G.O., and Phillips, A.O. 2004 Hyaluronan and proximal tubular cell migration. *Kidney Int* **65**(3), 823-833.

85. Camenisch, T. D., Schroeder, J.A., Bradley, J., Klewer, S.E., McDonald, J.A 2002. Heart-valve mesenchyme formation is Dependent on hyaluronan-Augmented activation of ErbB2-ErbB receptors. *Nat Med* **8** (8), 850-855.

86. Brech, M., Mayer, U., Schlosser, E. and Prehm, P., 1986. Increased Hyaluronate synthesis is required for fibroblast detachment and mitosis. *Biochem J*, **239**, 445-50.

87. Anttila M.A, Tammi R.H, Tammi M.I., Syrjanen, K.J., Saarikoski, S.V., Kosma, V.M. High levels of stromal hyaluronan predict poor disease outcome in epithelial ovarian cancer. *Cancer Res* **60**:150-155, 2000.

88. Auvinen P.K, Parkkinen JJ, Johansson RT., Agren, U.M., Tammi, R.H., Eskelinen, M.J., Kosma, V.M. Expression of hyaluronan in benign and malignant breast lesions. *Int J Cancer* **74**:477-481, 1997.

89. Iocono, J. A., Bisignani, G.J., Krummel, T.M., Ehrlich, H.P.1998. Inhibiting the differentiation of myocardiocytes by hyalyronic acid. *J Surg Res* **76** (2), 111-116.

90. Chen, W. Y. and Abatangelo, G. 1999. Functions of hyaluronan in wound repair. *Wound Repair Regen* **7**(2), 79-89.

Ras-transformed cells

91. Turley, E. A., Austen, L., Moore, D., Hoare, K.1993. Ras-transformed cells express both CD44 and RHAMM hyaluronan receptors: only RHAMM is essential for hyaluronan-promoted locomotion. *Exp Cell Res* **207** (2), 277-282.

92. Kobayashi, H., and Terao, T. Hyaluronic acid-specific regulation of cytokines by human uterine fibroblasts. (1997). *The American Journal of physiology* **273** (4 Pt1), C1151-1159.

93. Toole, B. P., Wight, T.N., Tammi, M.I. 2002. Hyaluronan-cell interactions in cancer and vascular disease. *J Biol Chem* **277** (7), 4593-4596.

94. Knudson, W. Biswas, C., Li, X. Q., Nemec, R. E., and Toole, B. P. The role and regulation of tumor-associated hyaluronan. *CIBA Found. Symp*. **13**: 150-159, 1989.

95. Rooney, P., Kumar, S., Ponting, j., and Wang, M. The role of hyaluronan in tumor neovascularisation. *Int. J. Cancer* , **60**:632-636, 1995.

96. Auvinen, P., Tammi, R., Parkkinen, J., Tammi, M., Agren, U., Johansson, R., Hirvikoski, P., Eskelinen, M., Kosma, V.M. Hyaluronan in Peritumoral stroma and malignant cells associates with breast cancer spreading and predicts survival. 2000, *Am J Pathol*, **156**(2): 529-36

97. Ropponen, K., Tammi, M., Parkkinen, J., Eskelinen, M., Tammi, R., Lipponen, P., Agren, U, Alhava, E., Kosma, V.M. 1998. Tumor cell-associated hyaluronan as an unfavourable prognostic factor in colorectal cancer. *Cancer Res* **58**(2), 342-347.

98. Setala, L. P., Tammi, M.I., Tammi, R.H., Eskelinen, M.J., Lipponen, P.K., Agren, U.M., Parkkinen, J., Alhava, E.M., Kosma, V.M. 1999. Hyaluronan expression in gastric cancer cells is associated with local and nodal spread and reduced survival rate. *Br J Cancer* **79**(7-8), 1133-1138.

99. Kosaki, R., Watanabe, K. and Yamaguchi, Y., 1999. Overproduction of hyaluronan expression of the Hyaluronan synthase Has2 enhances anchorage-independent growth and tumorigenicity. . *Cancer Res* **59**(5), 1141-1145.

100. Liu, N., Gao, F., Han, Z., Xu, X., Underhill, C.B., Zhang, L. Hyaluronan synthase 3 overexpression promoters the growth of TSU prostate cancer cells. *Cancer Res*, 2001. **61**(13), 5207-14.

101. Ichikawa, T., Itano, N.,Sawai, T., Kimata, K, Koganehira, Y., Saida, T., and Taniguchi, S. (1999). Increased synthesis of hyaluronate Enhances motility of human melanoma cells. *J. Invest. Dermatol*. **113**, 935-939.

102. Heldin, P. 2003. Importance of hyaluronan biosynthesis and degradation in cell differentiation and tumor formation. *Braz J Med Biol Res* **36**(8), 967-973.

103. Markku I. Tammi, Anthony J. Day, and Eva A. Turley, 2002.Hyaluronan and Homeostasis: A Balancing Act. **277**(15), 4581-84 *Biological Chemistry.*

104. Toole, B .P. Hyaluronan in morphogenesis (1997) *J. Intern*. *Med*. **242**, 35-40.

105. Rabinovitch, M. Cell- extracellular matrix interactions in the ductus arteriosus and perinatal pulmonary circulation. (1996) *Semin. Perinatol*, **20**, 531-541.

106. Spicer, A. P., Spicer A.P., Tien, J.L., Joo, A., Bowling, Jr.R.A. 2002. Investigation of hyaluronan function in the mouse through targeted mutagenesis. *Glycoconj* J **19** (4-5), 341-345.

107. Gibbs, D. A., Merrill, E.W., Smith, K.A. and Balazs, E.A., 1968. Rheology of hyaluronic acid. Biopolymers. 6,777-91.

108. Hansell, P., Goransson, V., Odlind, C., Gerdin, B. and Hallgren, R., 2000. Hyaluronan content in the kidney in different states of body hydration .Kidney Int, 58,2061-8.

109. Ginetzinsky, A.G.1958. Role of hyaluronidase in the re-absorption of water in renal tubules: the mechanism of action of the antidiuretic hormone. Nature,182,1218-9.

110. Pitcock, J.A., Lyons, H., Brown, P.S., Rightsel, W.A., Muirhead, E.E. Glycosaminoglycan of the rat renomedullary interstitium: ultrastructural and biochemical observations. *Exp Mol Pathol*, 1988. **49** (3), 373-87.

111. Zaman, A., Cui, Z., Foley, J.P., Zhao, H., Grimm, P.C., Delisser, H. M., and

Savani, R. C. (2005). Expression and role of the hyaluronan receptor RHAMM in inflammation after bleomycin injury. *American journal of respiratory cell and molecular biology* **33** (5), 447-454.

112. Stickel, F., Poeschl, G., Schuppan, D., Conradt, C., Strenge-Hesse, A., Fuchs, F.S.,Hofmann, W.J., Seitz, H.K. 2003. Serum hyaluronate correlates with histological progression in alcoholic liver disease. *Eur J Gastroenterlo Hepatol* **15** (9), 945-950.

113. Wang, T., Wang, B., Liu, X. 1998[Correlation of serum markers with fibrosis staging in chronic viral hepatitis]. *Zhonghua Bing Li Xue Za Zhi* **27** (3), 185-190.

114. Lewis, A., Steadman, R., Manley, P., Craig, K., De la Motte, C., Hascall, V, Phillips, A.O. 2008. Diabetic nephropathy, inflammation, hyaluronan and interstitial fibrosis. *Histol Histopathol* **23** (6), 731-739.

115. Lewington, A. J., Padanilam, B.J., Martin, D.R., Hammerman, M.R. 2000. Expression of CD44 in kidney after acute ischemic injury in rats. *Am J Physiol Regul Integr Comp Physiol* **278** (1), R247-254.

116. Johnsson, C., Tufveson, G., Wahlberg, J., Hallgren, R. 1996. Experimentally-induced warm renal ischemia induces cortical accumulation of hyaluronan in the kidney. *Kidney Int* **50**(4), 1224-1229.

117. Green, F. H. (2002). Overview of pulmonary fibrosis. *Chest* **122** (6 Suppl), 334S-339S.

118. Bjermer, L., Lundgren, R., and Hallgren, R. 1989. Hyaluronan and type III Procollagen peptide concentrations in bronchoalveolar lavage fluid in idiopathic pulmonary fibrosis. *Thorax* **44**(2), 126-131.

119.Zaman, A., Cui, Z., Foley, J.P., Zhao, H., Grimm, P.C., Savani, R. C. Delisser,

H.M. 2005, Expression and role of the hyaluronan receptor RHAMM in inflammation after bleomycin injury. *American journal of respiratory cell and molecular biology* **33** (5), 447-454.

120. Stickel, F., Poeschl, G., Schuppan, D., Conradt, C., Strenge-Hesse, A., Fuchs, F.S., Hofmann, W. J., and Seitz, H.K. 2003. Serum hyaluronate correlates with histological progression in alcoholic liver disease. *European journal of gastroenterology & hepatology* **15**(9), 945-950.

121. Wang, T., Wang, B., and Liu, X. (1998). Correlation of serum markers with fibrosis staging in chronic viral hepatitis. *Zhonghua bing li xue za zhi Chinese journal of pathology* **27**(3), 185-190

122. Nyberg, A., Engstrom-Laurent, A., and Loof, L. (1988). Serum hyaluronate in primary biliary cirrhosis a biochemical marker for progressive liver damage. *Hepatology Baltimore, Md* **8**(1), 142-146.

123. Mahadevan, P., Larkins, R.G., Fraser, J.R., Fosang, A.J and Dunlop, M.E., 1995. Increased hyaluronan production in the glomeruli from diabetic rats: a link between glucose-induced prostaglandin production and reduced sulphated proteoglycan. *Diabetological*, **38**, 298-305.

124. Sano, N., Kitazawa, K., and Sugisaki, T. 2001. Localization and roles of CD44, hyaluronic acid and osteopontin in IgA nephropathy. *Nephron* **89** (4), 416-421.

125. Nishikawa, K., Andres, G., Bhan, A. K., Mc Cluskey, R. T., Collins, A. B., Stow, J.L., and Stamenkovic, I. (1993).Hyaluronate is a component of crescents in rat autoimmune glomerulonephritis. *Laboratory investigation; a journal of technical methods and pathology* **68** (2), 146-153.

126. Feusi, E., Sun, L., Sibalic, A., Beck-Schimmer, B., Oertli, B., and Wuthrich, R.P. 1999. Enhanced hyaluronan synthesis in the MRL-Fas (IPr) kidney : role of

cytokines. *Nephron* **83**(1), 66-73.

127. Sibalic, V., Fan, X., Loffing, J., and Wuthrich, R. P. 1997. Upregulated renal tubular CD44, hyaluronan, and Osteopontin in kdkd mice with interstitial nephritis. *Nephrol Dial Transplant* **12**(7), 1344-1353.

128. Wells, A., Larsson, E., Hanas, E., Laurent, T., Hallgren, R., and Tufveson, G. 1993. Increased hyaluronan in acutely rejecting human kidney grafts. *Transplantation* **55**(6), 1346-1349.

129. Stenvinkel, P., Heimboreger, O., Wang, T., Lindhoim, B., Bergstrom, J., Elinder, C-G., High serum hyaluronan indicates poor survival in renal replacement therapy. *Am J Kidney Dis*, 1999. 34(6), 1083-8.

130. Kaissling, B. and M. Le Hir, Characterisation and distribution of interstitial cell types in the renal cortex of rats, *kidney Int*, 1994.45(3), 709-20.

131. Hewitson, T.D., Renal tubulointerstitial fibrosis: common but never simple. *Am J Physiol Renal Physiol,* 2009. 296(6), p.F1239-44.

132. Lama, V.N. and S.H. Phan, The extrapulmonary origin of fibroblasts: stem/ progenitor cells and beyond. *Proc Am Thorac Soc*, 2006. 3(4), 373-6.

133. Iwano, M., Plieth, D., Danoff, T.M., Xue, C., Okada, H., Neilson, E.G. 2002. Evidence that fibroblasts derive from epithelium during tissue fibrosis. *J Clin Invest* **110**(3), 314-350.

134. Zeisberg, M. and R. Kalluri, The role of epithelial-to-mesenchymal transition in renal fibrosis. *J Mol Med*, 2004. 82(3), 175-81.

135. Okada, H., Danoff, T.M., Kalluri, R., Neilson, E.G. Early role of Fsp1 in epithelial-mesenchymal transformation. *Am J Physiol*, 1997. 273(4 Pt 2), F563-74.

136. Samuel, S. K., Hurta, R.A., Spearaman, M.A., Wright, J.A., Turley, E.A.,

Greenberg, A.H.1993. TGF-beta 1 stimulation of cell locomotion utilizes the hyaluronan receptor RHAMM and hyaluronan. *J Cell Biol* **123** (3), 749-758.

137. Meran, S., Thomas, D. W., Stephens, P., Enoch, S., Martin, J., Steadman, R., and Phillips, A. O. (2008). Hyaluronan facilitates transforming growth factor- beta-1-mediated fibroblast proliferation. *J. Biol. Chem*. **283**, 6530-6545.

138. Meran, S., Thomas, D., Stephens, P., Martin, J., Bowen, T., Phillips, A., and Steadman, R. Involvement of hyaluronan in regulation of fibroblast phenotype. (2007) *J. Biol. Chem.* **282**, 25687-25697.

139. Jenkins, R. H., Thomas, G.J., Williams, J.D., Steadman, R. 2004. Myofibroblastic differentiation leads to hyaluronan accumulation through reduced hyaluronan turnover. *J Biol Chem* **279** (40), 41453-41460.

140. Webber J, Jenkins RH, Meran S, Phillips AO and Steadman R. Modulation of TGF-β1-Dependent Myofibroblast Differentiation by Hyaluronan. *Am J Patho*, **175**, 1, 2009, 148-160.

141. Webber J, Meran S, Steadman R, and Phillips AO, 2009. Hyaluronan orchestrates transforming growth factor-β1-dependent maintenance of myofibroblast phenotype. *J Biolo Chem* **284**.14, 9083-9092.

142. Lee, G.M., Johnstone, B., Jacobson, K. and Caterson, B., 1993. The dynamic structure of the pericellular matrix on living cells. *J Cell Biol*, **123**, 1899-907.

143.Knudson, C.B. and Knudson, W., 1993. Hyaluronan-binding proteins in development, tissue homeostasis, and disease. *Faseb J*, **7**, 1233-41.

144.Nishida, Y., Knudson, C.B., Niefeld, J.J., Margulis, A. and Knudson, W., 1999. Antisense inhibition of hyaluronan synthase-2 in human articular

chondrocytes inhibits proteoglycan retention and matrix assembly. *J Biol Chem*, **274**, 21893-9.

145. Evanko, S. P., Angello, J.C., Wight, T.N. 1999. Formation of hyaluronan and versican-rich pericellular matrix is required for proliferation and migration of vascular smooth muscle cells. Arterioscler *Thromb Vasc Biol* **19** (4), 1004-1013.

146. De la Motte, C. A., Hascall, V.C., Drazba, J., Bandyopadhyay, S.K., Strong, S.A. 2003. Mononuclear leukocytes bind to specific hyaluronan structures on colon mucosal smooth muscle cells treated with polyinosinic acid: polycytidylic acid: inter-alpha-trypsin inhibitor is crucial to structure and function. *Am J Pathol* **163**(1), 121-133.

147. Hinz, B., Formation and Function of the Myofibroblast during Tissue Repair. *J Invest Dermatol*, 2007.**127**(3), 526-537.

148. Sappino AP, Schurch W, Gabbiani G. Differentiation repertoire of fibroblastic cells: expression of cytoskeletal proteins as marker of phenotypic modulations. *Lab Invest*. 1990, **63**(2): 144-61.

149. Badid C, Desmouliere A, Laville M, Vincent M, and Fouque D. Myofibroblast: a prognostic marker and target cell in progressive renal disease. *Ren Fail*. 2001: **23**(3-4):543-9.

150. Clark, R. A. F. (1995) *Molecular and cellular Biology of Wound Repair*, 2nd Ed., 3-50, Plenum Publishing Corp., New York.

151. Grinnell, F. (1994). Fibroblast, myofibroblast, and wound contraction. *J. Cell Biol*, **124**, 401-404.

152. Desmouliere, A., Darby, I. A., and Gabbiani, G. (2003). Normal and Pathologic soft tissue remodelling : role of the myofibroblast, with special emphasis on liver and kidney fibrosis. *Lab. Investig*. **83**, 1689-1707.

153. Gabbiani, G. (2003). The myofibroblast in wound healing and fibrocontractive diseases. *J. Pathol* **200** (4), 500-503.

154. Evans, R. A., Tian, Ya. C, Steadman, R., and Phillips, A. O. 2003. TGF-beta-mediated fibroblast-myofibroblast terminal differentiation-the role of Smad proteins. *Exp Cell Res* **282**(2), 90-100.

155. Tomasek, J.J., Gabbiani, G., Hinz, B., Chaponnier, C., and Brown, R. A. 2002. Myofibroblasts and mechano-regulation of connective tissue remodelling. *Nat. Rev. Mol. Cell Biol*, **3**, 349-363.

156. Simpson, R., Meran, S., Thomas, D., Stephens, P., Bowen, T., Steadman, R., and Phillips, A. 2009. Age-Related Changes in Pericellular hyaluronan organization leads to impaired dermal fibroblast to myofibroblast differentiation. *Am J Path*, **175**(5), 1915-1928.

157. Simpson, R.M.L., Wells, A., Thomas, D., Stephens, P., Steadman, R.,A.O.,P.2010. Ageing fibroblasts resist phenotypic maturation due to impaired Hyaluronan-dependent CD44/EGF receptor signalling. *The Am J of Path*: 176 (3): 1215-28.

158. Meran, S., Luo, D.D., Simpson, R., Martin, J., Wells, A., Steadman, R., Phillips, A.O. Hyaluronan facilitates transforming growth factor-beta 1-dependent proliferation via CD44 and epidermal growth factor receptor interaction *J Biol Chem* 286, 17618-30. 2011.

159. Meran, S., Steadman, R. Fibroblasts and myofibroblasts in renal fibrosis.2011 *Int J Exp Pathol* 92, 158-67.

160.Goumenos D, Brown CB, Shortland J, El Nahas AM (1994). Myofibroblasts, predictors of progression of mesangial IgA nephropathy?. *Nephrology Dialysis Transplantation* **9**, 1418-1425.

161.Essawy M, Soylemezoglu O, Muchaneta-Kubara EC, Shortland J, Brown CB, El Nahas AM(1997). Myofibroblasts, predictors of progression of mesangial IgA nephropathy?. *Nephrology Dialysis Transplantation* **12**, 34-50.

162.Goumenous D, Tsomi k, Iatrou C, Oldroyd S., Sungur A, Papaioannides D, Moustakas G, Ziroyannis P, Mountokalis T, El Nahas AM (1998). Myofibroblasts, predictors of progression of mesangial Ig A nephropathy? *Nephrology Dialysis Transplantation* **13**, 1652-1661.

163.Roberts, I.S., Burrows, C., Shanks, J.H., Venning, M. and Mc William, L.J., 1997. Interstitial myofibroblasts: predictors of progression in membranous nephropathy. *J Clin Pathol*, **50**, 123-7.

164. Phillips AO, Topley N, Steadman R, et al: Induction of TGF-β1 synthesis in d-glucose primed human proximal tubular cells: Differential stimulation by the macrophage derived pro-inflammatory cytokines IL-1β and TNFα. *Kidney Int* **50**: 1546-1554, 1996.

165.Phillips AO, Steadman R, Morrisey K, Williams J D. Polarity of Stimulation and Secretion of Transforming Growth Factor-β1 by Cultured Proximal Tubular *Cells. Am J Path* **150**,3, 1101-1111, 1997.

166.Jones S G, Morrisey K, Williams JD, Phillips AO. TGF-β1 stimulates the release of pre-formed bFGF from renal proximal tubular cells. *Kidney International*, **56** (1999), 83-91.

167.Morrisey K, Steadman R, Williams JD, and Phillips AO. Renal proximal tubular cell fibronectin accumulation in response to glucose is polyol pathway dependent.

Kidney International, **55**(1999), 160-167.

168.Liu Y (2004). Epithelial to mesenchymal transition in renal fibrogenesis: pathologic significance, molecular mechanism and therapeutic intervention. *J Am Society of Nephrology* **15**, 1-12.

169. Cheng, J., Grande, J.P. Transforming growth factor-beta signal transduction and pro-gressive renal disease. *Exp Biol Med* (Maywood) 2002;227.943-56.

170.Grande, M., Franzen, A., Karlsson, J.O., Ericson, L.E., Heldin, N.E., Nilsson, M. Transforming growth factor-beta and epidermal growth factor synergistically stimulate epithelial to mesenchymal transition (EMT) through a MEK-dependent mechanism in primary cultured pig thyrocytes. *J Cell Sci* 2002;115:4227-36.

171.Tian, Y.C., Fraser, D., Attisano, L., Phillips, A.O. TGF-beta-1-mediated alterations of renal proximal tubular epithelial cell phenotype. *Am J Physiol Renal Physiol* 2003;285:F130-42.

172. Bommaya, G., Meran, S., Krup, A., Phillips, A.O., Steadman, R. Tumour necrosis Factor- stimulated gene (TSG)-6 controls epithelial- mesenchymal transition of Proximal tubular epithelial cells. *The international J of Bioch and Biolo* 43. 2011. 1739-1746.

173. Zoltan-Jones, A., Huang, L., Ghatak, S., Toole, B.P. 2003. Elevated hyaluronan production induces mesenchymal and transformed properties in epithelial cell. *J Biol Chem* **278** (46), 45801-45810.

174. Ahmed, S. and Nawshad, A. 2007. Complexity in interpretation of Embryonic Epithelial- Mesenchymal Transition in Response to Transforming Growth Factor-β Signaling. *Cells Tissues Organs*. **185**, 131-145.

175. Jones SG, Jones S, Phillips AO (2001). Regulation of renal proximal tubular epithelial cell hyaluronan generation: implications for diabetic nephropathy. *Kidney International* **59**, 1739-1749.

176. Wuthrich, R.P. 1999. The proinflammatory role of hyaluronan-CD44 interactions in renal injury. *Nephrol Dial Transplant*, **14**, 2554-6.

177.Li, Yuejuan., Rahmanian, M., Widstrom, C., Lepperdinger, G., Frost, G.I., Heldin, P. 2000. Irradiation- Induced Expression of HA Synthase 2 and hyaluronidase 2 Genes in Rat lung tissue accompanies active turnover of HA and Induction of types I and III collagen gene expression. *Am J Res Cell Mol Biol.***23**, 411-418.

178. Pienimaki, J. P., Rilla, K., Fulop, C., Sironen, R.K., Karvinen,S., Pasonen, S., Lammi, M.J. Tammi, R., Hascall, V.C., Tammi, M.I. 2001. Epidermal growth factor activates hyaluronan synthase 2 in epidermal keratinocytes and increases pericellular and intracellular hyaluronan. *J Biol Chem*, **276**, 20428-35.

179.Pasonen-Seppanen, S., Karvinen, S., Torronen, K., Hyttinen, J.M., Jokela, T., Lammi, M.J., Tammi, M.I., Tammi, R. 2003. EGF upregulates, whereas TGF-beta downregulates, the hyaluronan synthases Has2 and Has3 in organotypic keratinocyte cultures: correlations with epidermal proliferation and differentiation. *J Invest Dermatol*, **120**, 1038-44.

180. Karvinen, S., Pasonen-Seppanen, S., Hyttinen, J.M., Pienimaki, J.P., Torronen, K., Jokela, T.A., Tammi, M.I. and Tammi, R., 2003. Keratinocyte growth factor stimulates migration and hyaluronan synthesis in the epidermis byactivation of keratinocyte hyaluronan synthases 2 and 3. *J Biol Chem*, **278**, 49495-504.

181. Usui, T., Amano, S., Oshika, T., Suzuki, K., Miyata, K., Araie, M., Heldin, P. and Yamashita, H., 2000. Expression regulation of hyaluronan synthase in

corneal endothelial cells. *Invest Ophthalmol Vis Sci*, **41**, 3261-7.

182.Jacobson, A., Brinck, J., Briskin, M.J., Spicer, A.P. and Heldin, P., 2000. Expression of human hyaluronan synthases in response to external stimuli. *Biochem J*, **348 Pt 1**, 29-35.

183. Ijuin, C., Ohno, S., Tanimoto, K., Honda, K., Tanne, K. 2001. Regulation of hyaluronan synthase gene expression in human periodontal ligament cells by tumour necrosis factor-alpha, interleukin-1 beta and interferon-gamma. *Arch Oral Biol*, **46**, 767-72.

184. Carninci, P., Yasuda, J., and Hayashizaki, Y. Multifaceted mammalian transcriptome. (2008) *Curr Opin Cell Biol* **20**, 274-280.

185. Bowen, T., Yung, S., Martin, J., Morgan, L., Topley, N., Davies, M., & Williams, J.D. 2001.The effect of IL-1β stimulation on the expression of hyaluronan synthase isoforms and the rate of wound healing in a high-throughput in vitro model of human peritoneal mesothelial cells injury. *Journal of the American Society of Nephrology*, **12**, A3650.

186.Kennedy, C.I., Diegelmann, R. F., Haynes, J.H and Yager., 2000. Proinflammatory cytokines differentially regulate hyaluronan synthase isoforms in fetal and adult fibroblasts. *J Pediatr Surg*, **35**, 874-9.

187. Monslow J, Williams JD, Norton N, Guy CA, Price IK, Coleman SL, Williams NM, Buckland PR, Spicer AP, Topley N, Davies M, Bowen T, 2003. The human hyaluronan synthase genes: genomic structures, proximal promoters and polymorphic microsatellite markers. *International J Biochemistry and cell Biol*, **35**, 1272-1283.

188.Krawczak, M., Reiss, J., & Cooper, D.N. (1992). The mutational spectrum of single base-pair substitutions in messenger-RNA splice Junctions of human genes-

causes and consequences. *Human Genetics*, **90**, 41-54.

189. Monslow J, Williams JD, Guy CA, Price IK, Craig KJ, Williams HJ, Williams NM, Martin J, Coleman SL, Topley N, Spicer AP, Buckland PR, Davies M, Bowen (2004). Identification and analysis of the promoter region of the human hyaluronan synthase 2 gene. *J Biological Chemisty* **279**, 20576-20581.

190. Monslow J, Williams JD, Fraser DJ, Michael DR, Foka P, Kift-Morgan AP, Luo DD, Fielding CA, Craig KJ, Topley N, Jones SA, Ramji DP, Bowen T (2006). Sp1 and Sp3 mediate constitutive transcription of the human hyaluronan synthase 2 gene. *Journal of Biological Chemistry* **281**, 10843-10850.

191. Michael D R, Phillips A O, Krupa A, Neville R D, Webber J, Altaher A, Martin J, Kim M-Y, and Bowen T. The human hyaluronan synthase 2 gene and its natural antisense RNA exhibit coordinated expression in the renal proximal tubular epithelial cell. *Journal of Biological Chemistry*, 2011. 286(22): 19523-32

192. Saavalainen, K., Tammi, M.I., Bowen, T., Schmitz, M. L., and Carlberg, C. (2007). Integration of the activation of the human hyaluronan synthase 2 gene promoter by common cofactors of the transcription factors retinotic acid receptor and nuclear factor kappa B. *J. Biol. Chem.* ***282***, 11530-11539.

193. Saavalainen, K., Pasonen-Seppanen, S., Dunlop, T.W., Tammi,R., Tammi, M.I. and Carlberg, C. The human hyaluronan synthase 2 gene is a primary retinoic acid and epidermal growth factor responding gene. *2005*. *J Biol Chem*.**280**, 14636-14644.

194. Makkonen K. M, Pasonen-Seppanen S, Torronen K, Tammi M I, and Carlberg C, 2009. Regulation of the hyaluronan synthase 2 gene by convergence in cyclic AMP response element binding protin and retinoid acid receptor signaling. *J Biological Chemistry*, 284, 27, 18270-18281.

195. Chao, H., and Spicer, A.P. Natural antisense mRNAs to hyaluronan synthase 2 inhibit hyaluronan biosynthesis and cell proliferation. (2005) *J. Biol. Chem*. **280**, 27513-27522.

196. Vanhee-Brossollet, C., and Vaquero, C. Do natural antisense transcripts make sense in eukaryotes. (1998) *Gene* **211**, 1-9.

197.Herbert, A. (2004). The four Rs of RNA-directed evolution. *Nat. Genet*. **36**, 19-25.

198. Mattick, J.S. (2009). The genetic signatures of noncoding RNAs. *PLoS Genet*. 5, e1000459.

199. Phillips AO, Steadman R, Topley N, Williams JD: Elevated d-glucose concentration modulate TGF-β1 synthesis by human cultured renal proximal tubular cells: The permissive role of platelet derived growth factor. *Am J Pathol* **147**:362-374, 1995.

200. Sano N, Kitazawa K, Sugisaki T. 2001. Localization and roles of CD44, hyaluronic acid and osteopontin in IgA nephropathy. *Nephron*.**89**(4): 416-21.

201.Wahlestedt, C. 2006. Natural antisense and noncoding RNA transcripts as potential drug targets. *Drug Dscovery Today*. **11** (11-12), 503-508.

202. Bakker, W., Eringe, E., Sipkema. P. and van Hinsbergh .V. Endothelial dysfunction and diabetes: role of hyperglycemia, impaired insulin signalling and obesity, *Cell Tissue Res*, 335(2009), 165-189.

203. Schrijvers, B.F.,De Vriese, A.S and Flyvbjerg, A. From hyperglycaemia to Diabetic kidney disease: The role of metabolic, hemodynamic, intracellular factors and growth factors/ cytokines, *Endocr Rev*, 25 (2004), 971-1010.

204. Nitsch, D., Burden, R., Steenkamp. R., Ansell, D., Byrne, C., Caskey, F., Roderick,P. and Feest, T., Patients with diabetic nephropathy on renal

replacement therapy in England and Wales, *QJM*, 100 (2007), 551-560.

205. Hasslacher,H., Ritz, E., Walhl, P and Michael, C, Similar risks of nephropathy in patients with type I or type II diabetes mellitus, Nephrol Dial Transplant, 4(1989),859-863.

206. Mauer, S.M., Steffes, M.W., Ellis, E.N., Sutherland, D.E., Brown, D.M., and Goetz, F.C, Structural-functional relationships in diabetic nephropathy, *J Clin Invest*, 74 (1984), 1143-1155.

207. Fioretto, P., and Mauer, M. Histopathology of diabetic nephropathy, *Semin Nephrol*, 27(2007), 195-207.

208. Galkina, E and Ley, K. Leukocyte recruitment and vascular injury in diabetic nephropathy. *J Am Soc Nephrol*, 17 (2006), 368-377.

209. Girish, Bommaya., Soma, Meran., Aleksandra, Krup., Aled Owain, Phillips., Robert,Steadman. Tumour necrosis factor-stimulated gene (TSG)-6 controls epithelial-mesenchymal transition of proximal tubular epithelial cells. *The International Journal of Biochemistry and cell biology*.2011 (43)1739-1746].

210. Yamamoto, T., Nakamura, T., Noble, N.A., Ruoslahti, E., Border, W.A. Expressionof transforming growth factor-p is elevated in human and experimental diabetic nephropathy. *NatProc Natl Acad Sci USA* 1993. p. 1814-8.

211.Shankland, S.J., Scholey, J.W. Expression of transforming growth-factor-beta-during diabetic renal hypertrophy. *Kidney International*. 1994;46(2):430-42.

212. Huang, C., Kim, Y., Caramori, ML., Fish, AJ., Rich, SS., Miller, ME., Russell, GB., Mauer, M. Cellular basis of diabetic nephropathy: II. The transforming growthFactor-beta system and diabetic nephropathy lesion in type 1 diabetes. *Diabetes,*2002.51(12). 3577-81.

213. Okuda, S., Languino, L.R., Ruoslahti, E., Border, W.A. 1990. Elevated expression of transforming growth factor-beta and proteoglycan production in experimental glomerulonephritis. Possible role in expansion of the mesangial extracellular matrix. *J Clin Invest* **86**(2), 453-462.

214.Fraser, D., Wakefield, L., Phillips, A. 2002. Independent regulation of transforming growth factor-beta1 transcription and translation by glucose and platelet-derived growth factor. *Am J Pathol* **161**(3), 1039-1049.

215.Sanderson, N., Factor, V., Nagy, P., Kopp, J., Kondaiah, P., Wakerfield, L., Roberts., A.B., Sporn, M.B., Thorgeirsson, S.S. 1995. Hepatic expression of mature transforming growth factor beta 1 in transgenic mice results in multiple tissue lesion. *Proc Natl Acad Sci U S A* **92**(7), 2572-2576.

216.Border WA, Okuda S, Languino LR, Sporn MB, Ruoslahti E. 1990. Suppression of experimental glomerulonephritis by antiserum against transforming growth factor beta 1. *Nature*.**26**:346(6282):371-4.

217.Hou CC, Wang W, Huang X R, Fu P, Chen TH, Hamad DS, Lan HY, 2005. Ultrasound-Microbubble-Mediated Gene transfer of inducible Smad7 blocks transforming growth factor-β signalling and fibrosis in Rat remnant kidney. *Am J Pathology*, **166**,3,761-771.

218.Stahl, P.J. and Felsen, D., 2001. Transforming growth factor-beta, basement membrane, and epithelial-mesenchymal transdifferentiation: implication for fibrosis in kidney disease. *Am J Pathol*, **159**, 1187-92

219.Abrass, C.K., Berfield, A.K., Stehman-Breen, C., Alpers, C.E. and Davis, C.L., 1999. Unique changes in interstitial extracellular matrix composition are associated with rejection and cyclosporine toxicity in human renal allograft biopsies. *Am J Kidney Dis*, **33**, 11-20.

220. Brito, P.L., Fioretto, P., Drummond, K., Kim, Y., Steffes, M.W., Basgen, J.M., Sisson-Ross, S. and Mauer, M., 1998. Proximal tubular basement membrane width in insulin-dependent diabetes mellitus. *Kidney Int*, **53**, 754-61.

221. Miner, J.H. 1999. Renal basement membrance components. *Kidney Int*, **56**, 2016-24.

222. Holdsworth, S.R., Neale, T.J., Wilson, C.B. 1981. Abrogation of Macrophage-dependent injury in Experimental Glomerulonephritis in the Rabbit. *Am Soci Clinical Invest*.**68**,686-698.

223. Tesch, G, H., Schwarting, A., Kinoshita. K., Lan, H.Y., Rollins, B.J., Kelley, V.R. 1999. Monocyte chemoattractant protein-1 promotes macrophage-mediated tubular injury, but not glomerular injury, in nephrotoxic serum nephritis. *J. Clin. Invest*. **103**:73-80.

224. Ophascharoensuk, V., Giachelli, C.M., Gordon, K., Hughes, J., Pichler, R., Brown, P., Liaw, L., Schmidt, R., Shankland, S.J., Alpers, C.E., Couser, W.G., Johnson, R.J. 1999. Obstructive uropathy in the mouse: Role of osteopontin in interstitial fibrosis and apoptosis. *Kidney International*, **56**. 571-580.

225. Young, B.A., Johnson, R.J., Alpers, C.E., Eng, E., Gordon, K., Floege, J., Couser, W.G., Seidel, K. 1995. Cellular events in the evolution of experimental diabetic nephropathy. *Kidney International*, **47**, 935-944.

226. Lavaud, S., Michel, O., Sassy-Prigent, C., Heudes, D., Bazin, R., Bariety, J., Chevalier, J. 1996. Early influx of glomerular macrophages precedes glomerulosclerosis in the obese zucker rat model. *J. Am. Soc. Nephrol*. **7**, 2604-2615.

227. Furuta T, Saito T, Ootaka T, Soma J, Obara K, Abe K, Yoshinaga K. The role of macrophages in diabetic glomerulosclerosis. 1993 *Am J Kidney Dis*. **21**(5):480-5.

228. Fan, J.M., Huang, X.R., Ng, Y.Y, Nikolic-Paterson, D.J, Mu, W., Atkins, R.C, Lan,H.Y. Interleukin-1 induces tubular epithelial-myofibroblast transdifferentiation through a transforming growth factor-beta 1-dependent mechanism in vitro. *American Journal of Kidney Diseases*. 2001;37(4):820-31.

229. Vesey, D.A., Cheung, C.W., Cuttle, L., Endre, Z.A, Gobe, G., Johnson, D.W. Interleukin-1 beta induces human proximal tubule cell injury, alpha-smooth muscle actin expression and fibronectin production. *Kidney International*. 2002;62(1):31-40.

230. Phillips AO, Steadman R, Morrisey K, Martin J, Eynstone L, Williams JD. 1997. Exposure of human renal proximal tubular cells to glucose leads to accumulation of type IV collagen and fibronectin by decreased degradation. *Kidney Int*. **52**(4):973-84.

231.Riley SG, Steadman R, Williams JD, Floege J, Phillips AO. Augmentation of kidney injury by basic fibroblast growth factor or platelet-derived growth factor does not induce progressive diabetic nephropathy in the Goto Kakizaki model of non-insulin- dependent diabetes. *J Lab Clin Med.* 1999:***134***(3): 304-12.

232.Phillips AO, Baboolal K, Riley S, Grone H, Janssen U, Steadman R, Williams J, Floege J. Association of prolonged hyperglycemia with glomerular hypertrophy and renal basement membrane thickening in the Gto Kakizaki model of non-insulin-dependent diabetes mellitus. *Am J Kidney Dis*. 2001: **37**(2): 400-10.

233. Wolf, G., New insights into the pathophysiology of diabetic nephropathy: from Haemodynamics to molecular pathology. *Eur J Clin Invest*, 34,2004, 785-796.

234.Mason, R.M and Wahab, N.A, Extracellular matrix metabolism in diabetic Nephropathy. J Am Soc Nephrol, 2003. 14(5), 1358-73.

235 .Mc Lennan, S.V., Fisher, E.J., Yue, D.K., and Turtle, J.R.19994. High glucose

Concentration caueses a decrease in mesangium degradation. A factor in the Pathogenesis of diabetic nephropathy. *Diabetes*. 43: 1041-1045.

236. Sassy-Pringent, C., Heudes, D., Mandet, C., Belair, M.F., Michel, O., Perdereau,B.,Bariety, J., Bruneval, P. Early glomerular macrophage recruitment in streptozotocin Induced diabetic rats, *Diabetic* 49, 466-475,2000.

237. Furuta, T, Saito, T., Ootaka, T., Soma, J., Obara, K., Abe, K., Yoshinaga, K. The role of macrophages in diabetic glomerulosclerosis. *Am J Kidney Dis* 21, 480-485,1993.

238. Ksissling, B., Le Hir, M: Characterization and distribution of interstitial cell types in the renal cortex of rats. *Kidney Int* 45: 709-720, 1994.

239. Lonneman,G., Shapiro, L., Englerblum, G., Muller, G.A, Koch, K.M., Dinarello, C.A. Cytokines in human renal interstitial fibrosis.1. Interleukin-1 is a paracrine growth-factor for cultured fibrosis-derived kidney fibroblasts. *Kidney International*. 1995;47(3):837-44.

240. Lonnemann, G., Englerblum, G., Muller, G.A., Koch, K.M., Dinarello, C.A. Cytokines in human Renal interstitial fibrosis .2. Intrinsic interleukin (IL)-1 synthesis and IL-1-dependent production of IL-6 and IL-8 by cultured kidney fibroblasts. *Kidney International*. 1995;47(3):845-54.

241. Yang J, Liu Y. Dissection of key events in tubular epithelial to myofibroblast transition and its implications in renal interstitial fibrosis. *Am J Pathol*.2001.**159**(4):1465-75.

242.Li Y, Rahmanian M, Lepperdinger G, Widstrom C, Frost GI and Heldin P. 2000. Irradiation-induced expression of hyaluronan (HA) synthase 2 and hyaluronidase 2 genes in rat lung tissue accompanies active turnover of HA and induction of types I and III collagen gene expression. *Am. J. Respir. Cell Mol. Biol*. **23**, 411-

418.

243.El-Chemaly S, Malide D., Zudaire, E., Ikeda, Y., Weinberg, B. A., Pacheco-Rodriguez, G., Rosas, I.O., Aparicio, M., Ren, P., MacDonald, S. D., Wu, H.-P., Nathan, S. D., Cuttitta, F., Mc Coy, J.P., Gochuico, B.R., and Moss, J. Abnormal lymphangiogenesis in idiopathic pulmonary fibrosis with insights into cellular and molecular mechanisms. (2009) *Proc. Natl. Acad. Sci. U.S.A.* **106**, 3958-3963.

244.Lavorgna, G., Dahary D., Lehner B., Sorek R., Sanderson CM., and Casari G. In search of antisense. *Trends in Biochemical Sciences*.**29** (2),2004, 88-94.

245.Lapidot M, and Pilpel Y, 2006. Genome wide natural antisense transcription: coupling its regulation to its different regulatory mechanisms. *EMBO reports* **7**,12, 2006, 1216-1222.

246.Li Y.Y., Qin, L., Guo, Z.M., Liu, L., XU, H., Hao, P., Su, J., Shi, Y., He, W.Z., LI, Y.X. 2006. In silico discovery of human natural antisense transcripts. *BMC Bioinformatics*.7:18, 1-8.

247.Faghihi, M.A., Modarresi, F., Khalil, A. M., Wood, D.E., Sahagan, B.G., Morgan, T. E., Finch, C.E.,St. Laurent Iii, G., Kenny, P.J., and Wahlestedt, C. Expression of a non coding RNA is elevated in Alzheimer`s disease and drives rapid feed-forward regulation of beta-secretase. (2008) *Nat. Med*.**14**,723-730.

248.Cartharius, K., Frech, K., Grote, k., Klocke, B., Haltmeier, M., Klingenhoff, A., Frisch, M., Bayerlein, M., and Werner, T. Matlnspector and beyond : Promoter analysis based on transcription factor binding sites. (2005) *Bioinformatics***21**, 2933-2942.

249.Frith, M. C., Hansen, U., and Weng, Z. Detection of cis-element clusters in higher eukaryotic DNA. (2001) *Bioinformatics* **17**, 878-889.

250.Frith, MC, Li MC, Weng Z (2003). Cluster-buster: finding dense clusters of

motifs in DNA sequences. *Nucleic Acids Research* **31**, 3666-3668.

251. Dallosso, A. R., Hancock, A. L., Malik, S., Salpekar, A., King-Underwood, L., Pritchard-Jones, K., Peters, J., Moorwood, K., Ward, A., Malik, K. T., and Brown, K. W. (2007). Alternately spliced WT1 antisense transcripts interact withWT1 sense RNA and show epigenetic and splicing defects in cancer. *RNA* **13**, 2287-2299.

252. Matsui, K., Nishizawa, M., Ozaki, T., Kimura, T., Hashimoto, I., Yamada, M., Kaibori, M., Kamiyama, Y., Ito, S., and Okumura, T. Natural antisense transcript stabilizes inducible nitric oxide synthase messenger RNA in Rat hypatocytes. (2008) *Hepatology* **47**, 686-697.

253. Webber, M.M., Bello, D., Kleinman, H.K., Hoffman, M.P. Acinar differentiation by non-malignant immortalized human prostatic epithelial cells and its loss by malignant cells. *Carcinogenesis* vol.**18** (6), 1225-1231, 1997.

254.Sappino, A-P., Skalli, O., Jackson, B., Schurch, W., Gabbiani, G. Smooth muscle differentiation in stromal cells of malignant and non-malignant breast tissues. 2006, *International J of cancer* 707-712.

255. Yung S., Thomas, G.J., Davies, M. 2000. Induction of hyaluronan metabolism after mechanical injury of human peritoneal mesothelial cells in vitro. *Kidney International* **58**. 1953-1962.

256. Iwano M, Plieth D, Danoff TM, Xue C, Okada H, and Neilson EG. 2002. Evidence that fibroblasts derive from epithelium during tissue fibrosis. *J Clin. Invest*.**110:**341-350.

257.Udabage L, Brownlee GR, Nilsson SK, Brown TJ. The over-expression of HAS2, Hyal-2 and CD44 is implicated in the invasiveness of breast cancer. *Exp Cell Res*. 2005 15; 310(1):205-17.

Appendix 1

PCR gel- protocol:

1.5 % gel use 1.5% agarose powder.

150 ml gel = 2.25g Agarose +150 ml TAE buffer

(Tris base, acetic acid and **ethylenediaminetetraacetic acid**).

Microwave Agarose TAE mix, swirl periodically, caution it is very HOT.

Mix will bobble and go clear when ready

Swirl gently to “de-gas”

Add 1µl of stoch ethidum bromide for every 10 ml mix. So final concentration of 0.5 µg/ml.

For example 150ml =15µl Ethidum bromide.

Caution ethidum bromide = carcinogenic.

Pour into mould, move any bubbles to side with pipette tip.

Appendix 2

LB Amp selective plates preparation

Prepare 1 liter LB broth (Luria-Bertani broth)

Bacto Tryptone	10 g/litre
Bacto Yeast Extract	5 g/litre
NaCl	10 g/litre

Adjust PH to 7.5 with NaOH

Add Agar 1.5 g per 100ml (1.5% agar plates used)

Autoclave to sterilise and dissolve

Allow to cool to 65ºC

Add Ampicillin 100 µl of 50 mg/ml stock per 100 ml so final concentration of 50 µg/ml.

Pour 10 ml / 100mm plate.